

A PETROGRAPHIC, MINERALOGICAL, AND PETROPHYSICAL ANALYSIS OF CARBONATE
CORE IN THE FLORIDAN AQUIFER SYSTEM: COCKSPUR ISLAND, GEORGIA, USA

by

KATRINA SAMANTHA OSTROWICKI

(Under the Direction of Paul Schroeder)

ABSTRACT

The USGS Saline Aquifer Mapping Project is currently evaluating salinity variations in the Floridan aquifer system utilizing borehole geophysical logs to determine water quality throughout the aquifer system. This study, which contributes to the larger USGS mapping project, gives a detailed mineralogical, petrophysical, and petrographic analysis of core from Cockspur Island using XRD, image analysis software, minipermeametry, and laboratory resistivity measurements. This study investigates how a siliciclastic input in a carbonate aquifer, along with pore geometry, affects the geophysical logs used to calculate salinity. The Lower Floridan aquifer had a significant amount of clinoptilolite, which caused porosity to be underestimated from the sonic log, and illite and smectite, which likely has no effect on the resistivity well log. Cementation factors were found to be significantly larger for grainstones than packstones to wackestones. This study shows that mineralogy and lithology must be taken into account in the USGS's mapping project.

INDEX WORDS: Floridan Aquifer System, Clinoptilolite, Petrophysics, Carbonate Core, Resistivity, Conductivity, Well Logs, Cockspur Island, core hole, Savannah, Sonic, Gamma-ray

A PETROGRAPHIC, MINERALOGICAL, AND PETROPHYSICAL ANALYSIS OF CARBONATE
CORE IN THE FLORIDAN AQUIFER SYSTEM: COCKSPUR ISLAND, GEORGIA, USA

by

KATRINA SAMANTHA OSTROWICKI

BS, University of Florida, 2009

A Thesis Submitted to the Graduate Faculty of The University of Georgia in Partial Fulfillment of the
Requirements for the Degree

MASTER OF SCIENCE

ATHENS, GEORGIA

2012

© 2012

Katrina Samantha Ostrowicki

All Rights Reserved

A PETROGRAPHIC, MINERALOGICAL, AND PETROPHYSICAL ANALYSIS OF CARBONATE
CORE IN THE FLORIDAN AQUIFER SYSTEM: COCKSPUR ISLAND, GEORGIA, USA

by

KATRINA SAMANTHA OSTROWICKI

Major Professor: Paul Schroeder

Committee: John Dowd
Bruce Railsback

Electronic Version Approved:

Maureen Grasso
Dean of the Graduate School
The University of Georgia
December 2012

ACKNOWLEDGEMENTS

I would like to thank my family for their support, and especially my mother. I would also like to thank the USGS Georgia Water Science Center for the funding for trips to Reston, VA, and Denver, CO to collect samples and gather data. Art Schultz with the USGS in Reston and Bob Horton with the USGS in Denver provided invaluable advice, help, and guidance in collecting the samples and data for my thesis. I am very thankful for the opportunity to use the USGS Denver Federal Center's Petrophysics Laboratory and the USGS Core Repository in Reston, VA and for all of the people who made that a possibility. Lester Williams with the USGS in Atlanta, GA has been a great mentor and has given countless hours to this study, and I could never thank him enough. I would like to acknowledge Camille Ransom for collecting the geophysical logs in this study, and Lucy Edwards for her paleo work in the well used in this study.

Thank you to Gary Brown with Chevron for helping me to become a better geologist. A many thanks to former and current graduate students in the department for moral support, and would like to specifically mention Nicholas Radko. I would also like to acknowledge Allison Platsky for her statistical expertise, Kirk Fraley for some of the photographs used in this thesis, Dan Bulger for allowing me to use his minipermeameter and his lab in Atlanta, the UM Comparative Sedimentology Lab for letting me use their TSGui software, and the people at Bruker for answering the phone and walking me through Topas.

And of course I would like to give a big thanks to my advisor Paul Schroeder for mentoring me and for his invaluable input, and also for giving me the opportunity to be a TA for IFP three summers in a row. I will surely miss traveling across the U.S. and visiting National Parks during the summers. A huge thanks to my committee members Bruce Railsback, for his carbonate expertise and John Dowd, for his hydrogeology expertise.

This study would not have been possible without the generous support from the AAPG Grants-in-Aid Gustavus E. Archie Grant, Wheeler-Watts Grant, and the Joseph W. Berg Geophysics Scholarship

TABLE OF CONTENTS

	Page
ACKNOWLEDGEMENTS	iv
LIST OF TABLES	vii
LIST OF FIGURES	viii
CHAPTER	
1 INTRODUCTION	1
1.1 Background	1
1.2 Purpose of Study	2
1.3 Previous Studies Relating Borehole Well Logs to Salinity	5
2 GEOLOGY OF THE FLORIDAN AQUIFER SYSTEM	7
2.1 Stratigraphy	7
2.2 Occurrence of Zeolites and Glauconite in the Floridan Aquifer System	13
2.3 Hydrogeology	13
3 PETROPHYSICS OF CARBONATES	16
3.1 Principles of Borehole Resistivity Logs	16
3.2 Principles of Gamma-Ray and Sonic Borehole Logs	17
3.3 Application of the Resistivity-Porosity Method	18
3.4 Mineralogical Considerations	19
4 METHODS	21
4.1 General Description and Sampling	21
4.2 Permeability and Porosity Measurements	24
4.3 Laboratory Resistivity Measurements of Core	28
4.4 Image Analysis and Petrography	30

4.5 Mineralogy	32
4.6 Water Quality.....	34
5 RESULTS	35
5.1 Water Quality Sample Correlations.....	35
5.2 Mineralogy	36
5.3 Porosity and Permeability	44
5.4 Pore Geometry and Lithology	46
6 DISCUSSION	48
6.1 Pore Geometric Factors and Petrophysical Parameters	48
6.2 Porosity and Permeability and Relation to Well Logs.....	50
6.3 The Effects of Clays and Zeolites on Borehole Geophysical Logs.....	51
7 CONCLUSIONS.....	54
REFERENCES	55
APPENDICES	
A X-RAY DIFFRACTION DATA.....	60
B SIMILAR STUDIES IN THE FLORIDAN AQUIFER SYSTEM.....	62
C CORE PHOTOGRAPHS.....	67
D RESISTIVITY MEASUREMENTS	79
E PETROGRAPHY.....	87

LIST OF TABLES

	Page
Table 1: Pore geometric and petrophysical parameters for all samples.....	46

LIST OF FIGURES

	Page
Figure 1.1: Extent of the Floridan aquifer system.....	2
Figure 1.2: Site location of the Cockspur Island core hole and wells sampled for water quality	3
Figure 1.3: Well logs of the Cockspur Island core hole	4
Figure 1.4: Satellite image showing the Cockspur Island core hole and well sampled for water quality	5
Figure 2.1: Structural features affecting the Floridan aquifer system	8
Figure 2.2: Generalized stratigraphic column of the Floridan aquifer system	12
Figure 2.3: Regional hydrologic units of the Floridan aquifer system	15
Figure 4.1: Diagram showing methods used in this study.	22
Figure 4.2: Photographs depicting analytical instruments used in this study	23
Figure 4.3: Diagram of minipermeameter	24
Figure 4.4: Correlation of gas flow rate and permeability for PDPK and Hassler sleeve methods	25
Figure 4.5: Calibration between gas flow rate and permeability on low permeability standards.....	26
Figure 4.6: Calibration between gas flow rate and permeability on high permeability standards	26
Figure 4.7: Comparison of permeability measured from minipermeametry and conventional analysis	27
Figure 4.8: Complex impedance plot example.....	30
Figure 4.9: Photomicrograph of pore network modified by TSGui software	31
Figure 4.10: Graph showing DOMsize and its relation to the size equivalent diameter of pores	32
Figure 5.1: Box-and-whisker plots for water quality wells.	35
Figure 5.2: Calculated R_{w77} values from laboratory data.....	36
Figure 5.3: X-ray diffraction patterns for all samples, scaled to depth.....	38
Figure 5.4: Inset from Fig. 5.2.	39
Figure 5.5: Mineralogical changes with depth.....	40

Figure 5.6: X-ray diffraction patterns of air-dried and ethylene glycol solvated sedimented mounts	41
Figure 5.7: Model of mixed layering of illite and smectite using NEWMOD®	42
Figure 5.8: Laboratory porosities and resistivities compared with clay and zeolite mineral percentages ..	43
Figure 5.9: Standard deviation of permeability and laboratory derived porosity changes with depth	44
Figure 5.10: Resistivity and sonic porosity logs	45
Figure 5.11: Relationship between DOMsize, PoA, and cementation factor.....	47
Figure 6.1: Graph showing cementation factors calculated from this study and other similar studies.....	49
Figure 6.2: Vuggy porosity shown by ppl photomicrograph and digital photograph of core plug	51

LIST OF ABBREVIATIONS AND SYMBOLS

Ω	ohms		
ϕ	phase		
Φ	porosity		
$ Z $	magnitude		
Z'	real impedance		
Z''	imaginary impedance		
Z^*	complex impedance vector		
A	area		
a	tortuosity		
API	American Petroleum Institute		
atm	standard atmosphere		
BHT	bottom hole temperature	SPR	single point resistance
C	conductivity	STP	standard temperature and pressure
CEC	cation exchange capacity	TD	total depth
DI	deionized	X	reactance
DOMsize	dominant pore size	XRD	X-ray diffraction
F	formation factor		
FAS	Floridan aquifer system		
ft	feet		
GR	gamma-ray		
Hz	hertz		
K	permeability		
KPa	kilopascal		
L	inductance		
<i>m</i>	cementation factor		
m	meters		
mD	millidarcy		
μS	micro-Siemens		
ohm	ohms		
P	perimeter		
PoA	perimeter over area		
PDPK	pressure decay profile permeametry		
psi	pounds per square inch		
R	resistance		
R8	8 in normal resistivity		
R16	16 in normal resistivity		
R32	32 in normal resistivity		
R64	64 in normal resistivity		
R_o	resistivity of a water-filled formation		
R_{mf}	resistivity of the mud filtrate		
R_t	true formation resistivity		
R_w	pore-water resistivity		
R_{x_o}	resistivity of the flushed zone		
SP	spontaneous-potential		

CHAPTER 1
INTRODUCTION

1.1 Background

The Floridan aquifer system (FAS) is one of the most productive aquifers in the United States, and supplies potable water to large population centers in the southeast including Jacksonville, Daytona Beach, Tallahassee, and Orlando in Florida, and Savannah and Brunswick in Georgia (Johnson and Bush, 1988). Comprising a total area of approximately 100,000 square miles, this aquifer system underlies parts of Alabama, Georgia, South Carolina, Mississippi, and the entirety of Florida (Figure 1.1).

This system consists of Upper Paleocene to Lower Miocene limestone and dolomite rocks that are hydraulically connected in varying degrees. Typically the Floridan aquifer system consists of the Upper Floridan aquifer which is separated from the Lower Floridan aquifer by a confining unit.

The greatest amount of groundwater withdrawal is for irrigation purposes, followed by public supply, industrial, and domestic self-supply. In 2000 about 4,020 million gallons per day (Mgal/d) were withdrawn from the Floridan aquifer system (Berndt and Marella, 2005). However 90% of this withdrawal was from the Upper Floridan aquifer as opposed to the Lower Floridan aquifer due to high salinity and sulfate concentrations in the Lower Floridan aquifer and the increased cost of drilling wells with depth. A growing concern over saltwater intrusion in coastal areas such as Hilton Head, South Carolina and Brunswick, Georgia, along with intense withdrawals from the Upper Floridan aquifer, has caused limitations on pumping, and has created an interest in investigating alternative sources of groundwater, including the Lower Floridan aquifer.

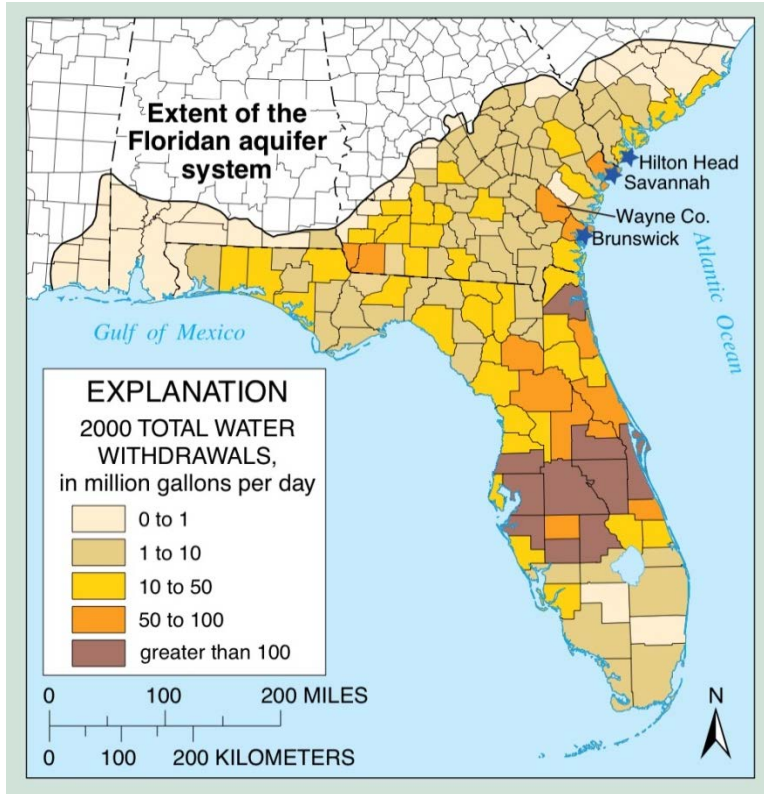


Figure 1.1 Extent of the Floridan aquifer system (modified from Marella and Berndt, 2005).

1.2. Purpose of Study

Part of a nationwide effort by the U.S. Geological Survey to map the saline aquifers in the United States is the Saline Aquifer Mapping Project of the Southeastern United States, which began in 2009 and investigates salinity variations in the Floridan aquifer system. This project utilizes borehole geophysical well logs from oil and gas and water wells, along with water quality data to calculate and map the salinity boundaries in the Floridan aquifer system.

Within the last 10 years several deep test well drilling projects have been completed for the purpose of further understanding the Lower Floridan aquifer and its potential for groundwater supply. One such deep test well, the Cockspur Island core hole (38Q237), located in Chatham County, Georgia (Figure 1.2), was cored to a total depth of 1,020ft in March 2010. The Cockspur Island core hole penetrates the Upper and Lower Floridan aquifer, along with the upper and middle confining unit. Several borehole geophysical

logs were run in this well, including gamma-ray (GR), spontaneous potential (SP), a suite of resistivity logs (SPR, R8, R16, R32, R64), and sonic porosity (Figure 1.3). Three nearby deep USGS wells (38Q002, 38Q004, 38Q196) provide water quality data at various depths in the aquifer (Figure 1.4). The Cockspur Island core hole is located near Savannah, Georgia, where the Floridan aquifer system is a major supplier of fresh water. Wells which are cored for their entire depth can provide very valuable mineralogical and petrophysical core data, which can be used to correlate with borehole geophysical logs, enabling for more accurate calculations of salinity from resistivity and porosity well logs.

The Cockspur Island core hole is located in an area where the sediments comprising the FAS have a significant siliciclastic component, which may involve an increase in clay minerals. The purpose of this study was to determine if and how the mineralogy of the rocks in this mixed carbonate siliciclastic environment affects the resistivity and sonic porosity well logs, and to determine if changes in the pore geometry of the various lithologies found in this core hole will affect petrophysical parameters such as the cementation factor. Similar previous studies have focused on the Floridan aquifer in South and Central Florida, which is composed only of carbonates, making this study critical to analyzing well logs in southeastern Georgia.

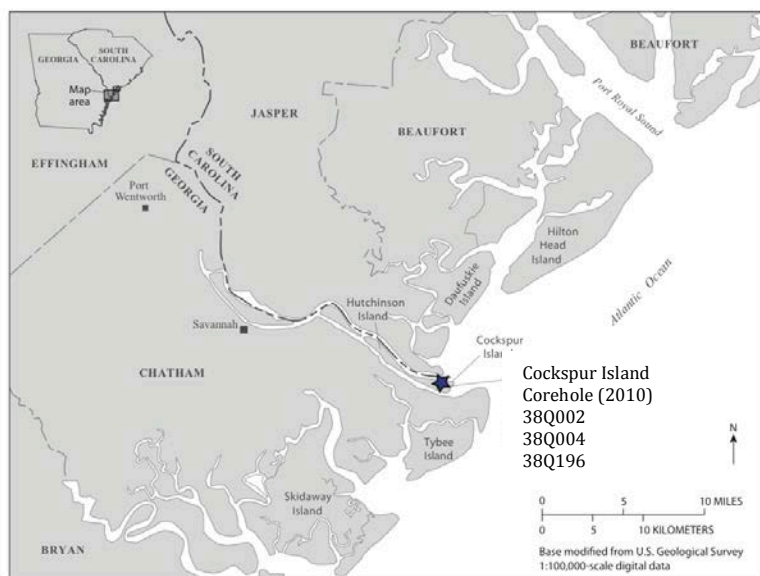


Figure 1.2 Site location of the Cockspur Island core hole and wells sampled for water quality (modified from Ostrowicki and Williams, 2011).

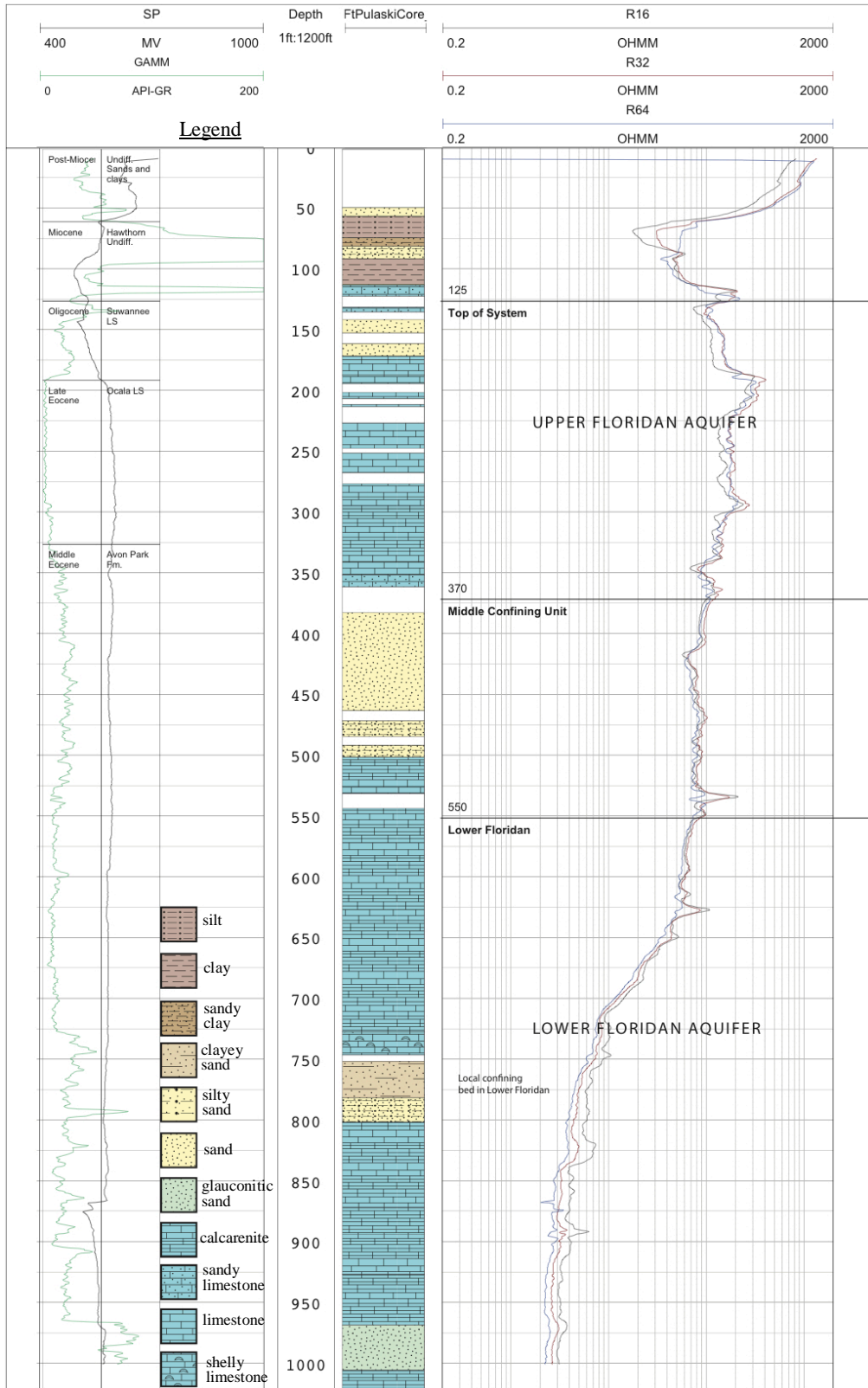


Figure 1.3 Well logs of the Cockspur Island core hole. Left track shows spontaneous potential (SP), and gamma ray (GR), and right track shows resistivity (R16, R32, R64). Lithological and hydrologic units with their ages are shown. (Figure produced by Lester J. Williams, USGS).



Figure 1.4 Satellite image showing the location of the Cockspur Island core hole (38Q237), and wells sampled for water quality (38Q002, 38Q004, 38Q196). Top of the image is North. See Fig. 1.2 for a broader-scale location.

1.3 Previous Studies Relating Borehole Well Logs to Salinity

Several other studies have related salinity changes in groundwater to borehole geophysical log response (Jorgenson and Petricola, 1994; Kwader, 1982; Reese 2000). Methods used to estimate water resistivity includes the cross-plot method, spontaneous-potential method, the microresistivity method, and the cementation-exponent method (Jorgenson and Petricola, 1994).

The cross-plot method assumes that there is a wide range of porosities for permeable zones with a constant resistivity. The sonic porosity log for the Cockspur Island core hole does not show substantial changes in porosity for similar resistivity values, therefore the cross-plot method is not an ideal method for calculating salinity in this well.

Although a spontaneous-potential (SP) log was run in the well being studied, there is a poor response, and no significant changes in the log with depth were recorded (Figure 1.3). There must be a large enough difference in salinity between the drilling fluid and the formation fluid to have a response in the SP log (Bowen, 1986; Keys, 1990), and this usually does not occur in the relatively fresh water of the Floridan aquifer system (less than 10,000 mg/L TDS). There also must be a shale layer and a clean sand layer to interpret the SP log, a condition not typically met in the formations which comprise the Floridan aquifer (Keys, 1990), therefore no methods utilizing the SP log were considered for this study.

In the micro-resistivity method, the following equation is used to calculate the resistivity of the pore water:

$$R_w \approx R_t R_{mf} / R_{xo} \quad [1]$$

where R_t is the true formation resistivity, R_{mf} is the resistivity of the mud filtrate, and R_{xo} is the resistivity of the flushed zone

The resistivity of the mud filtrate is not always recorded in oil and gas wells, and the resistivity of the flushed zone (R_{xo}) is typically determined from a microresistivity log, which is not always run in oil and gas and water wells in this area. Therefore there is not enough data for micro-resistivity method to be practical for use in the Saline Aquifer Mapping Project or this study.

Given the above limitations, the resistivity-porosity method is the optimal method to calculate salinity for the study area and for the Saline Aquifer Mapping Project. This method utilizes both a porosity and resistivity well log to determine the resistivity of the pore water. These logs are generally available for oil and gas, and water wells in the Floridan aquifer system. Both a sonic porosity and resistivity log were run in the Cockspur Island core hole.

CHAPTER 2
GEOLOGY OF THE FLORIDAN AQUIFER SYSTEM

2.1. Stratigraphy

Rocks in the Floridan aquifer system extend from the southern part of the Atlantic Coastal Plain, westward to the eastern part of the Gulf Coastal Plain, and southward into the Florida platform. These clastic and carbonate units are Paleocene to early Miocene age, and generally dip toward the Atlantic Ocean or Gulf of Mexico, except in local and sub-regional areas due to underlying structural features. Such features as the Southeast and Southwest Georgia Embayments can have major influences on the type and thicknesses of sediments deposited (Figure 2.1).

Coastal Plain sediments from the Fall Line southward towards the Gulf of Mexico and eastward towards the Atlantic Ocean are dominated by clastic rocks with minor amounts of limestone. Southeastern Georgia and the Floridan peninsula are underlain by a thick, continuous sequence of shallow-water platform carbonate rocks, and an interfingering between clastic and carbonate facies occurs in areas in north-central Floridan and Southeastern Georgia (Miller, 1986). In particular, the coastal areas of Georgia and South Carolina are underlain by a thick sequence of sand and clay, which ranges from unconsolidated to semi-consolidated, along with layers of limestone and dolostone (Williams and Gill, 2010). The stratigraphic nomenclature, ages, and hydrologic units used in this report are based upon those by Miller (1986) (Figure 2.2), although others have suggested different hydrologic and stratigraphic boundaries (Clarke et al, 1990, McCollum and Counts, 1964). Ages of sediments in the FAS are determined largely by assemblage of microfauna and not by lithologic changes. In this well the biostratigraphy, geophysical log response, and lithologic changes were used to identify the different formations and their age. The biostratigraphy of the Cockspur Island core hole was determined by the USGS and based on the zonation from Martini (1971).

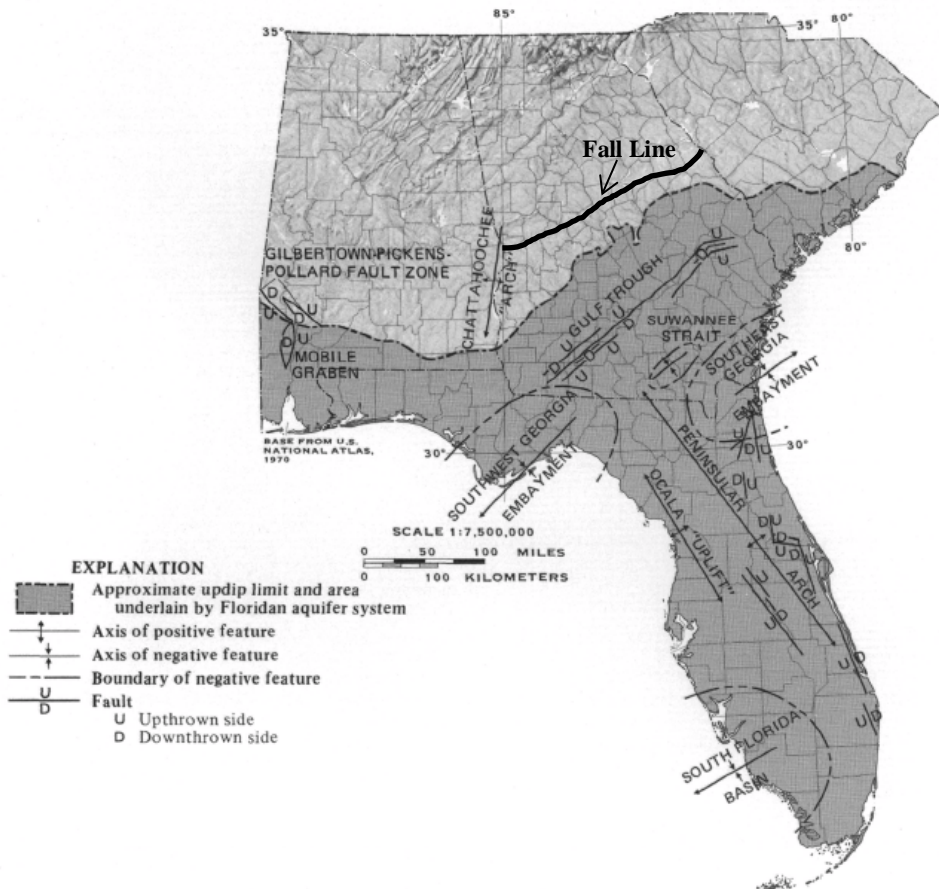


Figure 2.1 Structural features affecting the Floridan aquifer system (modified from Miller, 1986).

2.1.1 Middle Eocene

The Middle Eocene is present in the majority of the aquifer system, and is comprised of both carbonate and clastic facies. During the middle Eocene transgression of the sea was very extensive, and in the Savannah area sediments are clastic marine to marginal-marine. These sediments, known as the Avon Park Formation in the study area, were deposited in a shallow, warm-water carbonate bank, and this formation occurs throughout the Florida Peninsula, the eastern part of the Florida Panhandle, and South Georgia.

The Avon Park Formation is characterized by a sequence of predominantly brown variably fossiliferous limestone, which ranges from a grainstone to a wackestone, and rarely a mudstone. This unit is interbedded with dolomite that is crystalline, fossiliferous, and vuggy (Miller, 1986).

In most of the eastern part of the Florida peninsula and in southeastern Georgia, including the study area, this formation is comprised of a micritic finely pelletal limestone, which has a very low permeability. This formation grades into an argillaceous, moderately indurated micritic and glauconitic limestone to the north and west, which then grades into a calcareous, glauconitic sand and clay beds updip. In west-central peninsular Florida, the Avon Park Formation consists of gypsiferous limestone and dolomite. Around the study area, the thickness of this formation can reach up to 1,000 ft.

2.1.2 Upper Eocene

Upper Eocene rocks represent the most widespread transgression in the Southeastern United States during the Tertiary. This unit is comprised of carbonates everywhere but western Alabama and the Florida panhandle, where clastic sediments dominate, and in some updip outcropped areas, where mixing with clastics has occurred.

The Ocala Limestone is the upper Eocene stratum found in coastal areas of Georgia, and the depositional environment of this unit was in warm, shallow, and clear marine waters on a carbonate bank similar to the current Bahama Banks. These rocks are highly permeable and the upper part of the Ocala is a white, friable coquina, with bryozoan, foraminifera, and echinoid fossils. The basal layer of the Ocala is a white micritic limestone with foraminifera fossils, and is locally glauconitic in Georgia. In the counties to the north-west of Chatham, a clastic component increases. The Ocala Limestone unconformably overlies the Avon Park Formation.

2.1.3 Oligocene

Rocks of Oligocene age are predominantly carbonate, with clastic components in southwestern Alabama, the western part of the Florida panhandle, and areas of northeastern Georgia and southwestern

South Carolina. In the study area, Oligocene aged deposits are known as the Suwannee Limestone, and the depositional environment is a carbonate bank. The lithology of this unit is either a tan crystalline and vuggy limestone with abundant gastropod and pelecypod casts and molds, or a white pelletal, and sometimes micritic limestone with foraminifera, and is characterized by an absence of particulate phosphate. These two rock types can be interbedded with each other, and the latter rock type is dominant in most of Georgia and the eastern panhandle of Florida. The maximum thickness of the Suwannee Limestone is approximately 120 ft.

2.1.4 Miocene

Sediments from the Miocene are mostly clastic, however the Tampa Formation is characterized as a sandy limestone, and the Hawthorn Formation may have beds of dolomite in the lower section. The entire Floridan aquifer is overlain by Miocene aged rocks excluding northwestern peninsular Florida, where erosion has removed this unit. This time period is marked by an influx of clastic sediments, and changing chemical conditions of the Miocene ocean caused phosphatic and siliceous sediments to be deposited. The depositional environment during the Miocene in this area was inner to middle-shelf, and the sea during this time was colder than older Cenozoic epochs (Miller, 1986).

The Hawthorn Formation is the thickest and most extensive Miocene formation in the Southeastern United States, and is found in Peninsular Florida and southern Georgia and South Carolina. This formation is a sequence of complexly interbedded clay, silt, and sand, with phosphatic dolomite or dolomitic limestone common in the lower section. Three distinct units, which are each bounded above and below by an unconformity, compose the Hawthorn Formation: a lower carbonate layer, a middle clay layer, and an upper sand layer. In coastal Georgia this formation can range from 65-335ft thick.

2.1.5 Post-Miocene

Sediments which are Pliocene, Pleistocene, and Holocene aged are described as undifferentiated post-Miocene, because of a lack of geophysical, lithologic, and paleontological data. The Pliocene deposits

generally have marine characteristics, and consist of a locally micaceous and phosphatic clay. Terrace deposits of sand and gravel interbedded with clay were laid down during the Pleistocene, and during the Holocene fluvial and residual beds of sand and gravel were deposited.

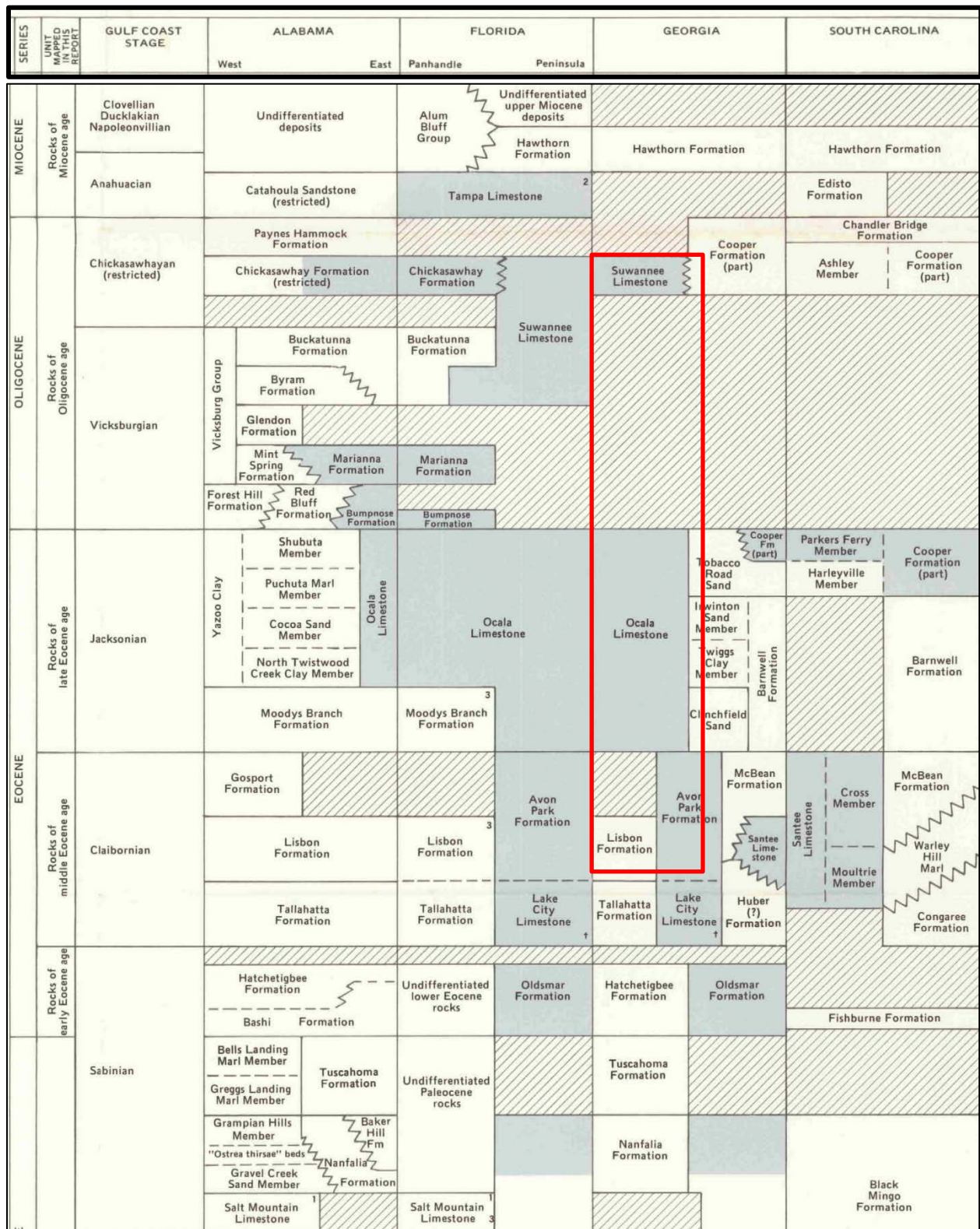


Figure 2.2 Generalized stratigraphic column of the Floridan aquifer system (Johnston and Bush, 1988). Blue denotes formations which comprise the Floridan aquifer system. Outlined in red are the formations which were sampled in this study.

2.2 Occurrence of Zeolites and Glauconite in the Floridan Aquifer System

The zeolite clinoptilolite has been previously found to occur as an extremely fine-grained aggregate in rocks that make up the Floridan aquifer system (Heron and Johnston, 1966; Weaver and Beck, 1977, Switzer and Boucot, 1955). Clinoptilolite was found in the Suwannee Limestone and the Eocene Santee Limestone in the Florida Panhandle (Switzer and Boucot, 1955) and in the Hawthorn Formation in coastal South Carolina (Heron and Johnson, 1966). It has been shown that in saline water, a reaction can occur with palygorskite that results in the formation of clinoptilolite, with clinoptilolite being favored in water with a relatively low pH and H_4SiO_4 concentration, and a high ratio of $[\text{Mg}^{2+}]/[\text{Na}^+]$ (Weaver and Beck, 1977). Heron and Johnson (1966) suggest the clinoptilolite found in the Santee Limestone and Hawthorn Formation in coastal South Carolina are an alteration product of volcanic ash. Newer studies in Miocene carbonate sediments of the Bahamas platform attribute the formation of clinoptilolite to the dissolution of biogenic silica and reaction with smectite (Karpoff et al., 2007).

Glauconite, which occurs in Middle Miocene rocks in this area, is found in almost exclusively marine environments, and can be detrital or authigenic. This mineral generally forms in suboxic conditions when there is a high supply of iron, and a low sediment influx (McRae, 1972).

2.3 Hydrogeology

The Floridan aquifer system is segregated based on changes in permeability and these boundaries typically but do not always correspond with geologic formation boundaries, time-stratigraphic breaks, or lithologic changes. The different layers are more or less vertically continuous sequence of carbonate rocks which are connected hydraulically in varying degrees based mostly on the mineralogy and texture of the rocks. The different units in this aquifer system are so variable in permeability, porosity, and lithology because the depositional environments change drastically throughout the area, diagenetic changes occurred after the rocks were deposited, and karst features caused by the dissolution of limestone have developed in local areas (Miller, 1986).

The Floridan aquifer system ranges from confined to semi-confined to unconfined depending on whether the Middle Miocene or younger aged rocks, which make up the upper confining unit, have been eroded. Generally this system is made up of an upper confining unit, the Upper Floridan aquifer, a middle confining unit, and the Lower Floridan aquifer. The upper confining unit retards the vertical movement of groundwater in the surficial aquifer based upon how thick this unit is and the amount of clay and low permeability rocks within the unit. The middle confining unit may be non-existent to leaky to virtually impermeable depending upon the lithology of the unit (Figure 2.3). When there is not a low permeability layer, the Upper and Lower Floridan aquifers merge.

Above the Floridan aquifer system exists an unconfined aquifer, which is a permeable layer of mostly unconsolidated to poorly consolidated clastic rocks, and can be highly productive in certain areas such as the Biscayne Aquifer in South Florida. Since the water quality in these aquifers is understood fairly well, the surficial aquifer is not addressed in this study.

The upper confining unit, where present, includes upper and middle-Miocene sediments. These beds have a low permeability and contain a high amount of phosphatic sand, clay, and sandy clay. In the study area, the Hawthorn Formation comprises most of this upper confining unit. The Oligocene aged Suwannee Limestone is part of the Upper Floridan aquifer along with the Late Eocene aged Ocala Limestone, which is one of the most permeable formations in the Floridan aquifer system. The upper Middle Eocene aged Avon Park formation, which is a low permeability micritic and glauconitic limestone, comprises the lower confining unit and the Lower Floridan aquifer.

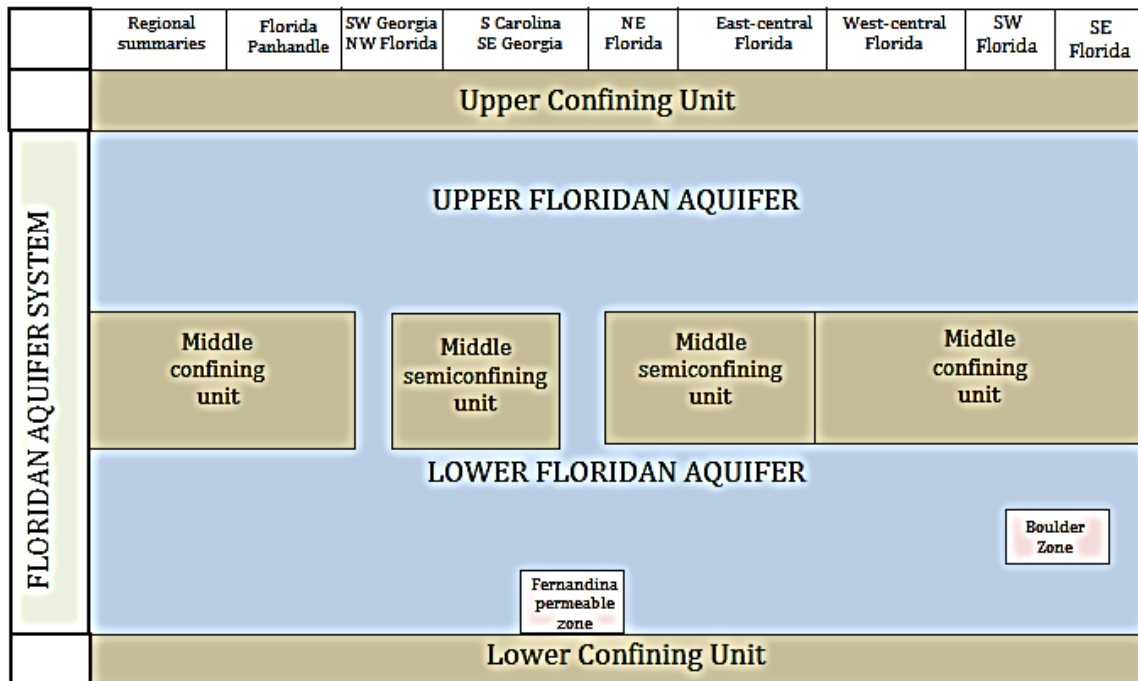


Figure 2.3 Regional hydrologic units of the Floridan Aquifer System (modified from Miller, 1986).

CHAPTER 3
PETROPHYSICS OF CARBONATES

3.1 Principles of Borehole Resistivity Logs

The borehole electrical resistivity log is an important tool to the petroleum industry and for hydrologic applications; the electrical log can aid in determining lithology and nature of the pore-fluid in sedimentary rocks, and for qualitatively estimating permeability. The 4 electrode resistivity tool run in this study includes normal resistivity with spacings of 8, 16, 32, and 64-inches (R8, R16, R32, R64) and single-point resistance (SPR). Increased spacing corresponds to resistivity measurements taken further away from the borehole (Asquith and Krygowski, 2004). The precision of this tool is 1%, and the user defined sampling interval was every 0.33 ft.

Since the matrix of sedimentary rocks is generally a poor conductor, the electrical current is conducted by the pore-water fluid. In the case of this study the pore-water fluid is a brine dominated by sodium chloride. Therefore, the shape, connectivity, and size of the pores and pore throats in the rock are the main influence of electrical conductivity if conductive minerals are not present.

Archie's law relates the resistivity of brine-saturated rocks to the resistivity of the pore-water as follows (Archie, 1942):

$$F=R_o/R_w \quad [2]$$

Where F is the formation factor, R_o is the resistivity of the water saturated formation, and R_w is the resistivity of the water in the formation.

A 64-inch spacing is usually accepted as the minimum electrode spacing required to measure the true resistivity of the formation with no borehole effects (Lindner-Lunsford and Bruce, 1995), therefore values from the R64 log were taken as R_o .

The formation factor of a non-shaley, carbonate, water saturated formation is also related to the porosity and cementation factor of that formation by the following equation (Archie, 1942):

$$F = \Phi^{-m} \quad [3]$$

Where Φ is the porosity (fraction) and m is the cementation factor.

3.2 Principles of Gamma-Ray and Sonic Borehole Logs

The gamma-ray (GR) tool measures the natural radioactivity of rocks adjacent to the borehole in American Petroleum Institute units (API), and is calibrated based on a permanent calibration facility at the University of Houston (American Petroleum Institute, 1959). The most common elements which emit gamma-rays in rocks are thorium, uranium, and potassium. As gamma radiation increases the curve deflects to the right, and generally this correlates to an increase in clays and shales (Asquith and Krygowski, 2004). There are a few instances of radioactive dolomites, sands, and limestones due to a high uranium content. Feldspathic, glauconitic, and micaceous rocks can also exhibit high gamma-ray values due to high potassium content, and phosphatic rocks can have high gamma-ray values due to high uranium content. However, clean sands and carbonates typically display levels of radioactivity from 15 to 20 API and shales and clays display levels from 120 to 240 API units (Asquith and Krygowski, 2004). The user defined sampling interval for the gamma-ray tool run in well 38Q237 was every 0.33ft.

The fullwave form sonic tool measures compressional, refracted shear, and Stoneley wave properties. During logging a sound wave is emitted from the tool and it travels through the formation and back to the receiver. The instrument measures the transit time of these waves in $\mu\text{S}/\text{ft}$. The precision of the fullwave form sonic instrument is 1% and the resolution is less than $1\mu\text{S}/\text{ft}$.

The transit time (Δt) of compressional waves, and the lithology and porosity of a fluid filled rock are related by the time-average relationship. This relationship is the most accurate in consolidated rocks, and decreases with poorly consolidated and shaly rocks. The most common way sonic log travel times can be converted to porosity is the Wyllie time-average equation (Wyllie et al., 1958), which is as follows:

$$\Phi_s = \frac{\Delta t_{\log} - \Delta t_{ma}}{\Delta t_{fl} - \Delta t_{ma}} \quad [4]$$

Where Φ_s is the sonic-derived porosity, Δt_{\log} is the interval transit time in the formation, Δt_{ma} is the interval transit time in the formation, and Δt_{fl} is the interval transit time in the fluid in the formation. The Δt_{ma} was assumed to be 47.6 $\mu\text{sec}/\text{ft}$ based on a pure limestone with intergranular porosity, and the Δt_{fl} was assumed to be 185 $\mu\text{sec}/\text{ft}$ based on a freshwater mud filtrate (Asquith and Krygowski, 2004).

3.3 Application of the Resistivity-Porosity Method

The most applicable method for calculating the resistivity of the pore fluid in this test well and other wells in the Saline Aquifer Mapping Project of the Southeastern United States is the resistivity-porosity method. To obtain cementation and formation factors, laboratory resistivity measurements can be made on core by saturating the core with a brine with a known resistivity, and measuring the resistance of the rock saturated with the brine at various frequencies (Tiab and Donaldson, 2004).

The cementation factor, also known as Archie shape factor and the cementation exponent, varies greatly based on the shape and size of the grains and pores, the lithological and mineral composition of the rock, and the types of pores (Salem and Chilingarian, 1999). It can also vary to a lesser extent based on specific surface area, anisotropy, tortuosity, and compaction or overburden pressure.

The cementation factor can vary greatly between different types of rocks, and even different types of carbonates, but values usually fall between 1.3 and 3.0. For example, it has been shown that m is 1.09 for porous dolomites, between 1.2 to 1.3 for fractured limestones, and between 1.8 to 3.0 for compacted limestones (Salem and Chilingarian, 1999, Asquith and Krygowski, 2004, Verwer et al., 2011). When clay minerals are present, the cementation factor can be even higher. The cementation factor has been shown to be 2.11 for illite, 2.70 for calcium montmorillonite, and 3.28 for sodium montmorillonite (Salem and Chilingarian, 1999).

3.4 Mineralogical Considerations

Smectite, illite, and glauconite are clay minerals, or hydrous aluminum phyllosilicates comprised of silica tetrahedral sheets and aluminum octahedral sheets. Smectite and illite are 2:1 clay minerals, and their structures are composed of repetitions of one octahedral sheet in between two tetrahedral sheets, with smectite being an expandable clay mineral. Glauconite is an Fe bearing mica, but can be classified as a 2:1 clay mineral. The interlayer space in the structure of these minerals can contain water and cations. Smectite has a high surface area per unit volume and usually has a higher cation exchange capacity (CEC) than non-expandable clays such as illite and glauconite (Erickson and Jarrard, 1999; Zorski et al., 2011).

Smectite can increase the electrical conductivity of a rock because it can act as an electrolytic conductor. The positive cations between and on the edges of the negatively charged clay structure are much more abundant than the ions in normal salt water, therefore the clay can provide a continuously conductive pathway through the rock if the clay is continuously bedded and not interspersed in the rock (Wyllie, 1963). Glauconite and illite typically do not contribute to the electrical conductivity of the rock because they have significantly lower CEC's than smectite.

Clinoptilolite, which is silica rich member of the heulandite group, is the most abundant authigenic zeolite mineral which occurs in sedimentary rocks (Sheppard, 1971). This hydrated aluminosilicate consists of many channels and cages filled with water and exchangeable cations (Reynolds and Williford, 1990). The CEC of clinoptilolite can be much higher than the majority of clay minerals, however previous studies have shown that in relatively fresh water and low temperatures the ions associated are not available for electrical conduction (Carroll, 1990). Clinoptilolite also rarely forms continuous networks, unlike clays, decreasing the rock's potential to conduct electrical current (Ijima, 2001)

Archie's equation [3] assumes that there are little to no conductive minerals in the system and that the rock containing the pore fluid is highly resistive. To account for conductive minerals, the Waxman-Smiths equation (Waxman and Smits, 1968) can be used. This equation quantifies the contributions of pore and clay conduction (C_t) using laboratory methods, and is as follows:

$$C_t = \Phi^m (C_w + BQ) / a \quad [5]$$

Where C_w is the electrical conductivity of the free pore water, B is counterion conductivity, Q is the cation exchange capacity (CEC) per unit pore volume, and a is the tortuosity.

CHAPTER 4

METHODS

4.1 General Description and Sampling

Samples representing various petrophysical properties and lithologies were selected from the 1,020 feet of core using resistivity, sonic, and gamma-ray borehole geophysical logs and from field core descriptions (see Appendix C for core photographs). The rocks primarily ranged from well consolidated to semi-consolidated limestones. Poorly consolidated rocks were not sampled because they would not be able to withstand the core plug extractions and/or the multiple saturations needed for the laboratory resistivity measurements. Geologic heterogeneity within each lithology sampled was addressed by sampling core that was visually homogeneous. A total of twenty-one 2.5” core samples were collected, and ~1” right angle cylinder core plugs were drilled perpendicular to the core axis and parallel to bedding planes, for each whole core sample, with exception to sample CI-977 which was sampled parallel to the core axis due to the friable nature of the sample (Figure 4.1; Figure 4.2E). Samples were labeled based on depth in feet.

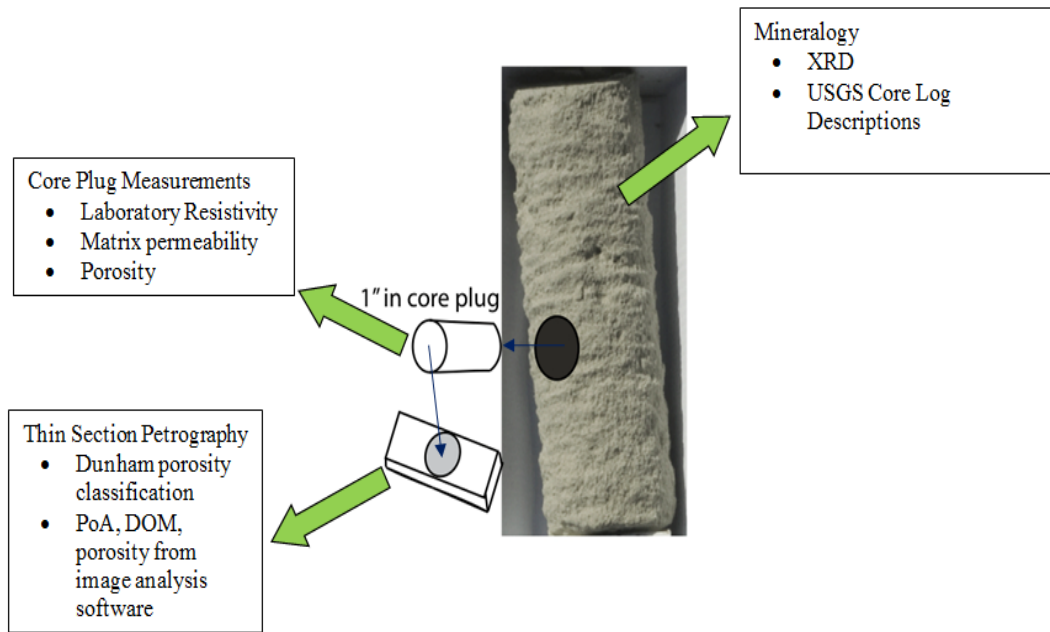


Figure 4.1 Diagram showing the methods used in this study.

Each core plug end was smoothed using a trim saw for minipermeameter and laboratory resistivity measurements, with attention paid to not leaving any saw markings, as described by Hurst and Goggin (1993), Sutherland et al.(1993), and Roberts and Lin (1997). Thin sections were prepared from the most homogeneous and representative end of each core plug (Figure 4.1). In addition to laboratory resistivity and permeability measurements, porosity, image analysis of thin sections, and X-ray diffraction (XRD) was performed.

The specific conductance of water quality samples from wells 38Q002, 38Q004, and 38Q196 was obtained from the U.S. Geological Survey National Water Information System Database, and compared to conductance calculated using the formation factors and cementation factors found in this study.

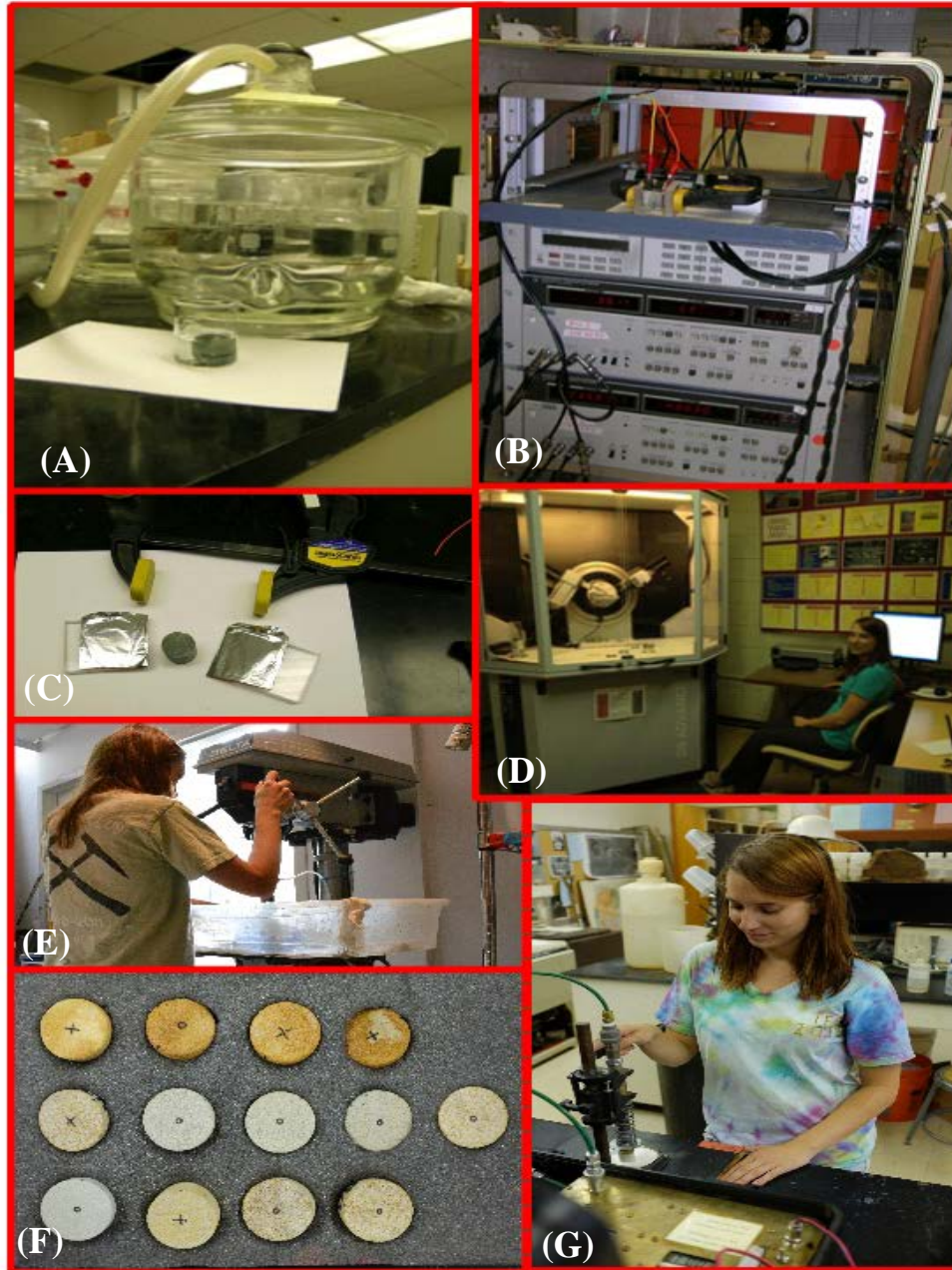


Figure 4.2. Photographs depicting analytical instruments used in this study: (A) Saturation of samples with saline water using a vacuum seal; (B) DC resistance measured using Hewlett LCR meters at the USGS Denver Federal Center Petrophysics Laboratory; (C) Set-up of tin foil, rubber, and plastic placed on the ends of the core plugs for resistance measurements; (D) Katrina Ostrowicki running samples on a Bruker D8 X-Ray Diffractometer at the UGA Geology Department; (E) Katrina Ostrowicki cutting 1-in core plugs from whole core samples using a water based saw at Dan Bulger's laboratory in Atlanta, GA; (F) Sandstone core plug standards used for minipermeameter measurements; (G) Katrina Ostrowicki measuring permeability using a mini-permeameter at the UGA Geology Department.

4.2 Permeability and Porosity Measurements

Matrix permeability was measured in millidarcys (mD) using a N_2 gas portable minipermeameter designed by the University of Colorado, and described by Goggin (1993), Sutherland et al. (1993), and Hurst and Goggin (1995) (Figure 4.3). To prepare the samples for these measurements and to ensure no drilling mud was left in the pores, each plug was cleaned with DI water and oven dried, following the procedures from Sutherland et al. (1993). A probe with an inner diameter (D_i) of $\frac{1}{4}$ in and an outer diameter (D_o) of $\frac{7}{16}$ in was lowered to each flat core plug face by a lever, attaining a uniform seal pressure on each sample (Figure 4.2G). The injection pressure was monitored using a pressure transducer with an precision of ± 0.1 psi (0.6895 kPa), and recorded manually. Measurements were made using 1.25 atm above ambient pressure for the higher permeability rocks (244 mD-off scale) and 2 atm above ambient pressure for the lower permeability rocks (12-167 mD); values were recorded after flow rates became stable and reached a steady state.

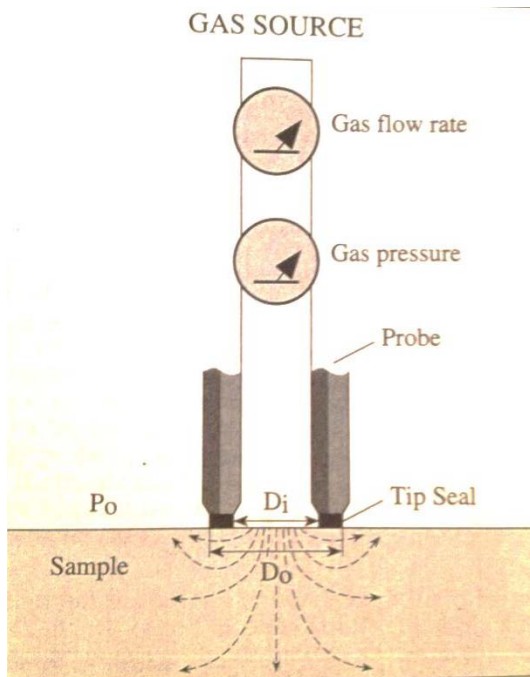


Figure 4.3. Diagram of minipermeameter (Hurst and Goggin, 1995)

It has been found that permeability on an entire plug generally matches well with the geometric mean of many minipermeameter spot analyses, but not with a single spot (personal communication with David Budd). In this study, five equally spaced measurements were taken on a face of each core plug and averaged together to obtain geometric mean k values. These permeability measurements represent matrix permeability (Budd, 2001). Vugs or molds which are larger than the diameter of the probe tip, and which contribute to the overall permeability of the rock, will not be accurately measured by a minipermeameter.

PDPK (pressure decay profile permeametry) gas permeability measurements show the best correlation between gas flow rate and permeability, as opposed to standard liquid permeability measurements such as Hassler-sleeve (Figure 4.4) (Budd, 2001). Thirteen low to high permeability sandstone 1" core plugs were used as standards (Figure 4.2F), and PDPK steady state measurements were performed on each standard using a 400 Pressure Decay Profile Permeameter of the standards by Core Laboratory Instruments in Houston, TX. K_{air} values were converted to liquid permeability values, using a Klinkenberg correction to account for the Klinkenberg gas-slippage effect (Klinkenberg, 1941). Flow rates of the sandstone standards were measured twice in between the low and high permeability samples, and a linear regression analysis was used on the measured flow rates and the Klinkenberg permeabilities reported by Core Laboratories (Figure 4.5 and Figure 4.6). The equations of the regression lines were used to calculate Klinkenberg permeabilities for all samples. Conventional liquid core plug permeability measurements correlate well with minipermeameter measurements (Figure 4.7).

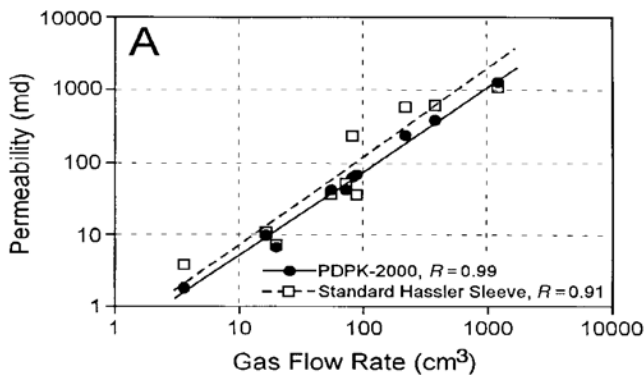


Figure 4.4 Correlation of gas flow rate and permeability for PDPK gas permeability, and standard Hassler sleeve liquid permeability methods. PDPK measurements show a better correlation between permeability and gas flow rate (Budd, 2001).

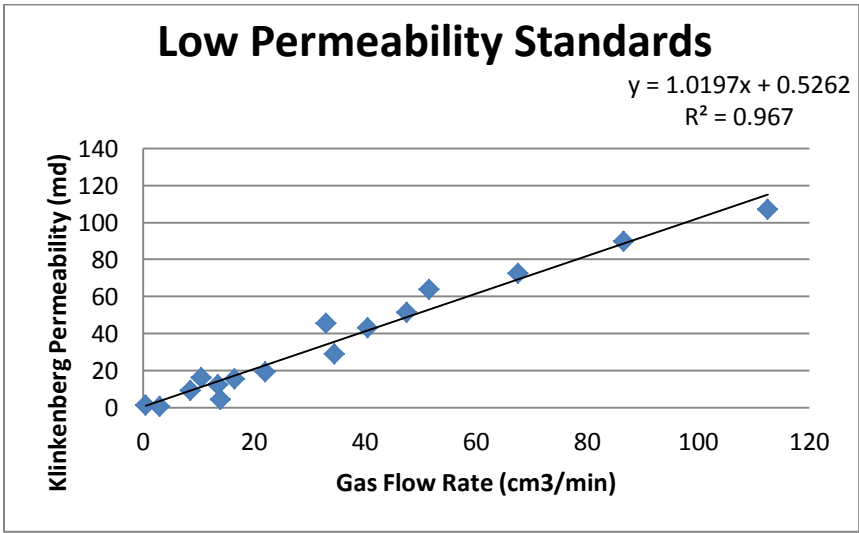


Figure 4.5 Empirical calibration between gas flow rate and Klinkenberg permeability on low permeability standards.

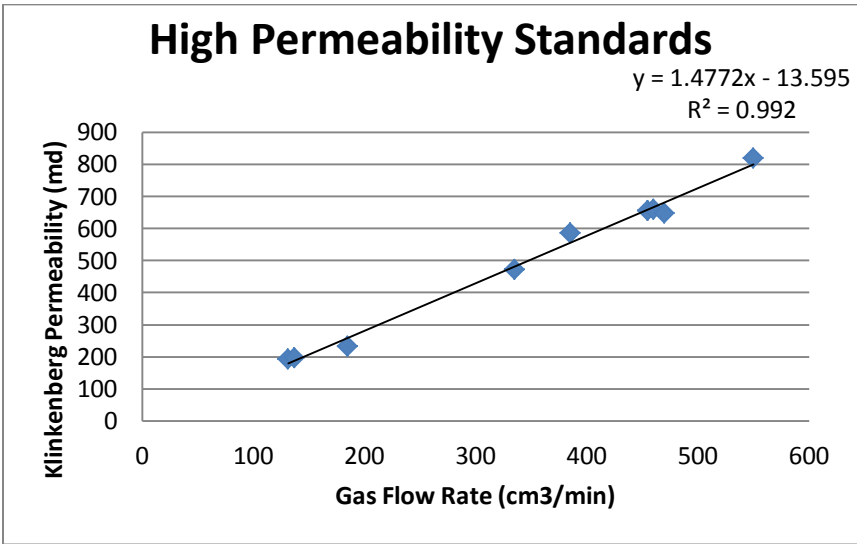


Figure 4.6 Empirical calibration between gas flow rate and Klinkenberg permeability on high permeability standards.

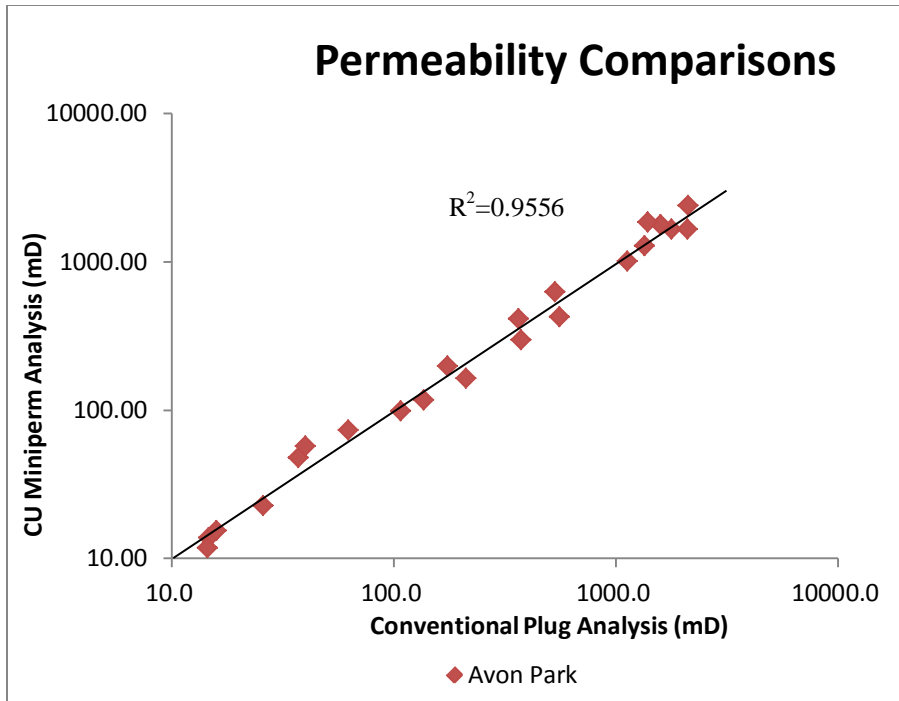


Figure 4.7 Comparison of permeability measured from minipermeametry and conventional liquid permeability measurements of 22 samples from the Avon Park Formation in Gulf Hammock, Florida (provided by David Budd). 1:1 line is shown.

Each sample was oven dried and weighed after no more water weight loss was observed, prior to the laboratory resistivity measurements. The plugs were weighed after each brine solution saturation, and the sediment left in the beaker was weighed and added to the saturated plug weight. The differences between the dry and saturated weights were calculated as the total volume of water in the pore spaces. The volume of each core plug was determined using a caliper tool, and the porosity of each sample was calculated with the following equation:

$$\Phi = \frac{\text{sat wt} - (\text{dry wt} + \text{sediment left in beaker})}{\text{volume of rock}} \quad [6]$$

Porosities were calculated for each of the three saturations, and the average of these was used as the porosity in this study.

4.3 Laboratory Resistivity Measurements of Core

The electrical properties of each sample were investigated over a mid-frequency range of 100 hertz (Hz) to 10 megahertz (MHz) at the USGS Petrophysical Laboratory at the Denver Federal Center. Operating frequencies of borehole resistivity tools typically fall within this range. The two-electrode complex electrical impedance was measured by two Hewlett Packard LCR meters (inductance (L), capacitance (C), and resistance (R)), which measured two overlapping frequency ranges (Figure 4.2B). A HP4274A meter recorded the lower frequency range (100 Hz and 100kHz) and a HP4275A meter recorded the higher frequency range (10kHz and 10 MHz). The LCR meters are computer controlled using an unpublished USGS program written in LabView and this program reads the data via an IEEE interface.

The reported resistance and impedance measurement errors range from $\pm 0.1\%$ to $\pm 3\%$. Typically, the lower errors are the lower frequency and low resistance measurements ($\pm 0.1\%$ to 0.3%), whereas the highest errors are the high frequency and high resistance (approximately $\pm 1\%$ to 3%).

Before the resistivity measurements were taken, each core plug was saturated with DI water and put under a vacuum seal for 24 hours to clean the samples. The samples were placed into 50 mL beakers and consecutively vacuum saturated with 3 separate brine solutions for approximately 4 hours (Figure 4.2A). The three brine solutions contained 100 mg, 1,000 mg, and 10,000 mg of NaCl per kilogram of distilled water, with conductivities of 210 $\mu\text{S/cm}$, 1,980 $\mu\text{S/cm}$, and 17,200 $\mu\text{S/cm}$, respectively. The brine compositions reflect the composition of the water samples taken from three nearby wells (38Q002, 38Q004, and 38Q196). The major cation and anion in the water samples collected at nearby wells were Na and Cl respectively, and the conductivities at the three sampled intervals were similar to the solutions prepared in the lab.

The conductivity of the brine was measured using a Horiba B-173 compact twin conductivity meter and the pH was measured using a Horiba B-213 pH meter at standard room temperature and pressure.

The conductivity and pH of the brine left in the beakers was recorded following each vacuum saturation, and this value was used as R_w in the porosity-exponent method.

Two pieces of insulating material covered with aluminum foil were put on each end of the saturated core plug to make good contact with the sample. Pieces of plastic were placed on the ends and kept together using a quick-grip mini bar clamp (Figure 4.2C). The electrodes were clamped onto the aluminum foil, and the inductance, capacitance, and resistance was measured.

Impedance is the total opposition to current in response to an AC applied voltage. Impedance is a complex quantity and can be expressed as a magnitude and phase ($|Z|, \phi$), as a real and imaginary component (Z', Z''), or as resistance and capacitance (R,C). The real and imaginary components can be calculated at a given frequency from the measured quantities $|Z|$ and ϕ as given by

$$Z' = |Z| \cos \phi \quad [7]$$

$$Z'' = |Z| \sin \phi \quad [8]$$

Where $|Z|$ is the impedance and ϕ is the phase angle. The real part of the complex impedance (Z') is the resistance (R), and the imaginary part of the complex impedance (Z'') is the reactance (X).

One commonly used method for analyzing the electrical response of porous rocks containing pore fluids is the use of complex plane plots. In this method the real versus the imaginary component of some complex electrical quantity is plotted for a wide range of frequencies. The complex planes generally used are the complex dielectric constant, the complex admittance, and the complex impedance. The physical nature of the system dictates which complex plane should be used (Jonscher, 1975). An inhomogeneous system consisting of a conducting bulk layer in series with an insulating barrier layer characterizes the system in this study, and in this situation a complex impedance (Z^*) plane is used to plot the data. In a complex impedance plot the reactance or the imaginary part of the impedance (-X) is plotted against the resistance or the real part (R). The plot can be divided into a semicircular arc (with the center below the real axis), which is the high frequency response, and a straight line (Figure 4.8), which is the low frequency response. The semicircular arc represents the bulk sample response, the inclined straight line

represents polarization at the sample-electrode interface, and the frequency separating the linear response and the semicircular response is f_o . The bulk sample resistance is the resistance at f_o (Knight and Nur, 1987; Raistrick et al., 1976; Denicol and Jing, 1998). The resistance of each sample was multiplied by a geometric factor (GF) to obtain resistivity.

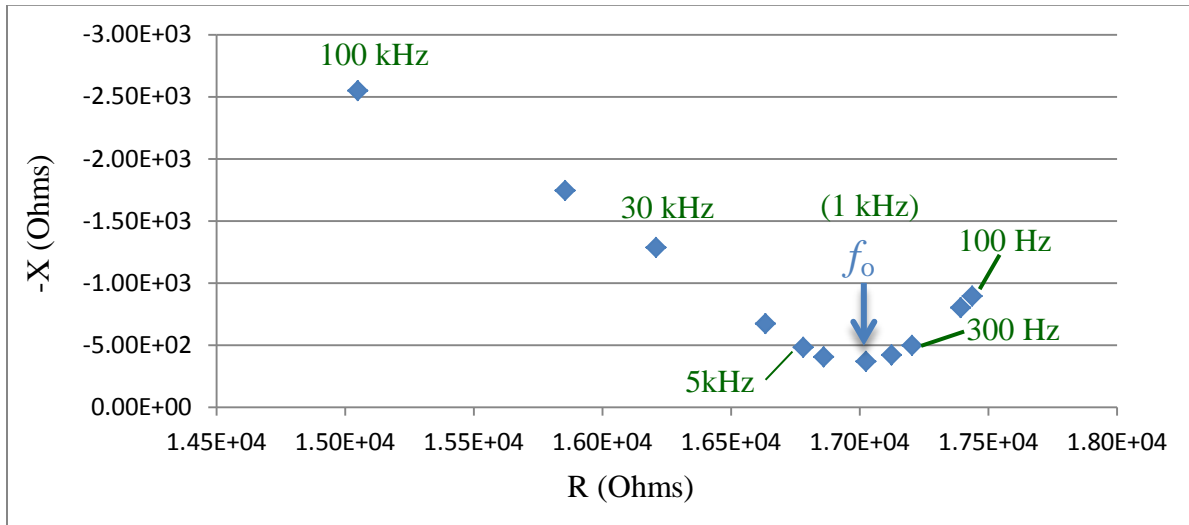


Figure 4.8 Complex impedance plot example.

4.4 Image Analysis and Petrography

Thin sections were prepared by Quality Thin Sections, and thin section blanks were impregnated with blue epoxy to aid in visual identification of pore space, and stained with alizarin red to determine between dolomite and calcite as detailed in Swanson (1981). Photomicrographs using digital cameras and optical light microscopes have been used in several other studies to investigate sandstone and carbonate pore networks by differentiating background from pores using manual selection to automated thresholding procedures (Crabtree et al. 1984, Ehrlich et al. 1991, Van den Berg et al, 2002, and Verwer et al., 2011). In this study photographs of thin sections were taken using a Leitz petrographic microscope with an attached SPOT idea microscope camera and a 2.5x Zeiss objective lens, and analyzed using TSgui Digital Image Analysis Software developed by the University of Miami Comparative Sedimentology Laboratory. Pore space was classified as any space with a blue color in plain polarized light. Carbonates often have

completely disconnected vugs and molds and epoxy resin does not always penetrate all pore space area in a thin section, therefore cross-polarized light images rotated to 0°, 20°, and 40° were also used in determining pore space. A threshold of pore space was set manually based upon visual examination of each thin section, and 4 adjacent photos representative of each sample were stitched together to enable the analysis of a larger more representative area.

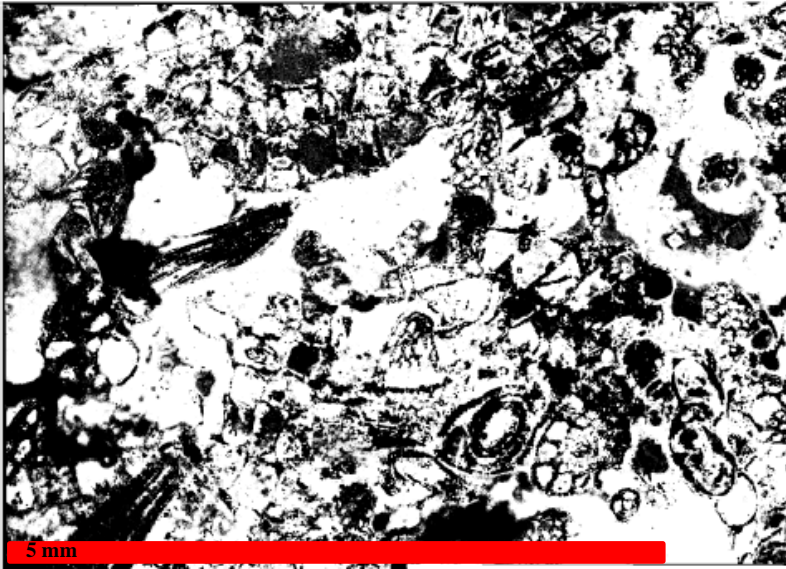


Figure 4.9 Photomicrograph of pore network modified by TSGui software. Manual thresholds were used for determining between pore space (white) and background (black).

Several different parameters were used to quantify the pore shape of each sample. The perimeter over pore space area (PoA), dominant pore size (DOM), and porosity were calculated for each sample using the TSGui software. The PoA is defined as the ratio of the sum of the perimeters of the pores identified on the thin section and the area of all of the pores analyzed as shown by the following equation:

$$PoA = \frac{\sum P}{\sum A} \quad [9]$$

Where P is the perimeter of all pores identified on a thin section and A is the area of all pores identified on a thin section.

This parameter describes the complexity and complicated nature of the enclosure of the pore system, regardless of the total porosity. The DOMsize is the maximum size of pores needed to occupy half of the pore space on a given thin section (Figure 4.10).

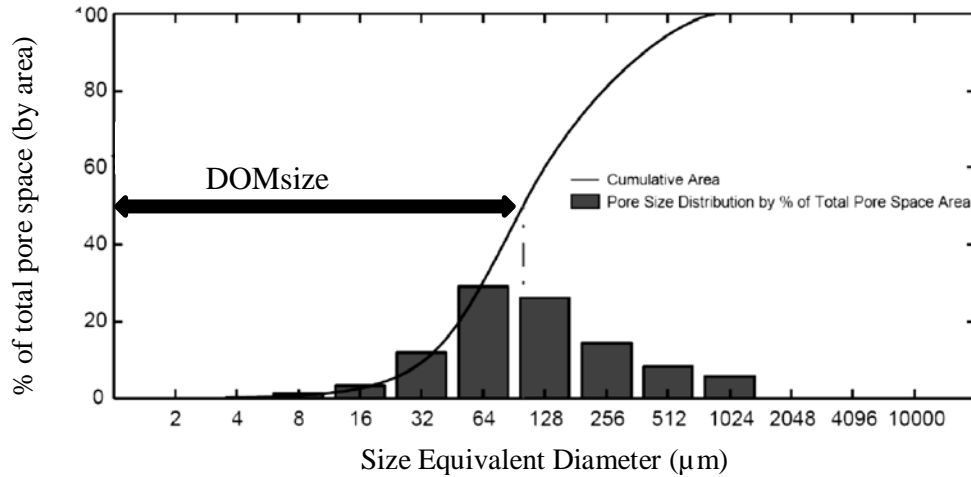


Figure 4.10 Graph showing DOMsize and its relation to the size equivalent diameter of pores. Modified from University of Miami Comparative Sedimentary Laboratory (2010)

The carbonate depositional texture of each sample was classified based on the using the Dunham classification (Dunham, 1962). Fabric and non-fabric selective porosity types for each sample were based on the Choquette and Pray (1970) carbonate porosity classification.

4.5 Mineralogy

For bulk mineralogical analysis, 1.2 grams of material from each sample was oven dried at approximately 100 °C, ground with a mortar and pestle and sieved using a 75µm diameter sieve. Samples were spiked with 0.3 grams of a zincite standard to make a mixture of 20% standard and 80% sample. Deionized water was added to this mixture, ultrasonicated for 1 minute to disaggregate the clay minerals, and further ground using a McCrone Micronising Mill for 10 minutes to analyze the <10 µM size fraction. Samples were oven dried for 24 hours at approximately 100° C, and resulting powders were prepared as press powder mounts for bulk analysis.

Samples were examined using a Bruker D8 Advance X-ray diffractometer at the University of Georgia Geology Department and CoK α radiation was used in all analyses (Figure 4.2D). Scans were performed utilizing a 0.6mm slit from 2-70° 2 theta at an interval of 0.02 and a scan speed of 5 degrees/minute.

To analyze the clays further, 900ml of Na Acetate buffered Acetic Acid with a pH of 5.0 was used to dissolve the carbonate material in sample CI-781, as described by Railsback (1993). 110g of sample in a 2000mL flask was digested at room temperature and agitated for 24 hours with a shaker. The sample was centrifuged for 20 minutes, washed with deionized water 3 times to remove any remaining acetic acid, and allowed to settle for 5 minutes. The finer fraction at the top of the sample was pipetted onto a glass slide, air dried at room temperature for 24 hours, and ethylene glycolated for 24 hours.

The mineralogy of each sample was quantified with Topas 4.2 software using a Rietveld refinement method (Rietveld, 1967). This semi-quantitative analysis of step-scan powder diffraction data uses least squares to fit a calculated pattern to an observed pattern, and is associated with an error of $\pm 5\%$ (Moore and Reynolds, 1997). The NIST standard LaB6 was used to determine the background parameters, Chebychev polynomial, and peak type. R_{wp} values were compared for each run, and the parameters from the run with the lowest R_{wp} value were used for all sample runs (Bruker, 2009). These parameters are as follows: 3rd order Chebychev polynomial, and the 1/x bkg function. A pseudo-Voigt peak type, which is a combination of Lorentzian and Gaussian functions, was the peak-shape model used in the refinement (Young and Wiles, 1982). CIF files for each mineral were obtained from the online MSA Crystal Structure Database. The platy nature of clinoptilolite causes preferred orientation to become a problem in Rietveld refinement (Taylor and Pcover, 1988). Preferred orientation was corrected in samples which contained clinoptilolite using a March-Dollase correction (Bruker, 2009).

Quantification of mixed-layering for sample CI-781 was accomplished with the software NEWMOD[®] (Reynolds, 1996).

4.6. Water Quality

Water quality and salinity are often defined by the total-dissolved solids (TDS) concentration, with a TDS concentration of 1,000 to 10,000 mg/L defined as brackish, 10,000 to 35,000 mg/L defined as moderately saline, and 35,000 to 100,000 mg/L as saline (Reese, 2000). Typically specific conductance is measured in water samples, and this parameter is directly correlated to TDS.

To determine the specific conductance of pore-water from well log data using the resistivity-porosity method, the resistivity of the pore-water must be corrected to 77°F using Arp's equation (Arps, 1953):

$$R_{w77} = \frac{R_o(T_f + 6.77)}{77 + 6.77} \quad [10]$$

Where R_{w77} is the formation water resistivity at 77°F and T_f is the formation temperature (°F).

The temperature of the formation at various depths can be estimated using the following equation (Asquith and Krygowski, 2004) :

$$T_f = \frac{BHT - AMST}{TD} \times FD + AMST \quad [11]$$

Where BHT is the bottom hole temperature (°F), TD is the total depth (ft), FD is the formation depth (ft), and AMST is the annual mean surface temperature (°F).

A temperature log was run in well 38Q201 on Cockspur Island and at 1,170 ft, a temperature of 89°F was recorded and used as the bottom hole temperature (BHT) of the Cockpur Island core hole, and the annual mean surface temperature was found to be 65.5° (Parker et al., 1994).

The specific conductance (SC) of the pore-water can be calculated using the following relationship between specific conductance and R_{w77} :

$$SC = \frac{10,000}{R_{w77}} \quad [12]$$

CHAPTER 5

RESULTS

5.1 Water Quality Sample Correlations

Forty-one water quality samples from well 38Q002 at a depth of 110-348ft were collected from 1991 to 2010, and an average specific conductance value of 256 $\mu\text{S}/\text{cm}$ at 25°C was calculated. A total of 106 samples were collected from well 38Q004 at a depth of 606-657ft from 1982 to 2002, and an average specific conductance value of 907 $\mu\text{S}/\text{cm}$ at 25°C was found. 103 water quality samples from well 38Q196, with an open interval of 870-900 ft., were collected between 1982 and 2002, and an average specific conductance value of 17,338 $\mu\text{S}/\text{cm}$ at 25°C was measured (Figure 5.1). In all three of these wells, there was not a significant change in water quality during the time periods in which samples were collected. The mean water sample resistivities correlated well with water resistivities calculated from the resistivity well logs and cementation and formation factors found in this study, with exception to sample CI- 977, which was collected parallel to bedding planes (Figure 5.2).

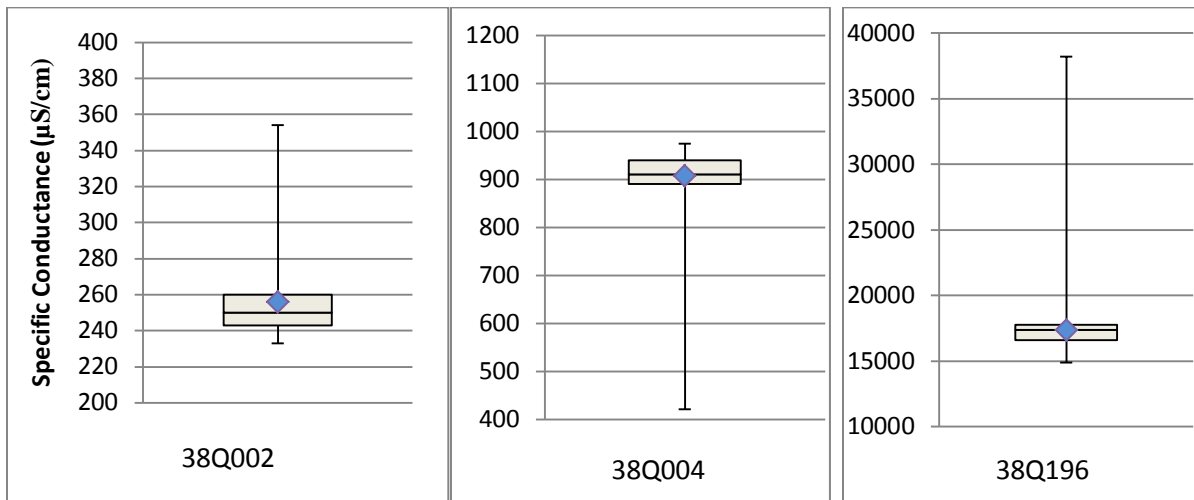


Figure 5.1. Box-and-whisker plots for water quality wells (38Q002, 38Q004, 38Q196). Diamond symbol represents mean.

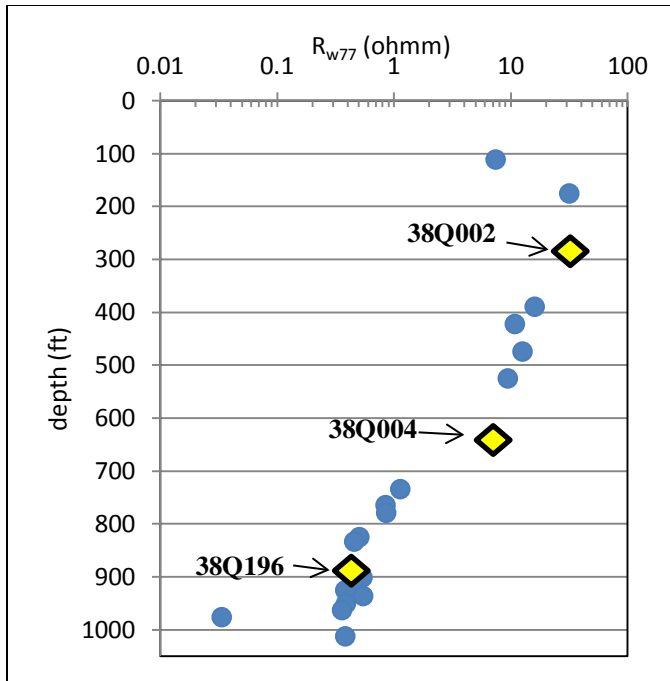


Figure 5.2 Calculated R_{w77} values from laboratory data. Diamonds show water quality results from nearby wells.

5.2. Mineralogy

The main mineral constituent of all of the samples was calcite, which ranged from 28 to 99%, with exception to samples CI-108, CI-977, and CI-1013, which contained high amounts of glauconite. Minor amounts of quartz (1-6%) occurred in each samples except for CI-108 and CI-112. A relatively large amount of quartz was found in the two shallowest samples, CI-108 and CI-112, which contained 23 and 14% quartz, respectively (Figure 5.2).

Minor amounts of clinoptilolite, illite, and smectite were found in some samples. Clinoptilolite was shown to generally increase with depth, and was identified only in the middle confining unit, and the Lower Floridan aquifer (Figure 5.3). Samples CI-390 and CI-424 in the middle confining unit contained 1 and 6% clinoptilolite respectively, and every sample analyzed in the Lower Floridan aquifer contained clinoptilolite except for the shallowest sample, CI-628. Those samples include CI-735, CI-766, CI-781, CI-826, CI-835, CI-902, CI-907, CI-926 CI-937, CI-952, CI-965, CI-977, and CI-1014 and the amount of clinoptilolite in these samples ranged from 2 to 10%.

The clay minerals which were identified in the Cockspur Island core hole include smectite, illite, and glauconite. Glauconite was identified in the two deepest samples, CI-977 and CI-1014, which contained 42 and 53% glauconite, respectively, and 49% glauconite was found sample CI-108, which is within the upper confining unit. Mixed layered illite-smectite was identified in sample CI-781 which is within the Lower Floridan aquifer. The intervals where clay minerals were found had high gamma-ray responses, with glauconitic areas exhibiting the highest response (Figure 5.4).

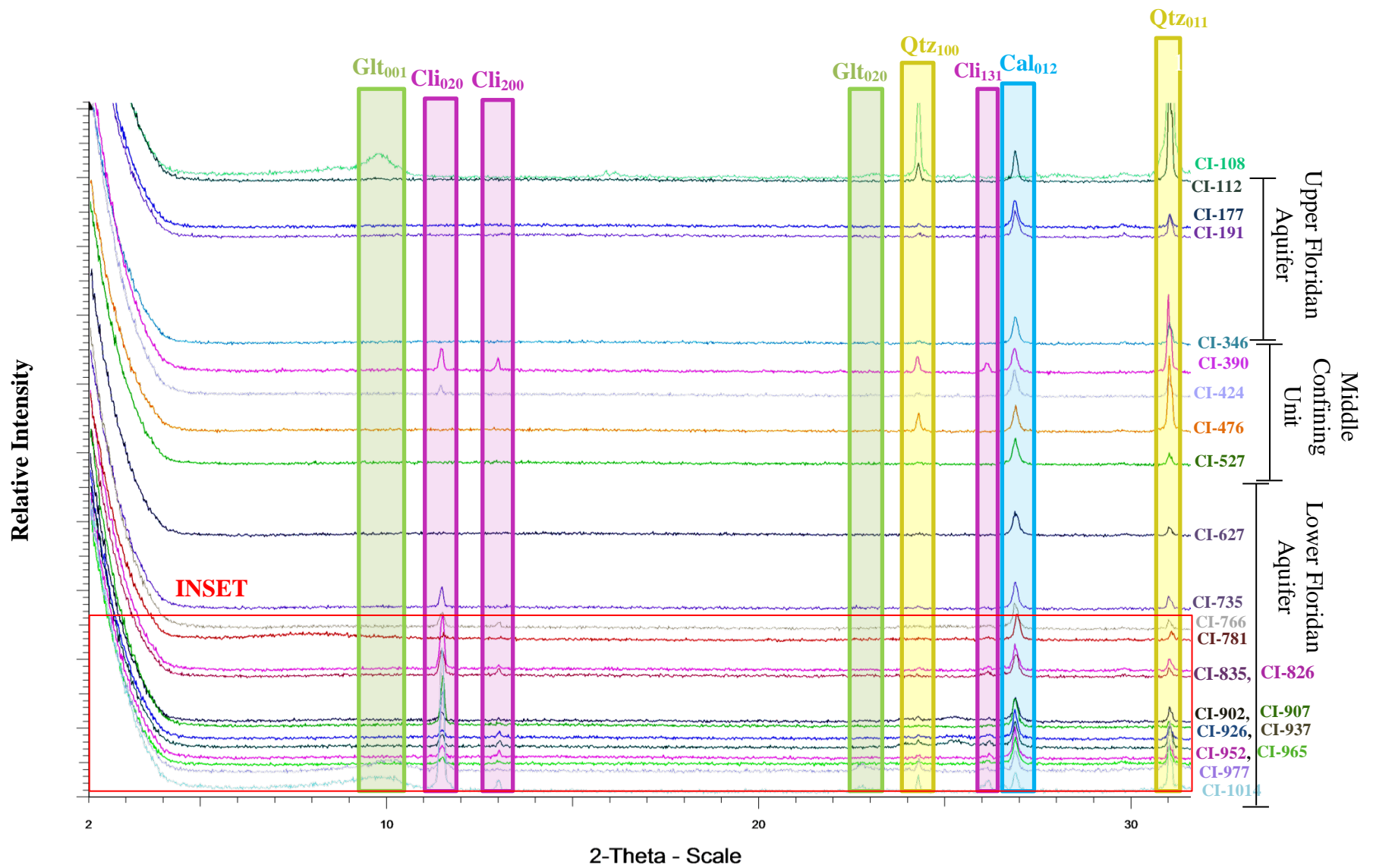


Figure 5.3 X-ray diffraction patterns for all samples, scaled to depth. Glt=glaucanite; Cli=clinoptilolite; Qtz=quartz; Cal=calcite. Samples were prepared as press powder mounts.

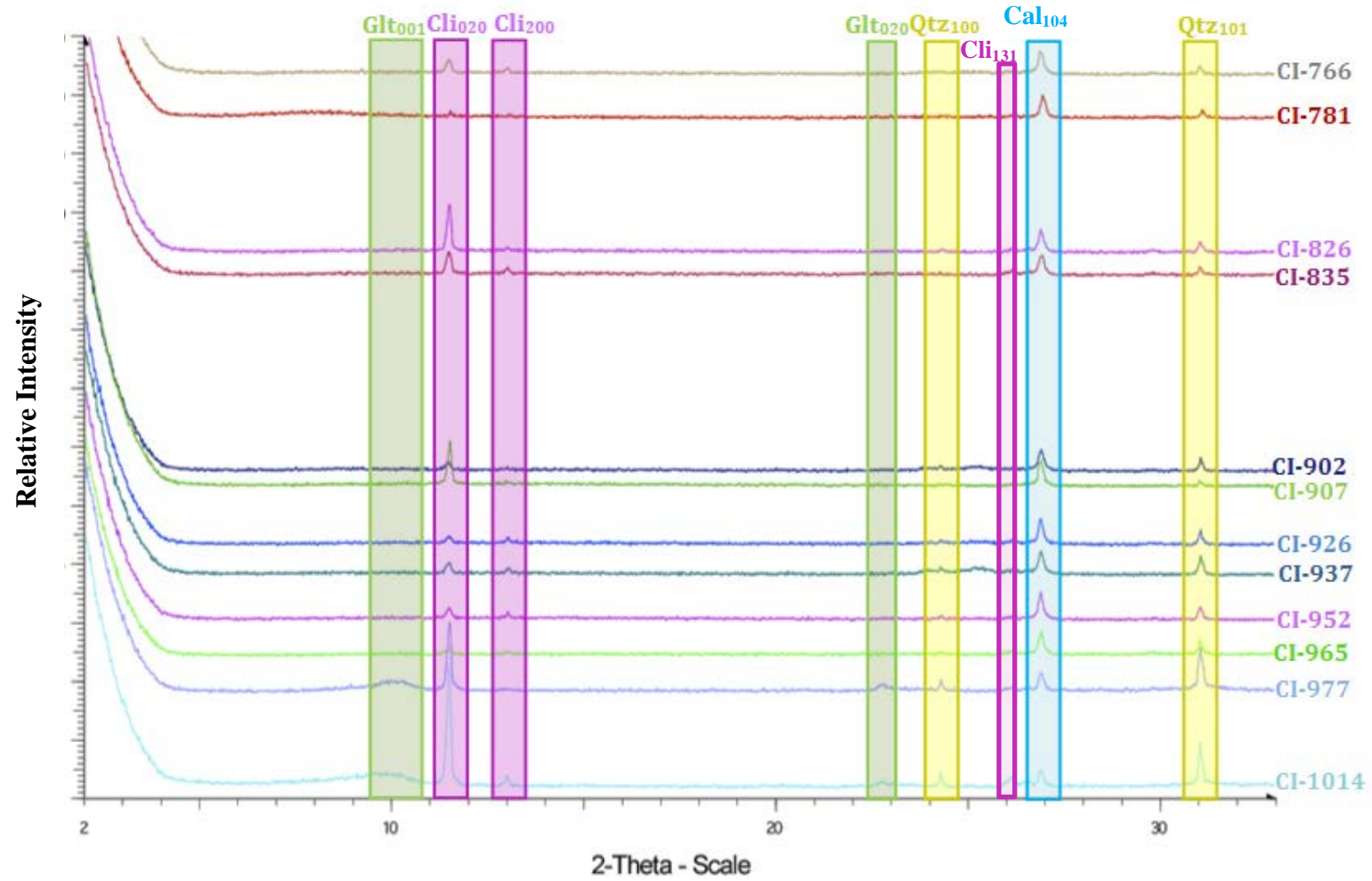


Figure 5.4 Inset from fig. 5.2.

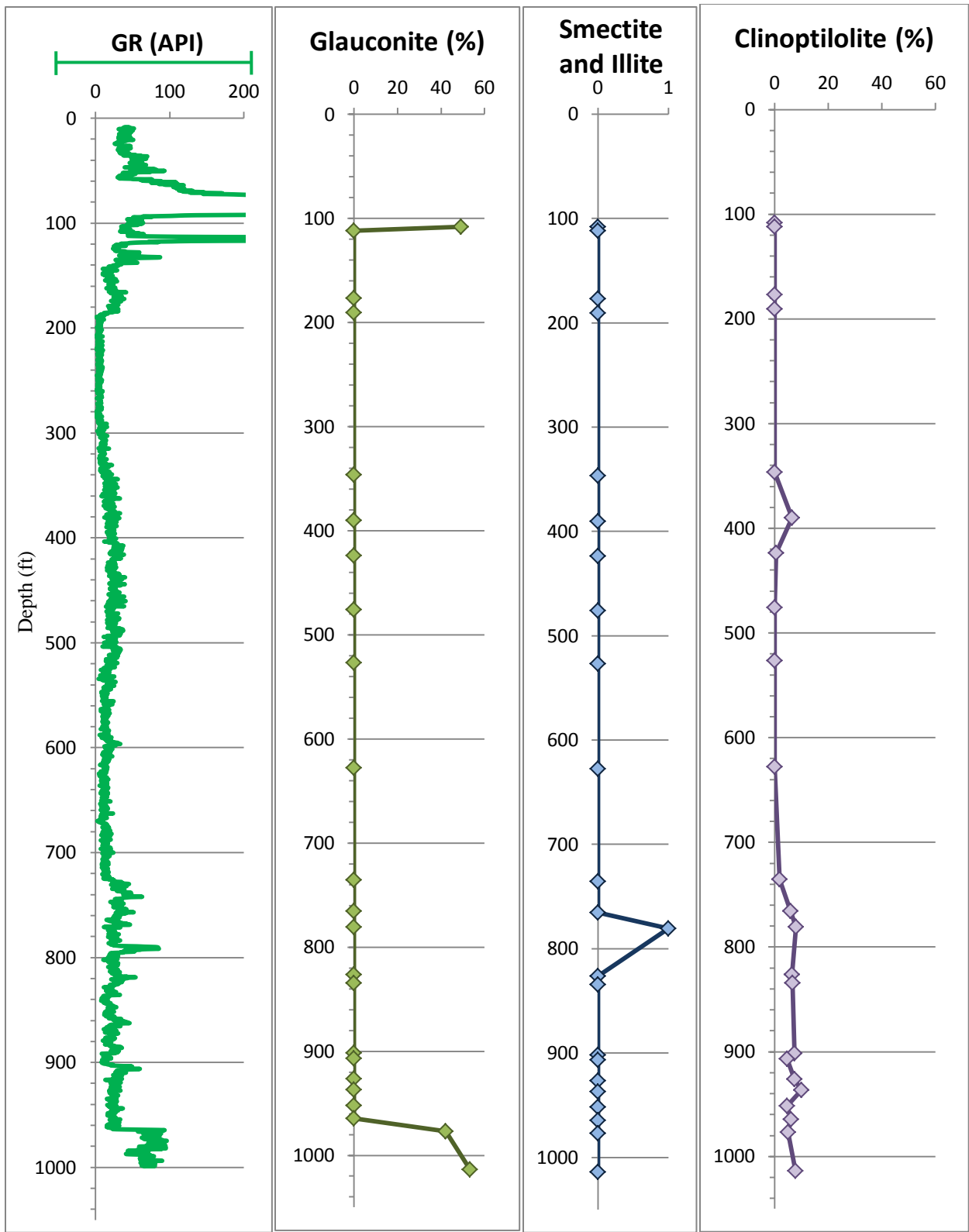


Figure 5.5 Mineralogical changes with depth. Values are in weight percent, except for smectite and illite which is denoted as 0 for not present and 1 for present, as determined from NEWMOD modeling and Rietveld Refinement utilizing Topas software.

Mixed layering of illite and smectite was identified by comparing the air-dried state to the ethylene glycol solvated state after acid treatment (Figure 5.5). When there is a significant change in the diffraction pattern after ethylene glycolation, there is most likely a smectite component, with the most abundant mixed layering in sedimentary rocks being illite/smectite (Moore and Reynolds, 1997) .

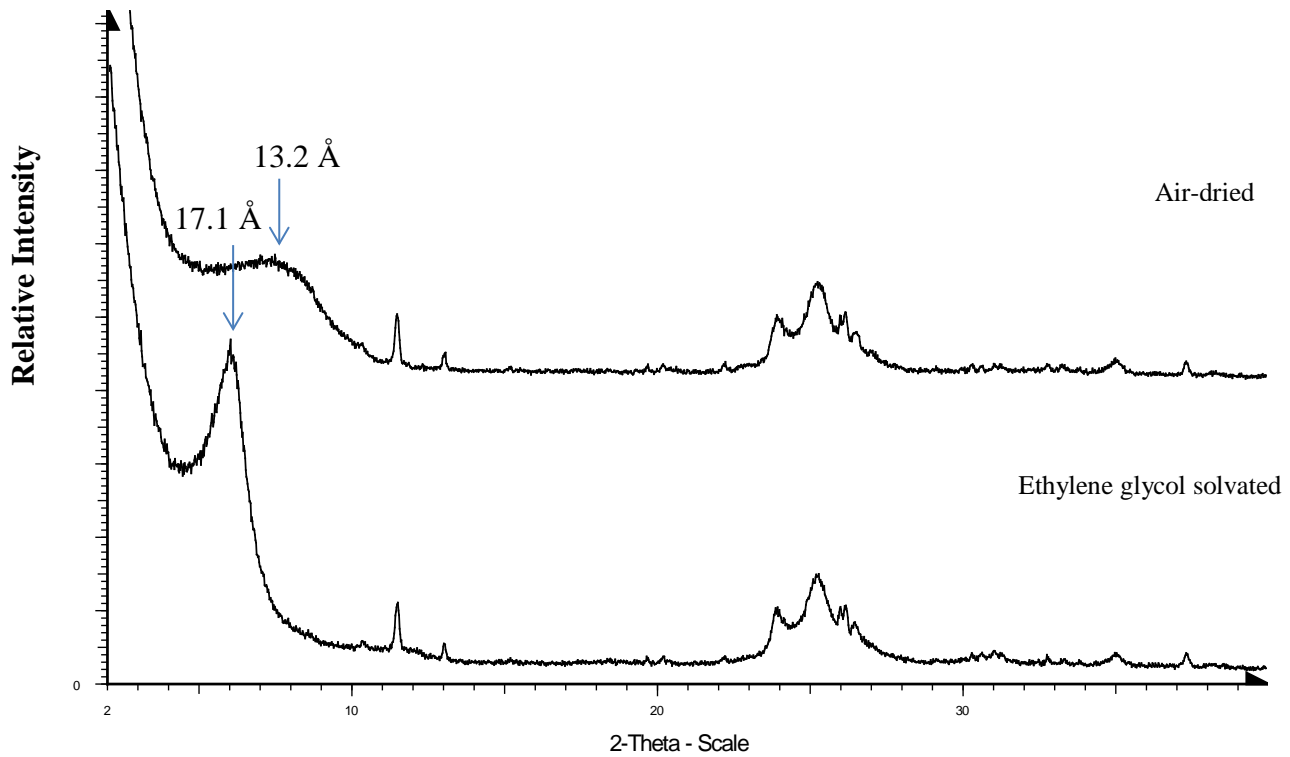


Figure 5.6 X-ray diffraction patterns of air-dried and ethylene glycol solvated sedimented mounts of sample CI-781.

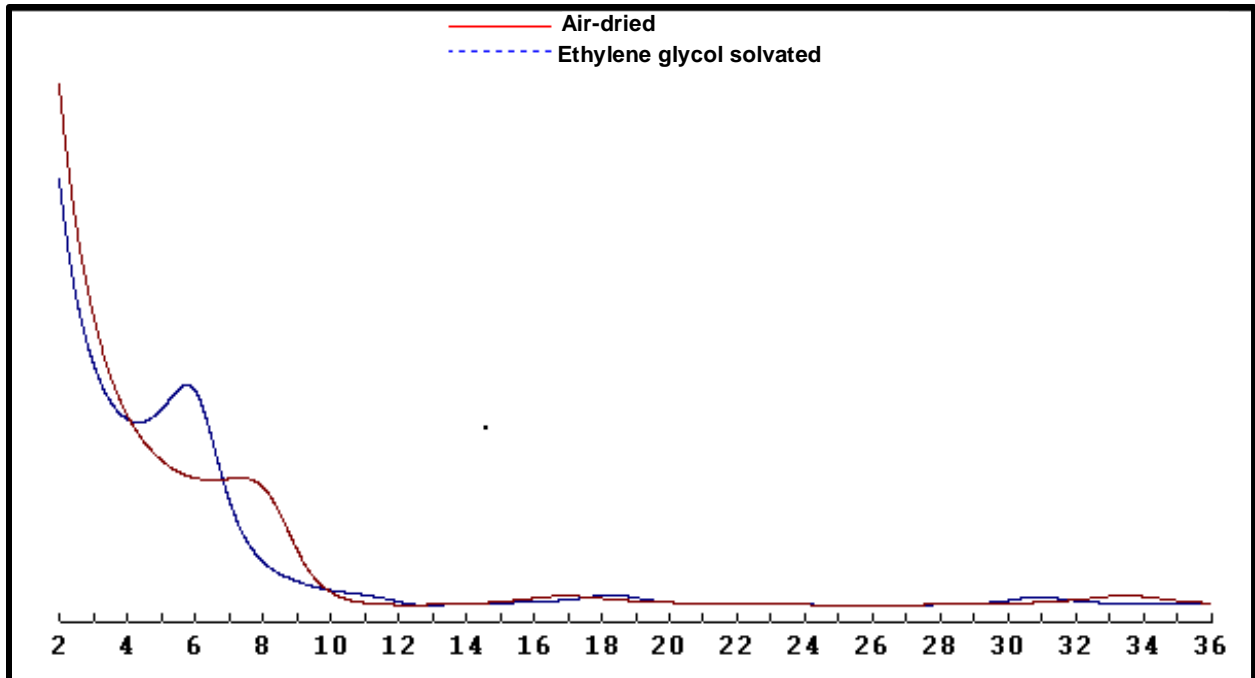


Figure 5.7 Model of mixed layering of illite and smectite using NEWMOD[®] (sample CI-781).

The mixed layering of illite and smectite in sample CI-781 was modelled using NEWMOD[®], and a ratio of 87% smectite and 12% illite was found (Figure 5.6), with an ordering of R=0.

The lowest laboratory resistivity measurements correspond to the highest porosities, which corresponds with the highest amounts of clinoptilolite, glauconite, illite, and smectite (Figure 5.7).

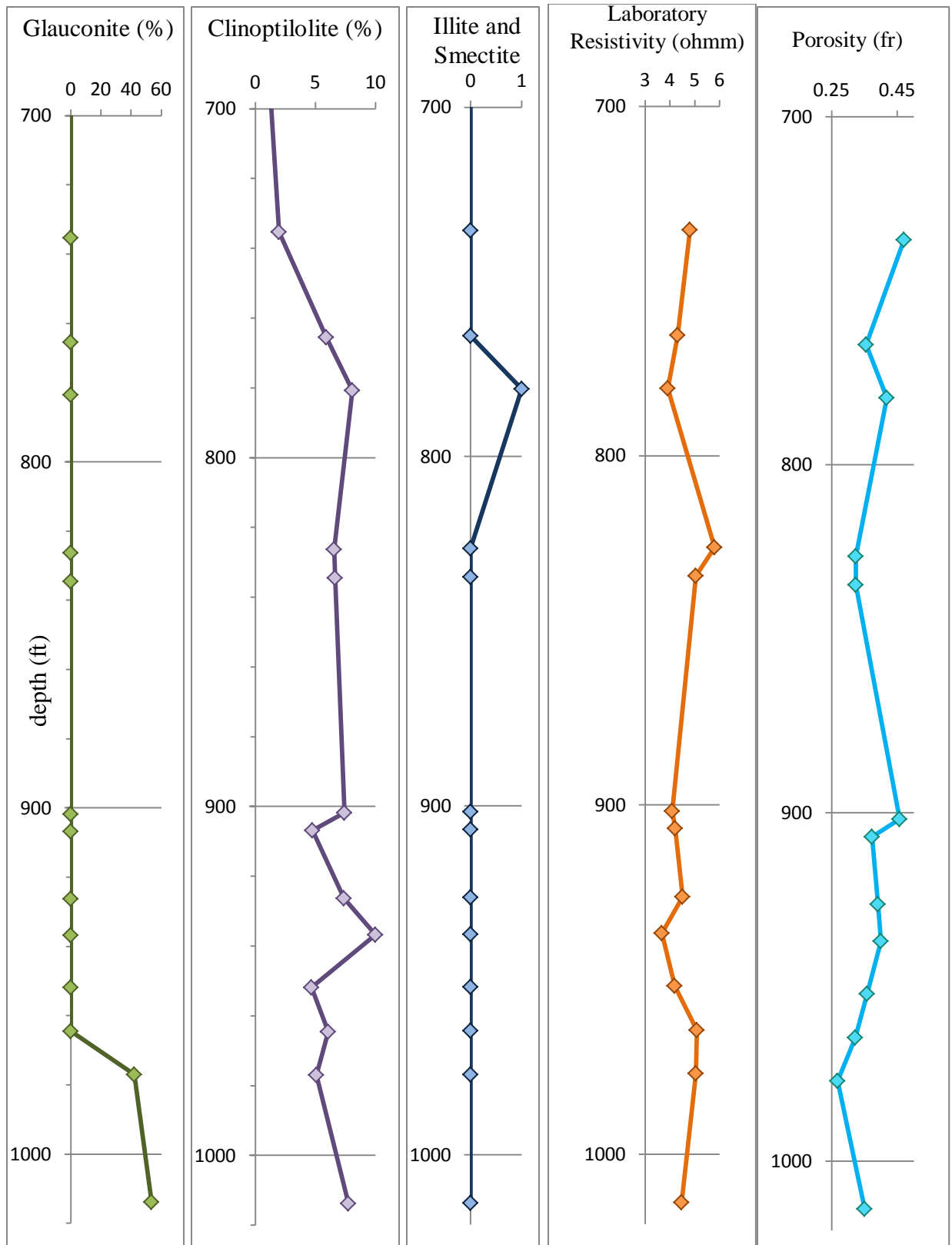


Figure 5.8 Laboratory porosities and resistivities compared with clay and zeolite mineral percentages for rocks saturated with the same brine concentration.

5.3. Porosity and Permeability

Permeability generally decreased with depth for the Cockspur Island core hole (Figure 5.7). Each sample which contained clay minerals and clinoptilolite had low to moderate permeabilities, with a geometric mean k range of 13mD to 168mD. Samples which contained clay minerals and clinoptilolite had fairly high porosities, ranging from 27 to 57%. Samples CI-112, CI-191, and CI-628 exhibited low sonic and laboratory porosities (Figure 5.7 and Figure 5.8), and a large range of spot permeability measurements (0 mD to 640 mD) (Figure 5.7; Figure 5.8).

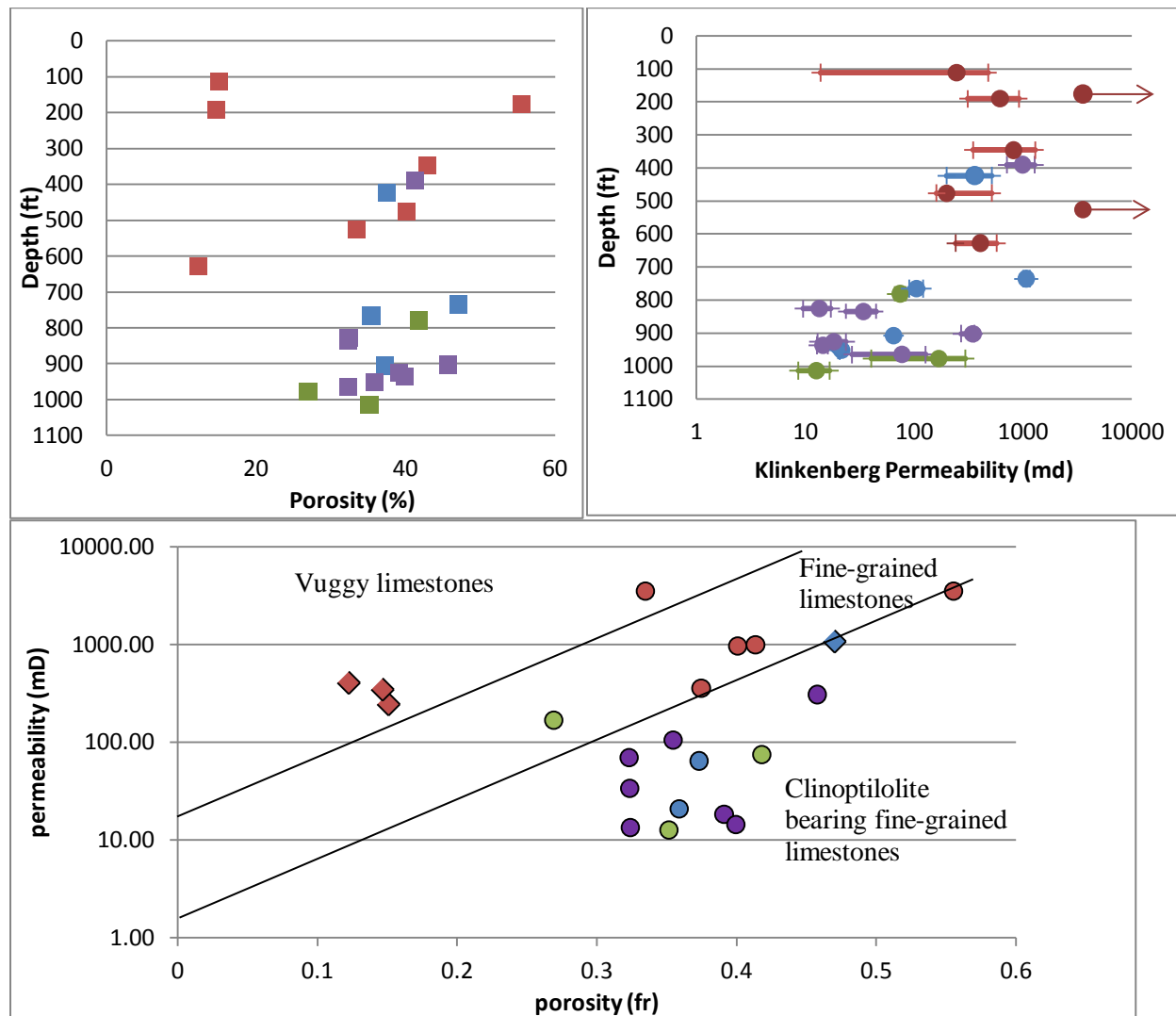


Figure 5.9 Upper Left: Standard deviation of permeability with depth. Circles represent average permeability. Upper Right: Lab derived porosity changes with depth. Bottom: Porosity vs Permeability. **red**: only calcite and quartz present; **green**: glauconite, illite, or smectite present; **blue**: <5 wt% clinoptilolite present; **purple**: >5 wt% clinoptilolite present; diamond shape: vuggy porosity

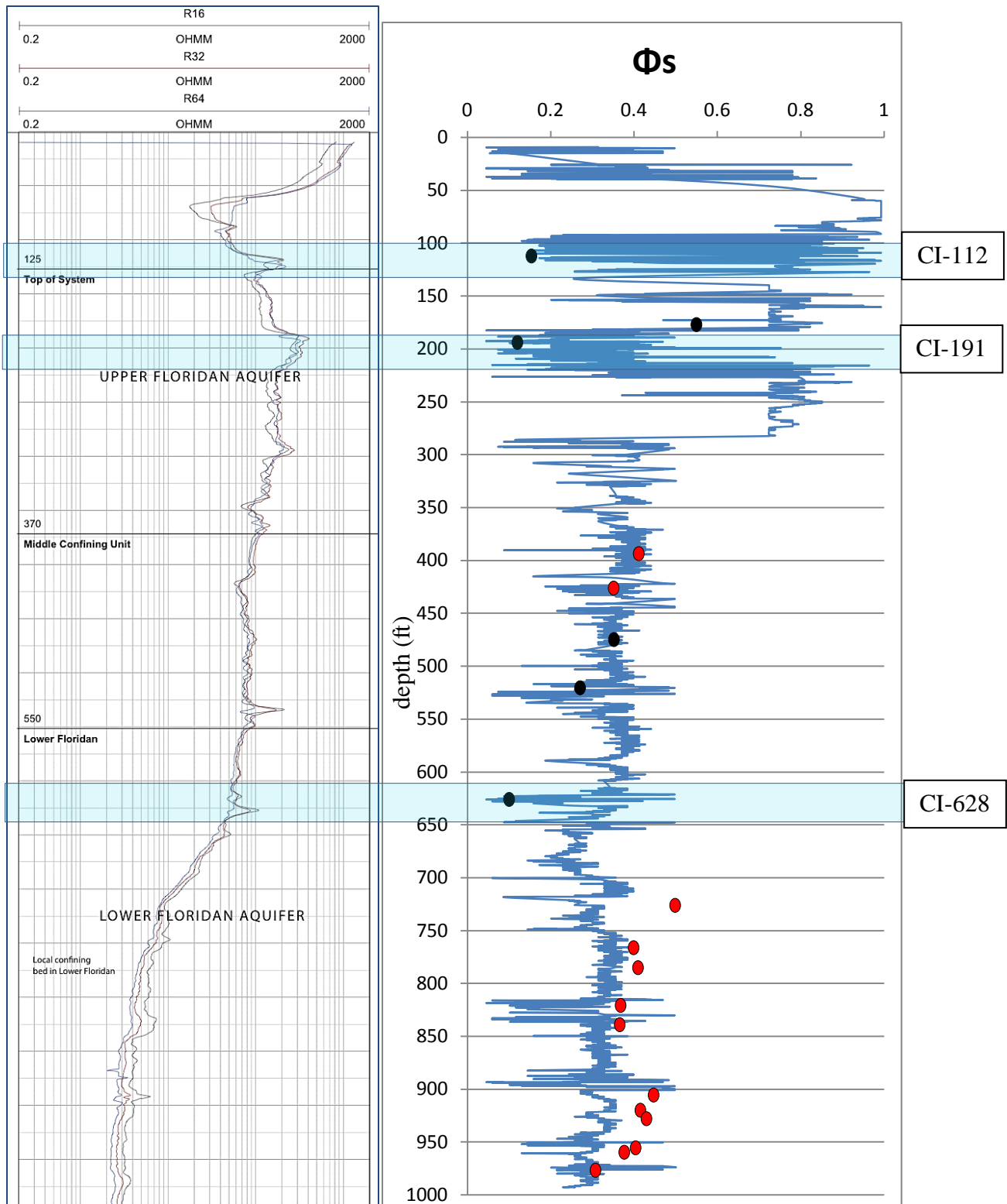


Figure 5.10 Resistivity and sonic porosity logs. Blue highlighted areas show rocks with disconnected pore networks; black circles represent samples with no clinoptilolite; red circles represent samples with clinoptilolite.

Porosities calculated from the sonic log using the Wyllie time-average equation were found to be in agreement with porosities calculated in the laboratory for all samples which did not contain clinoptilolite. Samples which did have clinoptilolite were typically found to have underestimated porosity values (Figure 5.9).

5.4. Pore Geometry and Lithology

Formation factors for all samples ranged from 5.24 to 11.36, and cementation factors ranged from 1.70 to 2.59, with exception to sample CI-1014, which had a cementation factor of 3.33 and a formation factor of 80. Cementation factors for the three grainstone samples were 2.12, 2.59, and 1.82 with an average of 2.18. Cementation factors ranged from 1.70 to 2.45 for fifteen wackestones to packstones samples, with an average of 1.89. No correlation was found between PoA, DOMsize, and cementation factor (Figure 5.9).

Table 5.1 Pore geometric and petrophysical parameters for all samples.

Sample ID	m	F	Avg k (md)	PoA (mm ⁻¹)	DOMsize (mm ⁻¹)	Rock Type
CI-177	2.59	4.58	Off scale	163	290	Grainstone
CI-390	1.86	9.27	993.86	185	138	Fine-grained Wackestone
CI-424	1.70	11.36	358.95	145	224	Fine-grained Packstone
CI-476	2.02	6.36	967.27	164	291	Fine-Grained Packstone
CI-527	1.82	7.32	Off scale	72	215	Fine-Grained Grainstone
CI-735	2.45	6.34	1073.62	173	270	Fine-Grained Packstone
CI-766	1.71	5.89	105.00	136	196	Fine-Grained Wackestone
CI-781	1.89	5.21	74.48	84	257	Fine-Grained Wackestone
CI-826	1.86	8.10	13.41	183	245	Packstone
CI-835	1.79	7.57	34.00	142	217	Packstone
CI-902	2.12	5.24	307.55	187	269	Fine-Grained Grainstone
CI-907	1.88	6.39	64.51	199	147	Fine-Grained Wackestone
CI-926	1.98	6.44	18.34	210	111	Fine-Grained Wackestone
CI-937	1.79	5.15	14.47	206	115	Fine-Grained Wackestone
CI-952	1.79	6.23	20.78	213	132	Fine-Grained Wackestone
CI-965	1.78	7.46	69.39	139	184	Fine-Grained Wackestone
CI-977	3.33	79.64	167.68	276	142	Glauconitic Fine-Grained Wackestone
CI-1014	1.87	7.06	12.64	156	328	Glauconitic Fine-Grained Wackestone

m is cementation factor, F is formation factor, k is permeability, PoA is perimeter over area, and DOMsize is dominant pore size.

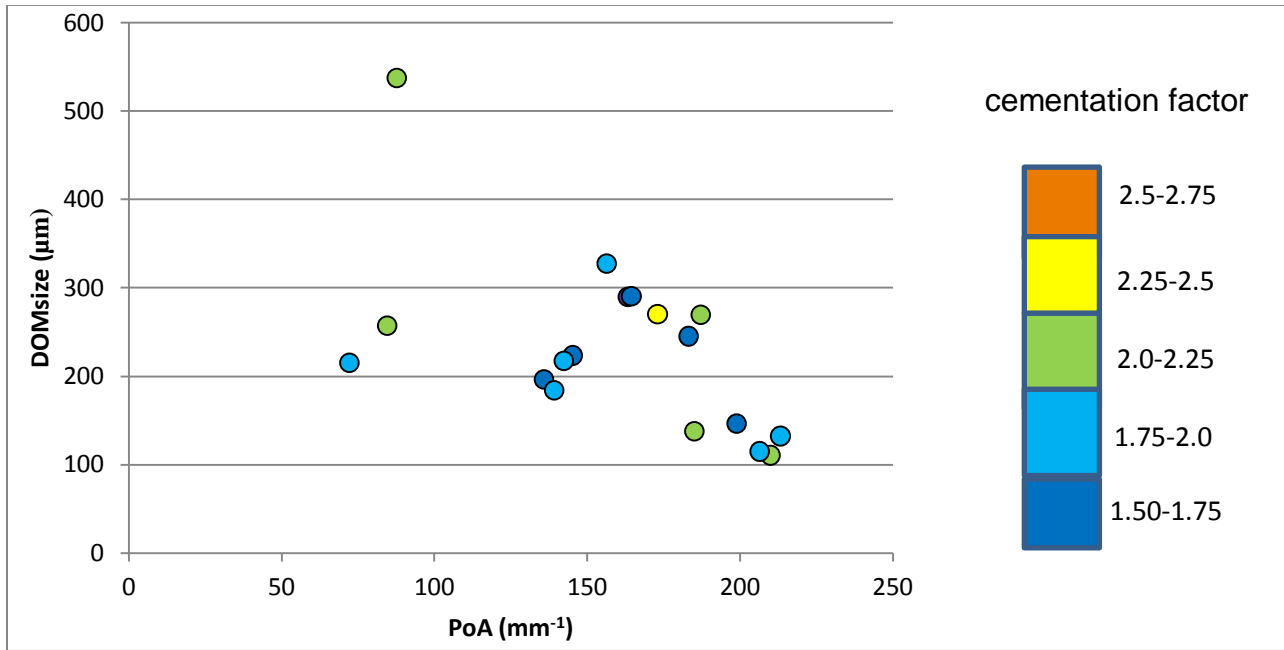


Figure 5.11 Relationship between DOMsize, PoA, and cementation factor

CHAPTER 6

DISCUSSION

6.1. Pore Geometric Factors and Petrophysical Parameters

Kwader (1985) reports that carbonate rocks in the FAS which are highly cemented and have an $m > 2.2$ will have a portion of the current conducted through the matrix because the pores are not interconnected. Samples with the highest cementation factors were found to have low permeabilities, large pores and a simple pore network. Samples with small pores and an intricate pore network had the lowest cementation factors. This may be because isolated pores do not contribute to the flow of electric charge, resulting in a higher m , while interparticle and intercrystalline pores are more connected with each other and provide a better pathway for the flow of electrical current, resulting in a lower m (Verwer et al., 2011). Ramakrishan et al. (1998) showed that cementation factor was related to carbonate texture, with a cementation factor of 1.65 to 1.70 in fine grained packstones and wackestones, and grainstones had cementation factors of 2.0-2.2. Verwer et al. (2011) found that pore structure and number of pores were the most important factors in controlling electrical resistivity, as opposed to the size of the pore throats.

Post, Buckley, Schuh, and Jernigan, Inc. (1989 and 1992) and Palm Beach County Water Utilities Department (2009) reported cementation factors and formation factors in the Avon Park formation and the Ocala Group in Sarasota, Palm Beach, and Charlotte County, Florida (Appendix B) (Figure 6.1). In those studies, cementation factors for nine grainstone samples ranged from 1.85 to 2.3, with an average of 2.05. Fifteen wackestone to packstone samples had cementation factors which ranged from 1.32 to 2.34, with an average of 1.88.

A t-test with a p value of 0.01512 rejects the null hypothesis that there is no difference in means for this study and other studies in the FAS (Figure 6.1), with grainstones having a mean of 2.083 and wackestones to packstones having a mean of 1.884. Based on this p value the difference in means

between grainstones and wackestone to packstones is statistically significant. This cementation factor trend can be attributed to the relatively simple pore structure of grainstones in which large vuggy pores do not contribute to the flow of electric current, while rocks with an intricate pore network, such as wackstones and packstones, have more connected pores which allow for electric current to pass easily through the sample.

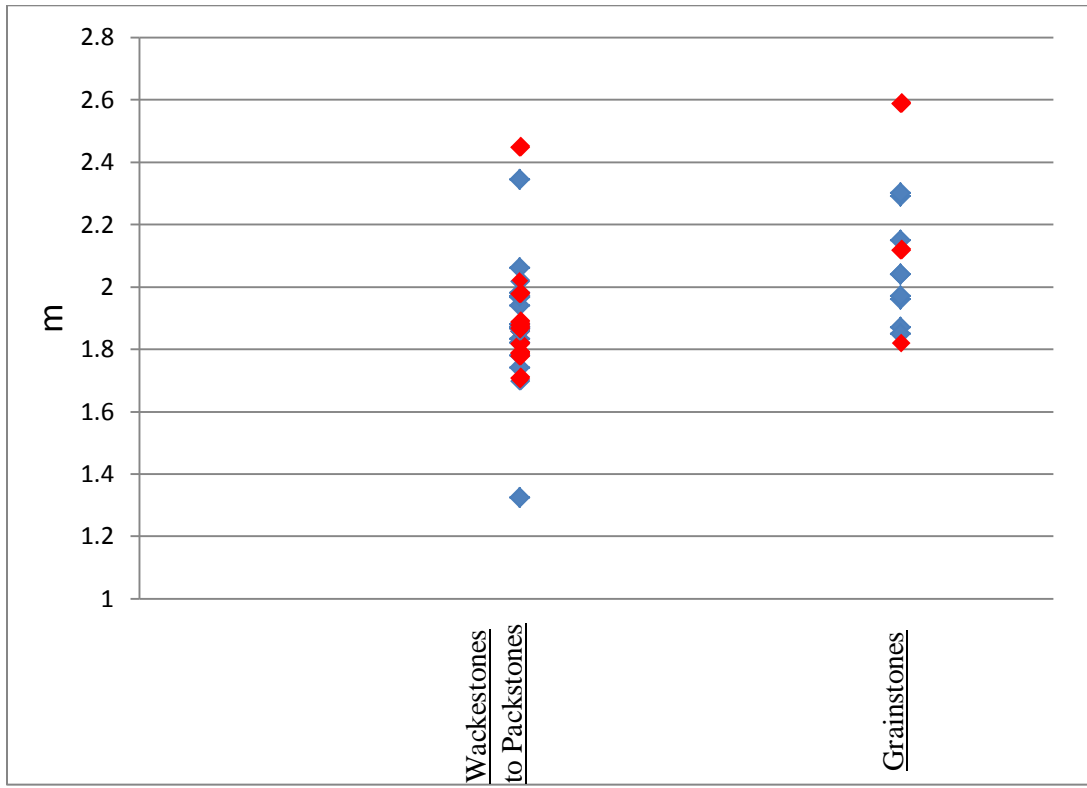


Figure 6.1 Graph showing cementation factors calculated from this study and other studies in the Floridan aquifer system (Post, Buckley, Schuh, and Jernigan Inc., 1989 & 1992; Palm Beach County Water Utilities Department, 2009). Red shows cementation factors calculated in this study.

The PoA and DOMsize did not correlate with cementation factors found in this study, although Verwer et al. (2011) found a general decrease in cementation factor with an increase in PoA, and an increase in cementation factor for a larger DOMsize. This was likely due to the difficulty of determining pore space in the image analysis due to the friable nature of the samples and the poor epoxy impregnation in most of the pore spaces.

Running laboratory resistivity measurements at ambient conditions may lead to errors, because mineral grains may be more compacted at in-situ pressures. However, studies show that at relatively shallow depths, such as the depth of the Cockspur Island core hole, the effects of confining pressures are insignificant (Schnoebelen et al., 1995).

6.2. Porosity and Permeability and Relation to Well Logs

Samples CI-112, CI-191 and CI-628 had very vuggy porosity and disconnected pore networks. Laboratory and sonic porosities were found to be very low, thin sections show large disconnected pores (Figure 6.1), and minipermeametry analysis shows a very large range of spot permeability measurements, ranging from 0 mD to 640 mD. Calculated formation and cementation factors for each saturation were significantly different, and measured laboratory resistivity for each sample was orders of magnitude greater than other samples measured. The inability for the electric current to flow through the brine solution in the sample was likely the cause of the high laboratory resistivity measurements, and no formation factors and cementation factors were used in the final analysis of this study. The sections where these three samples were collected show a sharp decrease in porosity on the sonic log, and a sharp increase in well log resistivity. Areas which exhibit these characteristics should be avoided when calculating water resistivity from well log data because these areas reflect low permeability and porosity rocks with vuggy, disconnected pore networks (Figure 6.2). The resistivity values of the well log in these sections may not be indicative of the resistivity of the pore fluid.

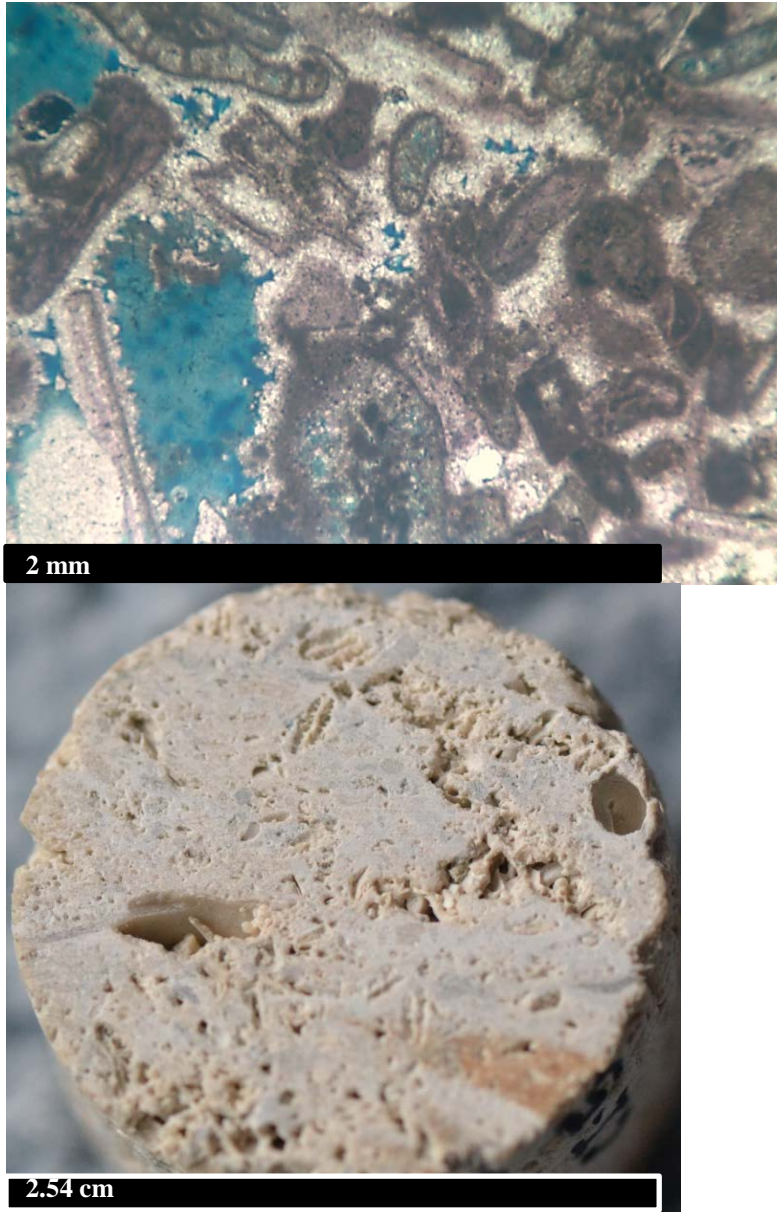


Figure 6.2 Upper: Vuggy porosity shown by plain polarized light photomicrograph of sample CI-628. Blue color is pore space. Lower: Digital photograph with macro lens of sample CI-628.

6.3 The Effects of Clays and Zeolites on Borehole Geophysical Logs

The increase in siliciclastic input in the study area most likely contributed to the presence of clinoptilolite in the lower Floridan aquifer and the middle confining unit. Clinoptilolite is most likely the product of diagenetic changes involving clay minerals, and clay minerals would likely be more abundant in a siliclastic environment.

The rocks which contained clinoptilolite generally exhibited high porosities (27-47%), low to moderate average permeabilities (13-355mD) and were typically found in fine-grained packstones to wackestones within the middle confining unit and throughout most of the Lower Floridan aquifer. It was found that as the percentage of clinoptilolite increased, porosity also generally increased. Therefore the presence of clinoptilolite is likely causing an increase in microporosity in the rocks in the Lower Floridan aquifer because of its microporous structure. Clinoptilolite usually forms as microcrystalline disseminated aggregates. These aggregates typically occur as a cement or grain replacements in sedimentary rocks (Iijima, 2001). Because of the disseminated nature of these aggregates, they rarely form continuous networks. Therefore, although this mineral has a high CEC it rarely contributes to the conduction of electric current, and is unlikely having an effect on the electrical conductivity of the rocks in this study. Other studies have also shown that the CEC of clinoptilolite is unavailable at conditions encountered in this well. Future studies involving measuring the CEC of these clinoptilolite containing rocks could confirm that these zeolites are in fact not contributing to the conduction of these carbonate rock matrices. Since clinoptilolite is usually unable to be identified in thin section, future studies involving imaging these zeolites with a scanning electron microscope must be performed to determine if they are occurring as disseminated cements and grain replacements, and are therefore not forming connected networks in the rock. Depending on if clinoptilolite is occurring as a cement in these rocks, this zeolite could also be contributing to a decrease in permeability in rocks in the middle confining unit and Lower Floridan aquifer.

XRD data show that rocks from the lower part of the Lower Floridan aquifer system contained clay minerals, in particular illite, smectite, and glauconite. Glauconite and illite have a low CEC and therefore doesn't usually contribute to the conduction in a rock. Smectite has a very high CEC, however and has the potential to have a significant influence on the conductive properties of these rocks. The resistivity of the water calculated from the resistivity well log and the cementation factors found in this study correlated well with the resistivity of the water quality samples collected from nearby wells. The cementation factor for the sample containing smectite was also very similar to cementation factors found for similar rocks in

this study. Therefore the smectite found in sample CI-781 is most likely not contributing to the electrical conductivity of this rock matrix. An increase in the amount, or a change in the distribution of smectite however, could have an effect on the electrical conductivity of the rock matrices in nearby wells. Minerals other than smectite, which cause an increase in the gamma-ray log, were found to occur in rocks in the Lower Floridan aquifer in this study making identification of where smectite occurs difficult. This includes the glauconite and illite identified by X-ray diffraction, and the minor amount of glauconite identified by thin section in most of the samples in the Lower Floridan aquifer (Appendix E). Although phosphate was not identified in any X-ray diffraction patterns or thin sections, it was described in the core log descriptions, and may also be causing an increase in gamma-ray response. A gamma-spectral log would be beneficial for parsing out which of these minerals are causing increases in gamma response, allowing for a quick way to identify which rocks are rich in smectite, and also allowing for estimations of the volume of clay from the gamma-ray log. The Wyllie time-average equation was used to estimate porosity from interval transit times. This method generally underestimated the porosity in rocks containing clinoptilolite in the Cockspur Island core hole.

CHAPTER 7

CONCLUSION

Cementation factors were significantly higher for grainstones than wackestones to packstones in the Floridan aquifer system (Figure 6.1). This can be attributed to the large simple pore networks in grainstones, as opposed to small more connected pore networks in wackestones to packstones. The more connected pore networks have a higher potential to conduct electric current.

Clinoptilolite has only been documented only in a few samples in previous studies of rocks comprising the Floridan aquifer system. These studies focused on rocks in Central and South Florida, and not Southeast Georgia. XRD data in this study shows a significant amount of clinoptilolite, ranging from 1-10%, in the middle confining unit of the Floridan aquifer system, and in the Lower Floridan aquifer (Figure 5.3). The rocks containing clinoptilolite were characterized as having a high porosity and lower permeability (Figure 5.9). This result is significant to the USGS Saline Aquifer Mapping Project on the Southeastern United States because zeolites will effect the interpretation of borehole geophysical well logs, in particular porosity logs (Figure 5.10).

REFERENCES

- American Petroleum Institute, 1959, Recommended Practice for Standard Calibration and Form for Nuclear Logs, API Recommended Practice 33.
- Archie, G.E., 1942, The electrical resistivity log as an aid in determining some reservoir characteristics, Petroleum Transactions of AIME, v. 146, 54-62.
- Arps, J.J., 1953, The effect of temperature on the density and electrical resistivity of sodium chloride solutions, Transactions of the American Institute of Mining, Metallurgical, and Petroleum Engineers, v. 198, 327-330.
- Asquith, G. and D. Krygowski, 2004, Basic Well Log Analysis, AAPG Methods in Exploration Series, 2nd edition, No. 16, 244 p.
- Budd, D.A., 2001, Permeability loss with depth in the Cenozoic carbonate platform of west-central Florida, AAPG Bulletin, v.85, no.7, 1253-1272.
- Budd, D.A., 2011, Personal communication.
- Berndt, M.P. and R.L. Marella, 2005, Water Withdrawals and Trends from the Floridan Aquifer System in the Southeastern United States, 1950-2000, A Contribution of the National Water Quality Assessment (NAWQA) Program 2005: Circular 1278, 24 p.
- Bowen, R., 1986, Groundwater. 2nd Ed., Elsevier, New York, NY, 444 p.
- Bruker, 2009, DIFFRAC^{plus} TOPAS, TOPAS 4.2 Tutorial and User Manual, Bruker AXS GmbH, Karlsruhe, Germany.
- Bush, P.W. and R.H. Johnston, 1988, Summary of the Hydrogeology of the Floridan Aquifer System in Florida and in Parts of Georgia, South Carolina, and Alabama: U.S. Geological Survey Professional Paper 1403-A, 80 p.
- Carroll, R.D., 1990, Electric logging and electrical properties of rocks in the Rainier Mesa Area, Nevada Test Site, Nevada, U.S. Geological Survey Open File Report 90-31, 90p.
- Clarke, J.S., Hacke, C.M., Peck, M.F., 1990, Geology and Ground-Water Resources of the Coastal Areas of Georgia, Georgia Geologic Survey Bulletin 113, 106 p.
- Choquette, P.W. and L.C. Pray, 1970, Geologic Nomenclature and Classification of Porosity in Sedimentary Carbonates, AAPG Bulletin, v. 54, no. 2, 207-250.
- Crabtree Jr., S. J., Ehrlich, R., Prince, C., 1984, Evaluation of strategies for segmentation of blue-dyed pores in thin sections of reservoir rocks: Computer Vision, Graphics and Image Processing, v. 28, 18.

- Denicol, P.S. and X.D. Jing, 1998, Effects of water salinity, saturation and clay content on the complex resistivity of sandstone samples, Geological Society, London, Special Publications, v. 136, 147-157.
- Dunham, R.J., 1962, Classification of carbonate rocks according to depositional texture, In: W.E. Ham (Editor) Classification of Carbonate Rocks-a symposium, AAPG Memoir 1, 108-121.
- Ehrlich, R., Crabtree, S.J., Horkowitz, K.O., Horkowitz, J.P., 1991, Petrography and reservoir physics: I. Objective classification of reservoir porosity, AAPG Bulletin v. 75, 1547-1562.
- Erickson, S.N. and R.D. Jarrard, 1999, Porosity-formation factor and porosity-velocity relationships in Barbados prism, Journal of Geophysical Research, v. 104, no. B7, 15,391-15, 407.
- Goggin, D.J., 1993, Probe permeametry: is it worth the effort?: Marine and Petroleum Geology, v. 10, 299-308.
- Heron, S.D. and H.S. Johnson, 1966, Clay mineralogy, stratigraphy, and structural setting of the Hawthorn Formation, Coosawhatchie District, South Carolina, Southeastern Geology, v. 7, no. 2, 51-63.
- Hurst, A., and D.J. Goggin, 1995, Probe permeametry: an overview and bibliography, AAPG Bulletin, v. 79, 463-473.
- Ijima, A., 2001, Zeolites in Petroleum and Natural Gas Reservoirs, Reviews in Mineralogy and Geochemistry, v.45, no. 1, 347-402.
- Jonscher, A.K., 1975, The interpretation of non-ideal dielectric admittance and impedance diagrams, physica status solidi (a), v. 32, no. 2, 665-676.
- Jorgensen, D.G. and M. Petricola, 1994, Petrophysical Analysis of Geophysical Logs of the National Drilling Company-U.S. Geological Survey Ground-Water Research Project for the Abu Dhabi Emirate, United Arab Emirates: U.S. Geological Survey Water-Supply Paper 2417, 35 p.
- Karpoff, A.M., Destrigneville, C., Stille, P., 2007, Clinoptilolite as a new proxy of enhanced biogenic silica productivity in lower Miocene carbonate sediments of the Bahamas platform: Isotopic and thermodynamic evidence, Chemical Geology, vol. 245, 285-304.
- Keys, W.S., 1990, Borehole Geophysics Applied to Ground-Water Investigations, U.S. Geological Survey Techniques of Water Resources Investigations, Book 2, Chapter E-2, 150 p.
- Klinkenberg, L.J., 1941, The Permeability Of Porous Media To Liquids and Gases, American Petroleum Institute Drilling and Production Practice, 200-213.
- Knight, R.J. and N. Amos, 1987, The dielectric constant of sandstones, 60kHz to 4 MHz, Geophysics, v. 52, no. 5, 644-654.
- Kwader, T., 1985, Estimating Aquifer Permeability from Formation Resistivity Factors, Ground Water, v.23, no.6, 762-766.
- Kwader, T., 1982, Interpretation of Borehole Geophysical Logs and Their Application to Water Resource Investigations, Florida State University dissertation, 201 p.

- Lin, W. and J.J. Roberts, 1997, Electrical properties of a partially saturated Topopah Spring Tuff: Water distribution as a function of saturation, *Water Resources Research*, v. 33, no. 4, 577-587.
- Lindner-Lunsford, J.B., and B.W. Bruce, 1995, Use of Electric Logs to Estimate Water Quality of Pre-Tertiary Aquifers, *Ground Water*, v. 33, no. 4, 547-555.
- Martini, E., 1971, Standard Tertiary calcareous nannoplankton zonation, In Farinacci, A. (Ed.), *Proceedings of the Second Planktonic Conference, Roma, 1970*, 739-785.
- McCullum, M.J. and H.B. Countd, 1964, Relation of salt-water encroachment to the major aquifer zones, Savannah area, Georgia and South Carolina, U.S. Geological Survey Water-Supply Paper 1613-D, 26 p.
- McRae, S.G., 1972, Glauconite, *Earth Science Reviews*, Elsevier Publishing Compant, Amsterdam, The Netherlands, 397-440.
- Miller, J.A., 1986, Hydrogeologic framework of the Floridan aquifer system in Florida and in parts of Georgia, Alabama, and South Carolina: U.S. Geological Survey Professional Paper 1403-B, 91 p.
- Moore, D.M., and R.C. Reynolds Jr., 1997, *X-Ray Diffraction and the Identification and Analysis of Clay Minerals*, 2nd edition, Oxford University Press, Inc., New York, NY, 378 p.
- Mount Sopris Instrument Company, Inc., 2012, personal communication.
- Ostrowicki, K. and L.J. Williams, 2011, Saline aquifers in coastal Georgia: assessment using borehole geophysical logs at the Fort Pulaski Core Site, Chatham County, Georgia, Abstract for Georgia Water Resources Conference 2011, 5 p.
- Palm Beach County Water Utilities Department, 2009, Lake Region Water Treatment Plant Concentrate Injection Well System PBCWUD Project No. 03-169, Manuscript on file.
- Parker, D.E., Jones, P.D., Folland, C.K., Bevan, A., 1994, Interdecadal changes of surface temperature since the late nineteenth century, *Journal of Geophysical Research*, vol.99, no.D7, 14,373-14,399.
- Post, Buckley, Schuh, and Jernigan, Inc., 1992, Zemel Rd. Landfill Test/Injection Well Project, Charlotte County, Florida, Project No. 10-231.46, Manuscript on file.
- Post, Buckley, Schuh, and Jernigan, Inc., 1989, Atlantic Utilities Test/Injection Well, Project No. 01-196.08, Manuscript on file.
- Ramakrishan, T.S., Rabaute, A., Fordham, E.J., Ramamoorthy, R., Herron, M., Matteson, A., Ranghurman, B., 1998, A petrophysical and petrographic study of carbonate cores from the Thamama Formation: SPE Paper 49502, 14 p.
- Railsback, L.B., 1993, Effect of acidic buffers on clay minerals recovered from calcareous soils: an X-ray diffraction study, *Soil Science*, v. 155, no.3, 206-210.
- Raistrick, I.D., Ho, C., Huggins, R.A., 1976, Ionic conductivity of some Lithium silicates and aluminosilicates, *Journal of the Electrochemical Society*, v. 123, no. 10, 1,469-1,476.
- Reese, R.S. 2000, Hydrogeology and the Distribution of Salinity in the Floridan Aquifer System, Southwestern Florida: U.S. Geological Survey Water-Resources Investigations Report 98-4253.

Reynolds, R.C., Jr., and R.C. Reynolds, 1996, NEWMOD-FOR WINDOWS™. THE CALCULATION OF ONE-DIMENSIONAL X-RAY DIFFRACTION PATTERNS OF MIXED-LAYERED CLAY MINERALS, Hanover, NH, 24 p.

Reynolds, W.R. and C.W. Williford, 1991, Zeolite and clay-mineral induced resistivity in simulated reservoir sand. *Journal of Petroleum Science and Engineering*, v. 5, 163-172.

Rietveld, H.M., 1969, A profile refinement method for nuclear and magnetic structures, *Journal of Applied Crystallography*, v. 2, 65-71.

Riggs, S.R., 1979, Phosphorite sedimentation in Florida- A model phosphogenic system: *Economic Geology*, v. 74, no.2, 285-315.

Salem, H.M. and G.V. Chilingarian, 1999, The cementation factor of Archie's equation for shaly sandstone reservoirs, *Journal of Petroleum Science and Engineering*, v. 23, no. 2, 83-93.

Schnoebelen, D.J., Bugliosi, E.F., Krothe, N.C., 1995, Delineation of a Saline Ground-Water Boundary from Borehole Geophysical Data, v. 33, no. 6, 965-976.

Sheppard, R.A., 1971, Clinoptilolite of Possible Economic Value in Sedimentary Deposits of the Conterminous United States, *United States Geological Survey Bulletin* 1332-B, 15 p.

Sutherland, W.J., Halvorsen, J.A., Hurst, A., McPhee, C.A., Robertson, G., Whattler, P.R., Worthington, P.F., 1993, Recommended practices for probe permeametry: *Marine and Petroleum Geology*, v. 10, 309-317.

Swanson, R.G., 1981, *Sample Examination Manual, Methods in Exploration Series*, AAPG, Tulsa, OK, 45p.

Switzer, G. and A.J. Boucot, 1955, The mineral composition of some microfossils, *Journal of Paleontology*, v. 29, no. 3, 525-533.

Taylor, J.C., and S.R. Pecover, 1988, Quantitative Analysis of Phases of Zeolite Bearing Rocks from Full X-ray Diffraction Profiles, *Australian Journal of Physics*, vol. 41, 323-335.

Tiab, D. and E.C. Donaldson, 2004, *Petrophysics*, Gulf Professional Publishing, Burlington, MA, 889p.

University of Miami Comparative Sedimentary Laboratory, 2010, *TSGui Digital Image Analysis Software Manual*, ver. 1, 102 pp.

Van den Berg, E.H., Meesters, A.G.C.A, Kenter, J.A.M., Schlager, W., 2002, Automated separation of touching grains in digital images of thin sections: *Computers and Geosciences*, v. 28, 179-190.

Verwer, K., Eberli, G.P., Weger, R.J., 2011, Effect of pore structure on electrical resistivity in carbonates, *AAPG Bulletin*, v. 95, no. 2, 175-190.

Waxman, M.H. and L.M. Smits, 1968, Electrical Conductivities in Oil-Bearing Shaly Sands, *Trans. AIME*, v. 243, 107-122.

- Weaver, C.E. and K.C. Beck, 1977, Miocene of the S.E. United States: A Model for Chemical Sedimentation in a Peri-Marine Environment, *Sedimentary Geology*, v. 17, no. 1-2, 324 p.
- Weger, R.J., Eberli, G.P., Baechle, G.T., Masafferro, J.L., Sun, Y., 2009, Quantification of pore structure and its effect on sonic velocity and permeability in carbonates, *AAPG Bulletin*, v. 93, no. 10, 1297-1317.
- Williams, L.J. and H.E. Gill, 2010, Revised Hydrogeologic Framework of the Floridan Aquifer System in the Northern Coastal Area of Georgia and Adjacent Parts of South Carolina, U.S. Geological Survey Scientific Investigations Report 2010-5158, 115 p.
- Wyllie, M.R.J., 1963, *The fundamentals of well log interpretation*, 3rd edition, Academic Press, Inc., New York, NY, 238 p.
- Wyllie, M.R.J., Gregory, A.R., and G.H.F. Gardner, 1958, An experimental investigation of the factors affecting elastic wave velocities in porous media, *Geophysics*, v. 23, 459-493.
- Young, R.A., and D.B. Wiles, 1982, Profile shape functions in Rietveld refinements, *Journal of Applied Crystallography*, v. 15, no.3, 430-438.
- Zorski, T., Ossowski, A., Srodon, J., Kawiak, T., 2011, Evaluation of mineral composition and petrophysical parameters by the integration of core analysis data and wireline well log data: the Carpathian Foredeep case study, *Clay Minerals*, v. 46, 25-45.

APPENDIX A

X-RAY DIFFRACTION DATA

Sample ID	Quartz (%)	Calcite (%)	Clinoptilolite (%)	Glauconite (%)	K-Feldspar (%)	R _{wp}
CI-108	22.57	28.23	0.00	49.20	0.00	27.89
CI-112	13.60	86.40	0.00	0.00	0.00	18.06
CI-177	1.08	98.92	0.00	0.00	0.00	12.01
CI-346	2.67	96.74	0.00	0.00	0.59	12.49
CI-390	5.30	88.26	6.44	0.00	0.00	11.41
CI-424	1.55	97.85	0.60	0.00	0.00	10.49
CI-476	7.21	92.79	0.00	0.00	0.00	11.10
CI-526	0.81	99.19	0.00	0.00	0.00	10.54
CI-628	1.48	98.52	0.00	0.00	0.00	10.65
CI-735	1.28	96.76	1.96	0.00	0.00	10.33
CI-781	4.56	87.37	8.07	0.00	0.00	10.25
CI-826	2.42	91.04	6.53	0.00	0.00	10.50
CI-835	1.42	91.93	6.65	0.00	0.00	10.49
CI-902	4.14	88.44	7.41	0.00	0.00	10.90
CI-907	0.82	94.43	4.75	0.00	0.00	11.48
CI-926	2.94	89.69	7.37	0.00	0.00	11.20
CI-937	5.89	84.13	9.98	0.00	0.00	12.30
CI-952	2.59	92.72	4.69	0.00	0.00	11.04
CI-965	3.45	90.48	6.07	0.00	0.00	10.60
CI-977	5.72	46.98	5.06	42.24	0.00	10.60
CI-1013	3.17	35.68	7.74	53.40	0.00	12.75

Data excludes clay minerals and amorphous phases

APPENDIX B

SIMILAR STUDIES IN THE FLORIDAN AQUIFER SYSTEM

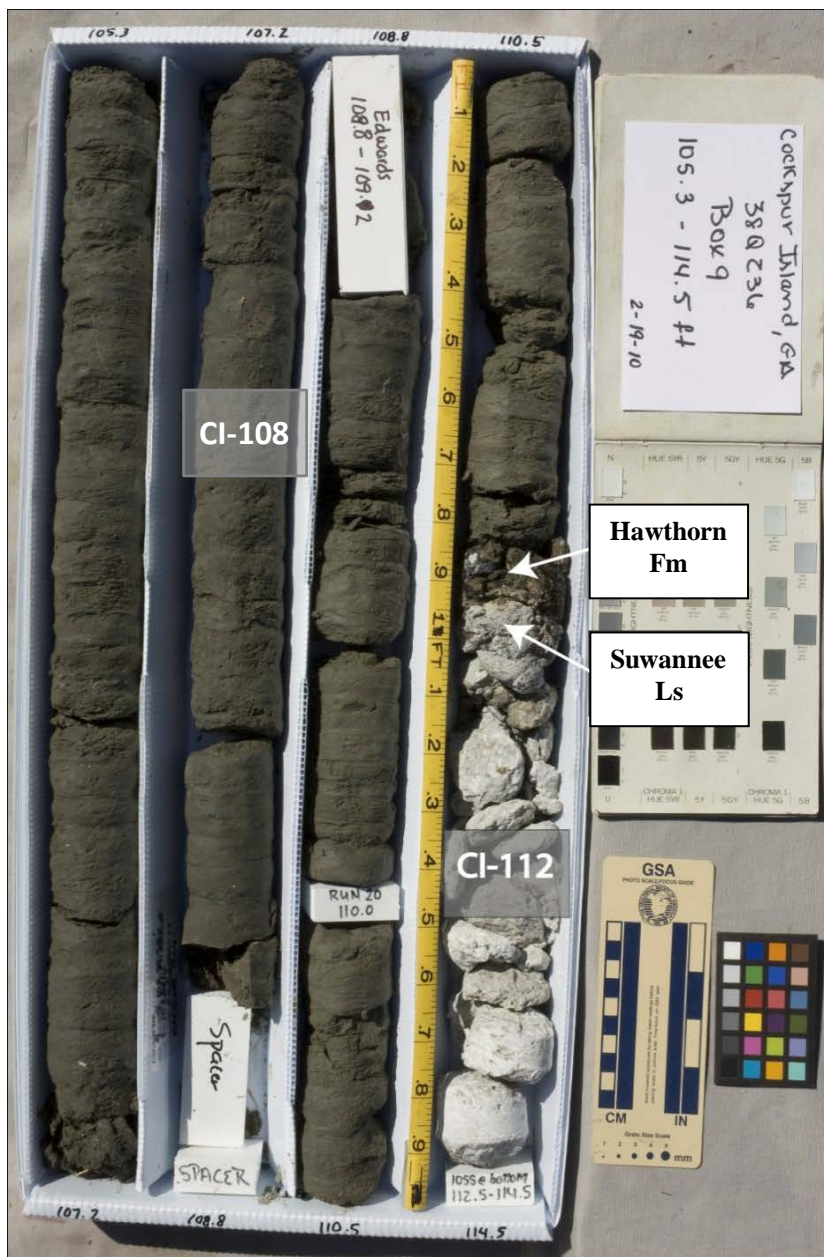
<u>Study</u>	<u>County, State</u>	<u>Depth (ft)</u>	<u>Formation</u>	<u>Rock Type</u>	<u>porosity (%)</u>	<u>Perm (mD)</u>	<u>F</u>	<u>m</u>	<u>Mineralogy</u>
Palm Beach Co Water Utilities Department,2009	Palm Bch, FL	1956.4	Avon Park	Dolomitized micrite to packstone	21.4	Low(secondary)	17.94	1.87	100%Dol
Palm Beach Co Water Utilities Department,2009	Palm Bch, FL	1959	Avon Park	Brecciated packstone dolomite	6.4	Low (primary); moderate-high (secondary)	1956	2.75	100%Dol
Palm Beach Co Water Utilities Department,2009	Palm Bch, FL	2354.5	Avon Park	Packstone	4.5	Low-moderate (secondary)	1016	2.24	100%Dol
Palm Beach Co Water Utilities Department,2009	Palm Bch, FL	2359.4	Avon Park	Packstone	6.1	Low-moderate (secondary)	1326	2.57	100%Dol
Palm Beach Co Water Utilities Department,2009	Palm Bch, FL	2522	Avon Park	Wackestone	12.4	Very low	38.17	1.74	100%Ls
Palm Beach Co Water Utilities Department,2009	Palm Bch, FL	2531.5	Avon Park	Wackestone	14	Very low	36.84	1.83	100%Ls
Palm Beach Co Water Utilities Department 2009	Palm Bch, FL	2788.1	Avon Park	Packestone to wackestone	24.1	Low to very low	14.27	1.87	100%Ls
Palm Beach Co Water Utilities Department 2009	Palm Bch, FL	2793.5	Avon Park	Packestone to wackestone	26.3	Low to very low	12.21	1.87	100%Ls
Palm Beach Co Water Utilities Department 2009	Palm Bch, FL	2807.7	Avon Park	Packestone to wackestone	11.6	Moderate	68.74	1.97	100%Ls
Palm Beach Co Water Utilities Department 2009	Palm Bch, FL	2812	Avon Park	Packestone to wackestone	26.1	Moderate	23.24	2.34	100%Ls
Palm Beach County Water Utilities Department 2009	Palm Bch, FL	2819.2	Avon Park	Packestone to grainstone	16.4	High	10.94	1.32	100%Ls
Post, Buckley, Schuh, and Jernigan, Inc.,1989	Sarasota, FL	1047-1048	Ocala Group	Dolomitized grainstone	20.5	21	13.4	1.64	96%Dol,3%Clay, 1%Qtz

<u>Study</u>	<u>County, State</u>	<u>Depth (ft)</u>	<u>Formation</u>	<u>Rock Type</u>	<u>porosity (%)</u>	<u>Perm (mD)</u>	<u>F</u>	<u>m</u>	<u>Mineralogy</u>
Post, Buckley, Schuh, and Jernigan, Inc.,1989	Sarasota, FL	1054.5-1055	Ocala Group	Dolomitized grainstone	24.1	124	15.8	1.94	97%Dol,2%Clay, 1%Qtz
Post, Buckley, Schuh, and Jernigan, Inc.,1989	Sarasota, FL	1241-1242	Avon Park	Dolomitized grainstone	22.9	1.4	14.9	1.83	72%Cal,22%Dol,5%Clay
Post, Buckley, Schuh, and Jernigan, Inc.,1989	Sarasota, FL	1244-1245	Avon Park	Grainstone	28.9	344	11.4	1.96	90%Cal,6%Dol,4%Clay
Post, Buckley, Schuh, and Jernigan, Inc.,1989	Sarasota, FL	1272.5-1273	Avon Park	Dolomitized packstone/ grainstone	3.8	.0020	912	2.08	96%Dol,3%Clay,1%Cal
Post, Buckley, Schuh, and Jernigan, Inc.,1989	Sarasota, FL	1281-1282	Avon Park	Dolomitized packstone/ grainstone	1.4	.00047	1199	1.66	97%Dol,2%Clay,1%Cal
Post, Buckley, Schuh, and Jernigan, Inc.,1989	Sarasota, FL	1302-1303	Avon Park	Dolomitized wackstone/ packstone	3.0	.0016	779	1.90	95%Dol,3%Clay,1%Cal
Post, Buckley, Schuh, and Jernigan, Inc.,1989	Sarasota, FL	1310-1311	Avon Park	Dolomitized wackstone/ packstone	3.9	.00034	216	1.66	96%Dol,4%Clay
Post, Buckley, Schuh, and Jernigan, Inc.,1989	Sarasota, FL	1331.5-1332	Avon Park	Dolomitized packstone/ grainstone	4.0	.00038	189	1.63	96%Dol,3%Clay,1%K-Feldspar
Post, Buckley, Schuh, and Jernigan, Inc.,1989	Sarasota, FL	1324.5-1325	Avon Park	Dolomitized packstone/ grainstone	6.1	.00074	98.1	1.64	96%Dol,4%Clay
Post, Buckley, Schuh, and Jernigan, Inc.,1989	Sarasota, FL	1350-1351	Avon Park	Dolomitized grainstone	7.0	.00017	1132	2.64	98%Dol,2%Clay
Post, Buckley, Schuh, and Jernigan, Inc.,1989	Sarasota, FL	1345-1345.4	Avon Park	Dolomitized packstone/ grainstone	5.1	.0012	126	1.63	92%Dol,6%Clay,2%K-spar

<u>Study</u>	<u>County, State</u>	<u>Depth (ft)</u>	<u>Formation</u>	<u>Rock Type</u>	<u>Porosity (%)</u>	<u>Perm (mD)</u>	<u>F</u>	<u>m</u>	<u>Mineralogy</u>
Post, Buckley, Schuh, and Jernigan, Inc.,1989	Sarasota, FL	1377-1378	Avon Park	Dolomitized packstone/ grainstone	2.1	.00044	1959	1.96	89%Dol,10%Clay, 1%Qtz
Post, Buckley, Schuh, and Jernigan, Inc., 1989	Sarasota, FL	1399-1400	Avon Park	Dolomitized grainstone	4.4	.00057	1838	2.41	88%Dol,9%Clay,
Post, Buckley, Schuh, and Jernigan, Inc.,1989	Sarasota, FL	1395-1396	Avon Park	Dolomitized grainstone	4.2	.0026	870	2.14	89%Dol,9%Clay,1%Qtz, 1%K-spar
Post, Buckley, Schuh, and Jernigan, Inc.,1989	Sarasota, FL	1427-1428	Avon Park	Dolomitized grainstone	27.1	184	17	2.17	97%Dol,3%Clay
Post, Buckley, Schuh, and Jernigan, Inc., 1989	Sarasota, FL	1419.5-1420	Avon Park	Dolomitized grainstone	20.7	1340	59.9	2.6	97%Dol,3%Clay
Post, Buckley, Schuh, and Jernigan, Inc.,1989	Sarasota, FL	1575-1576	Avon Park	Dolomitized grainstone	4.0	0.77	861	1.22	97%Dol,2%Clay,1%Qtz
Post, Buckley, Schuh, and Jernigan, Inc.,1992	Charlotte, FL	1325	Ocala Group	Finely crystalline limestone	34.4	14.8	9.03	2.06	98%Cal,1%Qtz,1%Dol
Post, Buckley, Schuh, and Jernigan, Inc.,1992	Charlotte, FL	1334	Ocala Group	Finely crystalline limestone	32.5	5.94	8.89	1.94	98%Cal,1%Qtz,1%Dol
Post, Buckley, Schuh, and Jernigan, Inc.,1992	Charlotte, FL	1442	Ocala Group	Finely crystalline limestone	33.7	7.01	8.65	1.98	94%Cal,5%Dol,1%Qtz
Post, Buckley, Schuh, and Jernigan, Inc.,1992	Charlotte, FL	1457	Ocala Group	Finely crystalline	28.9	3.63	11.60	1.97	87%Cal,12%Dol,1%Qtz
Post, Buckley, Schuh, and Jernigan, Inc.,1992	Charlotte, FL	1623	Avon Park	Crystalline limestone	35.3	15.1	8.39	2.04	100%Cal
Post, Buckley, Schuh, and Jernigan, Inc.,1992	Charlotte, FL	1636	Avon Pak	Crystalline limestone	30.5	28.1	11.29	2.04	99%Cal,1%Qtz

<u>Study</u>	<u>County, State</u>	<u>Depth</u>	<u>Formation</u>	<u>Rock Type</u>	<u>Porosity (%)</u>	<u>Perm (mD)</u>	<u>F</u>	<u>m</u>	<u>Mineralogy</u>
Post, Buckley, Schuh, and Jernigan, Inc.,1992	Charlotte, FL	1732	Avon Park	Crystalline/ sparry limestone	34.3	28.1	7.43	1.87	97% Cal,2% Dol,1% Qtz
Post, Buckley, Schuh, and Jernigan, Inc.,1992	Charlotte, FL	1771	Avon Park	Crystalline limestone	30.3	8.36	9.07	1.85	98% Cal,2% Dol,
Post, Buckley, Schuh, and Jernigan, Inc.,1992	Charlotte, FL	1780	Avon Park	Microcrystalline limestone	26.5	1.86	11.56	1.84	98% Cal,1% Dol,1% Qtz
Post, Buckley, Schuh, and Jernigan, Inc.,1992	Charlotte, FL	1898	Avon Park	Coarsely crystalline limestone	31.4	273	14.20	2.29	99% Cal,1% Qtz
Post, Buckley, Schuh, and Jernigan, Inc.,1992	Charlotte, FL	1902	Avon Park	Coarsely crystalline limestone	30.1	172	13.20	2.15	99% Cal,1% Qtz
Post, Buckley, Schuh, and Jernigan, Inc.,1992	Charlotte, FL	2078	Lake City	Microcrystalline dolomite	2.7	.001	1474	2.02	91% Cal,8% Dol,1% Qtz
Post, Buckley, Schuh, and Jernigan, Inc.,1992	Charlotte, FL	2116	Lake City	Crystalline limestone	23.6	2.95	27.56	2.30	48% Dol,51% Celestite
Post, Buckley, Schuh, and Jernigan, Inc.,1992	Charlotte, FL	2249	Lake City	Crystalline in micirtic matrix limestone	15.5	.15	27.59	1.78	52% Cal,45% Dol,2% Qtz
Post, Buckley, Schuh, and Jernigan, Inc.,1992	Charlotte, FL	2260	Lake City	Crystalline in micirtic matrix limestone	20.6	.94	17.69	1.82	72% Cal, 26% Dol, 2% Qtz
Post, Buckley, Schuh, and Jernigan, Inc.,1992	Charlotte, FL	2320	Lake City	Finely crystalline /cryptocrystalline dolomite	24.2	2.3	31.09	2.42	97% Dol, 2% Cal, 1% Qtz
Post, Buckley, Schuh, and Jernigan, Inc.,1992	Charlotte, FL	2327	Lake City	Finely crystalline /cryptocrystalline dolomite	23.8	1.8	42.65	2.61	98% Dol,1% Cal, 1% Qtz
Post, Buckley, Schuh, and Jernigan, Inc.,1992	Charlotte, FL	2432	Lake City	Crystalline limestone	24.9	6.65	15.43	1.97	91% Cal,8% Dol,1% Qtz
Post, Buckley, Schuh, and Jernigan, Inc.,1992	Charlotte, FFL	2446	Lake City	Crystalline dolomite	9.3	.17	91.70	1.90	65% Dol,34% Cal,1% Qtz

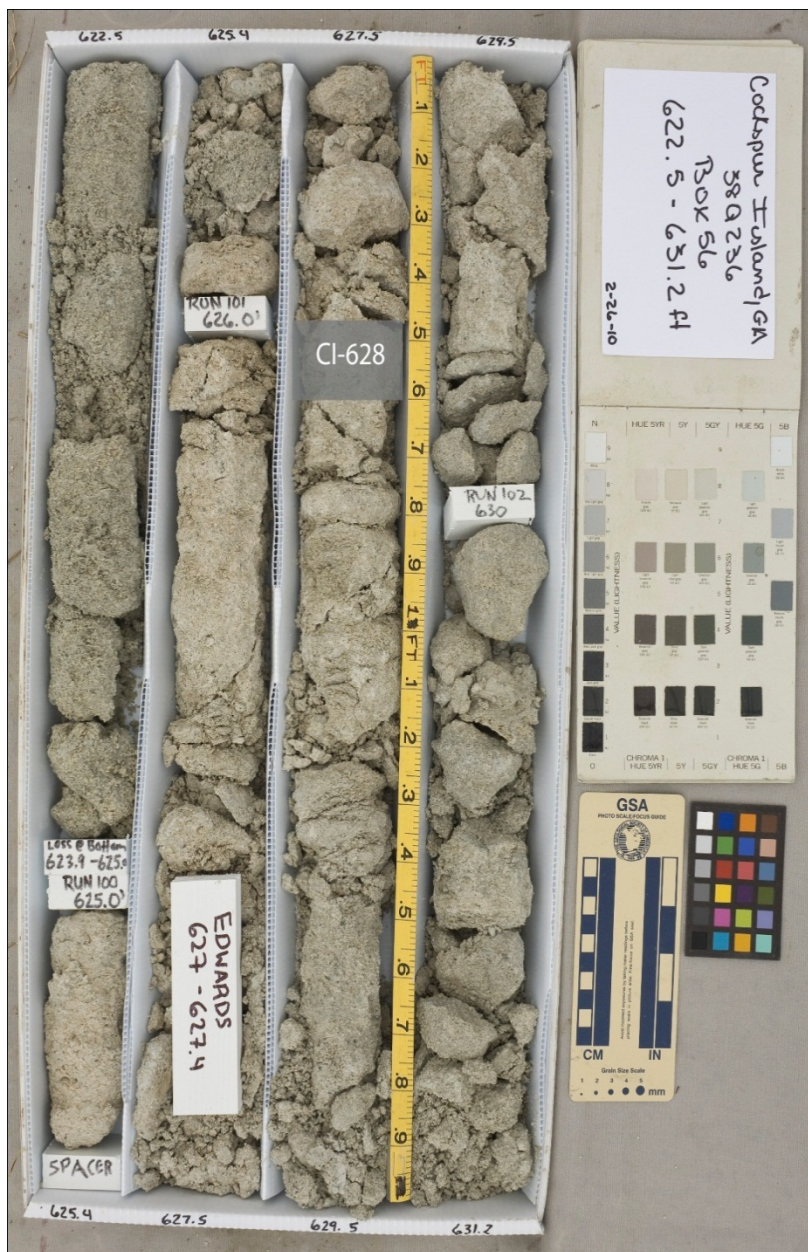
APPENDIX C
CORE PHOTOGRAPHS























APPENDIX D
RESISTIVITY MEASUREMENTS

CI-112

TestDesc:CI-1-111.9-112-33.733g		Oper:KO		Sample:CI sample suite saturated					
Comments:saturated 210mS/cm sample			DispB:Q or L/C		Trig:Internal			CktMode:Parallel	Mult:X 1
Dev:OFF		Date:04/20/2011		Time:16:49:21		L:0	C:0	R:1	Z :1
TimeDelt:0.000		OscLvl:1.000		Mode:No 3488A					
FreqMeas:Low Only									
Freq	L	C	R	Z	L(B)	C(B)	R(B)	Z (B)	
1.00E+02	0.00E+00	0.00E+00	9.69E+03	9.67E+03	0.00E+00	0.00E+00	1.08E-08	-3.76E+00	
1.20E+02	0.00E+00	0.00E+00	9.66E+03	9.65E+03	0.00E+00	0.00E+00	8.02E-09	-3.33E+00	
3.00E+02	0.00E+00	0.00E+00	9.52E+03	9.52E+03	0.00E+00	0.00E+00	1.98E-09	-2.03E+00	
5.00E+02	0.00E+00	0.00E+00	9.47E+03	9.47E+03	0.00E+00	0.00E+00	9.86E-10	-1.68E+00	
1.00E+03	0.00E+00	0.00E+00	9.40E+03	9.40E+03	0.00E+00	0.00E+00	4.30E-10	-1.45E+00	
3.00E+03	0.00E+00	0.00E+00	9.28E+03	9.28E+03	0.00E+00	0.00E+00	1.41E-10	-1.40E+00	
5.00E+03	0.00E+00	0.00E+00	9.22E+03	9.23E+03	0.00E+00	0.00E+00	8.86E-11	-1.47E+00	
1.00E+04	0.00E+00	0.00E+00	9.14E+03	9.14E+03	0.00E+00	0.00E+00	5.04E-11	-1.65E+00	
3.00E+04	0.00E+00	0.00E+00	8.98E+03	8.98E+03	0.00E+00	0.00E+00	2.29E-11	-2.22E+00	
5.00E+04	0.00E+00	0.00E+00	8.91E+03	8.90E+03	0.00E+00	0.00E+00	1.66E-11	-2.66E+00	
1.00E+05	0.00E+00	0.00E+00	8.79E+03	8.77E+03	0.00E+00	0.00E+00	1.15E-11	-3.63E+00	

CI-177

TestDesc:CI-9h 15.673g		Oper:808		Sample:CI sample suite saturated					
Comments:saturated 10g/L			DispB:Q or L/C		Trig:Internal			CktMode:Parallel	Mult:X 1
Dev:OFF		Date:04/25/2011		Time:15:50:59		L:0	C:0	R:1	Z :1
TimeDelt:0.000		OscLvl:1.000		Mode:No 3488A					
FreqMeas:Low Only									
Freq	L	C	R	Z	L(B)	C(B)	R(B)	Z (B)	
1.00E+02	0.00E+00	0.00E+00	1.25E+03	6.08E+02	0.00E+00	0.00E+00	2.28E-06	-6.10E+01	
1.20E+02	0.00E+00	0.00E+00	9.98E+02	5.29E+02	0.00E+00	0.00E+00	2.12E-06	-5.79E+01	
3.00E+02	0.00E+00	0.00E+00	3.99E+02	3.15E+02	0.00E+00	0.00E+00	1.03E-06	-3.77E+01	
5.00E+02	0.00E+00	0.00E+00	3.03E+02	2.71E+02	0.00E+00	0.00E+00	5.24E-07	-2.64E+01	
1.00E+03	0.00E+00	0.00E+00	2.54E+02	2.46E+02	0.00E+00	0.00E+00	1.69E-07	-1.51E+01	
3.00E+03	0.00E+00	0.00E+00	2.35E+02	2.34E+02	0.00E+00	0.00E+00	2.33E-08	-5.88E+00	
5.00E+03	0.00E+00	0.00E+00	2.32E+02	2.32E+02	0.00E+00	0.00E+00	9.14E-09	-3.80E+00	
1.00E+04	0.00E+00	0.00E+00	2.30E+02	2.30E+02	0.00E+00	0.00E+00	2.59E-09	-2.14E+00	
3.00E+04	0.00E+00	0.00E+00	2.29E+02	2.29E+02	0.00E+00	0.00E+00	3.66E-10	-9.04E-01	
5.00E+04	0.00E+00	0.00E+00	2.29E+02	2.29E+02	0.00E+00	0.00E+00	1.57E-10	-6.46E-01	
1.00E+05	0.00E+00	0.00E+00	2.28E+02	2.29E+02	0.00E+00	0.00E+00	6.23E-11	-5.10E-01	

CI-390

TestDesc:CI-15 14.403g		Oper:808		Sample:CI sample suite saturated					
Comments:saturated 10g/L			DispB:Q or L/C		Trig:Internal			CktMode:Parallel	Mult:X 1
Dev:OFF		Date:04/25/2011		Time:15:08:33		L:0	C:0	R:1	Z :1
TimeDelt:0.000		OscLvl:1.000		Mode:No 3488A					
FreqMeas:Low Only									
Freq	L	C	R	Z	L(B)	C(B)	R(B)	Z (B)	
1.00E+02	0.00E+00	0.00E+00	8.95E+02	4.32E+02	0.00E+00	0.00E+00	3.25E-06	-6.16E+01	
1.20E+02	0.00E+00	0.00E+00	7.37E+02	3.78E+02	0.00E+00	0.00E+00	3.01E-06	-5.92E+01	
3.00E+02	0.00E+00	0.00E+00	2.90E+02	2.19E+02	0.00E+00	0.00E+00	1.59E-06	-4.10E+01	
5.00E+02	0.00E+00	0.00E+00	2.12E+02	1.84E+02	0.00E+00	0.00E+00	8.66E-07	-3.00E+01	
1.00E+03	0.00E+00	0.00E+00	1.70E+02	1.62E+02	0.00E+00	0.00E+00	3.04E-07	-1.80E+01	
3.00E+03	0.00E+00	0.00E+00	1.52E+02	1.50E+02	0.00E+00	0.00E+00	4.53E-08	-7.40E+00	
5.00E+03	0.00E+00	0.00E+00	1.49E+02	1.49E+02	0.00E+00	0.00E+00	1.82E-08	-4.88E+00	
1.00E+04	0.00E+00	0.00E+00	1.47E+02	1.47E+02	0.00E+00	0.00E+00	5.30E-09	-2.81E+00	
3.00E+04	0.00E+00	0.00E+00	1.46E+02	1.46E+02	0.00E+00	0.00E+00	7.74E-10	-1.23E+00	
5.00E+04	0.00E+00	0.00E+00	1.46E+02	1.46E+02	0.00E+00	0.00E+00	3.34E-10	-8.80E-01	
1.00E+05	0.00E+00	0.00E+00	1.46E+02	1.46E+02	0.00E+00	0.00E+00	1.20E-10	-6.33E-01	

CI-424

TestDesc:CI-16-423.7-423.8-19.413g		Oper:KO		Sample:CI sample suite saturated		Comments:saturated					
2,000 mS/cm sample		DispB:Q or L/C		Trig:Internal		CktMode:Parallel		Mult:X 1	Dev:OFF		
Date:04/21/2011		Time:11:39:45		L:0	C:0	R:1	Z :1	TimeDelt:0.000	OscLvl:1.000	Mode:No 3488A	FreqMeas:Low Only
Freq	L	C	R	Z	L(B)	C(B)	R(B)	Z (B)			
1.00E+02	0.00E+00	0.00E+00	2.00E+20	1.18E+04	0.00E+00	0.00E+00	1.21E-07	-6.37E+01			
1.20E+02	0.00E+00	0.00E+00	2.00E+20	1.02E+04	0.00E+00	0.00E+00	1.16E-07	-6.33E+01			
3.00E+02	0.00E+00	0.00E+00	9.68E+03	5.17E+03	0.00E+00	0.00E+00	8.63E-08	-5.75E+01			
5.00E+02	0.00E+00	0.00E+00	5.99E+03	3.68E+03	0.00E+00	0.00E+00	6.80E-08	-5.19E+01			
1.00E+03	0.00E+00	0.00E+00	3.40E+03	2.51E+03	0.00E+00	0.00E+00	4.25E-08	-4.22E+01			
3.00E+03	0.00E+00	0.00E+00	1.89E+03	1.70E+03	0.00E+00	0.00E+00	1.35E-08	-2.57E+01			
5.00E+03	0.00E+00	0.00E+00	1.63E+03	1.53E+03	0.00E+00	0.00E+00	6.90E-09	-1.95E+01			
1.00E+04	0.00E+00	0.00E+00	1.44E+03	1.40E+03	0.00E+00	0.00E+00	2.54E-09	-1.29E+01			
3.00E+04	0.00E+00	0.00E+00	1.30E+03	1.30E+03	0.00E+00	0.00E+00	4.68E-10	-6.56E+00			
5.00E+04	0.00E+00	0.00E+00	1.28E+03	1.27E+03	0.00E+00	0.00E+00	2.14E-10	-4.90E+00			
1.00E+05	0.00E+00	0.00E+00	1.25E+03	1.25E+03	0.00E+00	0.00E+00	8.13E-11	-3.66E+00			

CI-476

TestDesc:CI-17h-475.8-476.3-17.715g		Oper:KO		Sample:CI sample suite saturated		Comments:saturated					
2,000 mS/cm sample		DispB:Q or L/C		Trig:Internal		CktMode:Parallel		Mult:X 1	Dev:OFF		
Date:04/21/2011		Time:09:34:05		L:0	C:0	R:1	Z :1	TimeDelt:0.000	OscLvl:1.000	Mode:No 3488A	FreqMeas:Low Only
Freq	L	C	R	Z	L(B)	C(B)	R(B)	Z (B)			
1.00E+02	0.00E+00	0.00E+00	1.20E+05	4.53E+04	0.00E+00	0.00E+00	3.25E-08	-6.78E+01			
1.20E+02	0.00E+00	0.00E+00	1.05E+05	3.89E+04	0.00E+00	0.00E+00	3.16E-08	-6.81E+01			
3.00E+02	0.00E+00	0.00E+00	4.71E+04	1.84E+04	0.00E+00	0.00E+00	2.00E+20	-6.69E+01			
5.00E+02	0.00E+00	0.00E+00	2.81E+04	1.22E+04	0.00E+00	0.00E+00	2.00E+20	-6.42E+01			
1.00E+03	0.00E+00	0.00E+00	1.36E+04	7.30E+03	0.00E+00	0.00E+00	1.83E-08	-5.75E+01			
3.00E+03	0.00E+00	0.00E+00	5.14E+03	3.87E+03	0.00E+00	0.00E+00	9.00E-09	-4.10E+01			
5.00E+03	0.00E+00	0.00E+00	3.77E+03	3.17E+03	0.00E+00	0.00E+00	5.42E-09	-3.26E+01			
1.00E+04	0.00E+00	0.00E+00	2.86E+03	2.64E+03	0.00E+00	0.00E+00	2.32E-09	-2.26E+01			
3.00E+04	0.00E+00	0.00E+00	2.32E+03	2.28E+03	0.00E+00	0.00E+00	4.73E-10	-1.17E+01			
5.00E+04	0.00E+00	0.00E+00	2.23E+03	2.20E+03	0.00E+00	0.00E+00	2.20E-10	-8.72E+00			
1.00E+05	0.00E+00	0.00E+00	2.15E+03	2.13E+03	0.00E+00	0.00E+00	8.49E-11	-6.52E+00			

CI-527

TestDesc:CI-21-526.5-526.6-21.257g		Oper:KO		Sample:CI sample suite saturated		Comments:saturated					
2,000 mS/cm sample		DispB:Q or L/C		Trig:Internal		CktMode:Parallel		Mult:X 1	Dev:OFF		
Date:04/21/2011		Time:09:23:35		L:0	C:0	R:1	Z :1	TimeDelt:0.000	OscLvl:1.000	Mode:No 3488A	FreqMeas:Low Only
Freq	L	C	R	Z	L(B)	C(B)	R(B)	Z (B)			
1.00E+02	0.00E+00	0.00E+00	4.35E+03	3.62E+03	0.00E+00	0.00E+00	2.43E-07	-3.35E+01			
1.20E+02	0.00E+00	0.00E+00	3.95E+03	3.41E+03	0.00E+00	0.00E+00	1.96E-07	-3.02E+01			
3.00E+02	0.00E+00	0.00E+00	2.96E+03	2.84E+03	0.00E+00	0.00E+00	5.39E-08	-1.67E+01			
5.00E+02	0.00E+00	0.00E+00	2.76E+03	2.70E+03	0.00E+00	0.00E+00	2.37E-08	-1.16E+01			
1.00E+03	0.00E+00	0.00E+00	2.61E+03	2.60E+03	0.00E+00	0.00E+00	7.41E-09	-6.93E+00			
3.00E+03	0.00E+00	0.00E+00	2.53E+03	2.52E+03	0.00E+00	0.00E+00	1.16E-09	-3.15E+00			
5.00E+03	0.00E+00	0.00E+00	2.51E+03	2.50E+03	0.00E+00	0.00E+00	5.12E-10	-2.30E+00			
1.00E+04	0.00E+00	0.00E+00	2.49E+03	2.49E+03	0.00E+00	0.00E+00	1.88E-10	-1.68E+00			
3.00E+04	0.00E+00	0.00E+00	2.46E+03	2.46E+03	0.00E+00	0.00E+00	5.59E-11	-1.48E+00			
5.00E+04	0.00E+00	0.00E+00	2.45E+03	2.45E+03	0.00E+00	0.00E+00	3.74E-11	-1.65E+00			
1.00E+05	0.00E+00	0.00E+00	2.43E+03	2.43E+03	0.00E+00	0.00E+00	2.48E-11	-2.16E+00			

CI-628

TestDesc:CI-50 32.537g		Oper:808		Sample:CI sample suite saturated			Comments:saturated		
10g/L		DispB:Q or L/C		Trig:Internal	CktMode:Parallel	Mult:X 1	Dev:OFF		
Date:04/25/2011 Time:13:43:52		L:0	C:0	R:1	Z :1	TimeDelt:0.000	OscLvl:1.000	Mode:No 3488A	FreqMeas:Low Only
Freq	L	C	R	Z	L(B)	C(B)	R(B)	Z (B)	
1.00E+02	0.00E+00	0.00E+00	4.68E+03	4.63E+03	0.00E+00	0.00E+00	4.87E-08	-8.13E+00	
1.20E+02	0.00E+00	0.00E+00	4.63E+03	4.60E+03	0.00E+00	0.00E+00	3.57E-08	-7.09E+00	
3.00E+02	0.00E+00	0.00E+00	4.49E+03	4.48E+03	0.00E+00	0.00E+00	7.63E-09	-3.68E+00	
5.00E+02	0.00E+00	0.00E+00	4.45E+03	4.45E+03	0.00E+00	0.00E+00	3.27E-09	-2.61E+00	
1.00E+03	0.00E+00	0.00E+00	4.41E+03	4.42E+03	0.00E+00	0.00E+00	1.11E-09	-1.75E+00	
3.00E+03	0.00E+00	0.00E+00	4.38E+03	4.38E+03	0.00E+00	0.00E+00	2.52E-10	-1.19E+00	
5.00E+03	0.00E+00	0.00E+00	4.37E+03	4.37E+03	0.00E+00	0.00E+00	1.45E-10	-1.14E+00	
1.00E+04	0.00E+00	0.00E+00	4.35E+03	4.35E+03	0.00E+00	0.00E+00	8.28E-11	-1.29E+00	
3.00E+04	0.00E+00	0.00E+00	4.30E+03	4.30E+03	0.00E+00	0.00E+00	4.71E-11	-2.18E+00	
5.00E+04	0.00E+00	0.00E+00	4.27E+03	4.27E+03	0.00E+00	0.00E+00	3.89E-11	-2.99E+00	
1.00E+05	0.00E+00	0.00E+00	4.21E+03	4.20E+03	0.00E+00	0.00E+00	3.09E-11	-4.67E+00	

CI-735

TestDesc:CI-29h 24.544g		Oper:808		Sample:CI sample suite saturated			Comments:saturated		
10g/L		DispB:Q or L/C		Trig:Internal	CktMode:Parallel	Mult:X 1	Dev:OFF		
Date:04/25/2011 Time:15:16:44		L:0	C:0	R:1	Z :1	TimeDelt:0.000	OscLvl:1.000	Mode:No 3488A	FreqMeas:Low Only
Freq	L	C	R	Z	L(B)	C(B)	R(B)	Z (B)	
1.00E+02	0.00E+00	0.00E+00	9.42E+02	5.85E+02	0.00E+00	0.00E+00	2.13E-06	-5.15E+01	
1.20E+02	0.00E+00	0.00E+00	7.76E+02	5.26E+02	0.00E+00	0.00E+00	1.86E-06	-4.73E+01	
3.00E+02	0.00E+00	0.00E+00	4.17E+02	3.73E+02	0.00E+00	0.00E+00	6.33E-07	-2.64E+01	
5.00E+02	0.00E+00	0.00E+00	3.61E+02	3.45E+02	0.00E+00	0.00E+00	2.78E-07	-1.75E+01	
1.00E+03	0.00E+00	0.00E+00	3.33E+02	3.29E+02	0.00E+00	0.00E+00	8.11E-08	-9.64E+00	
3.00E+03	0.00E+00	0.00E+00	3.21E+02	3.21E+02	0.00E+00	0.00E+00	1.08E-08	-3.75E+00	
5.00E+03	0.00E+00	0.00E+00	3.20E+02	3.19E+02	0.00E+00	0.00E+00	4.32E-09	-2.48E+00	
1.00E+04	0.00E+00	0.00E+00	3.18E+02	3.18E+02	0.00E+00	0.00E+00	1.32E-09	-1.51E+00	
3.00E+04	0.00E+00	0.00E+00	3.16E+02	3.16E+02	0.00E+00	0.00E+00	2.50E-10	-8.53E-01	
5.00E+04	0.00E+00	0.00E+00	3.16E+02	3.16E+02	0.00E+00	0.00E+00	1.30E-10	-7.39E-01	
1.00E+05	0.00E+00	0.00E+00	3.15E+02	3.15E+02	0.00E+00	0.00E+00	6.42E-11	-7.27E-01	

CI-766

TestDesc:CI-28 19.668g		Oper:808		Sample:CI sample suite saturated			Comments:saturated		
100g/L		DispB:Q or L/C		Trig:Internal	CktMode:Parallel	Mult:X 1	Dev:OFF		
Date:04/25/2011 Time:13:48:48		L:0	C:0	R:1	Z :1	TimeDelt:0.000	OscLvl:1.000	Mode:No 3488A	FreqMeas:Low Only
Freq	L	C	R	Z	L(B)	C(B)	R(B)	Z (B)	Radians
1.00E+02	0.00E+00	0.00E+00	8.78E+02	4.82E+02	0.00E+00	0.00E+00	2.75E-06	-5.64E+01	-0.98512
1.20E+02	0.00E+00	0.00E+00	7.11E+02	4.26E+02	0.00E+00	0.00E+00	2.49E-06	-5.31E+01	-0.92719
3.00E+02	0.00E+00	0.00E+00	3.25E+02	2.69E+02	0.00E+00	0.00E+00	1.10E-06	-3.39E+01	-0.59247
5.00E+02	0.00E+00	0.00E+00	2.57E+02	2.36E+02	0.00E+00	0.00E+00	5.43E-07	-2.37E+01	-0.41371
1.00E+03	0.00E+00	0.00E+00	2.22E+02	2.16E+02	0.00E+00	0.00E+00	1.71E-07	-1.34E+01	-0.23403
3.00E+03	0.00E+00	0.00E+00	2.08E+02	2.08E+02	0.00E+00	0.00E+00	2.28E-08	-5.10E+00	-0.08898
5.00E+03	0.00E+00	0.00E+00	2.07E+02	2.07E+02	0.00E+00	0.00E+00	8.81E-09	-3.27E+00	-0.05707
1.00E+04	0.00E+00	0.00E+00	2.06E+02	2.06E+02	0.00E+00	0.00E+00	2.53E-09	-1.87E+00	-0.03264
3.00E+04	0.00E+00	0.00E+00	2.05E+02	2.05E+02	0.00E+00	0.00E+00	4.18E-10	-9.20E-01	-0.01606
5.00E+04	0.00E+00	0.00E+00	2.04E+02	2.04E+02	0.00E+00	0.00E+00	2.01E-10	-7.35E-01	-0.01283
1.00E+05	0.00E+00	0.00E+00	2.04E+02	2.04E+02	0.00E+00	0.00E+00	8.79E-11	-6.43E-01	-0.01122

CI-781

TestDesc:CI-30h 19.391g		Oper:808		Sample:CI sample suite saturated			Comments:saturated		
10g/L		DispB:Q or L/C		Trig:Internal	CktMode:Parallel	Mult:X 1	Dev:OFF		
Date:04/25/2011 Time:14:40:50		L:0	C:0	R:1	Z :1	TimeDelt:0.000	OscLvl:1.000	Mode:No 3488A	FreqMeas:Low Only
Freq	L	C	R	Z	L(B)	C(B)	R(B)	Z (B)	
1.00E+02	0.00E+00	0.00E+00	8.97E+02	4.78E+02	0.00E+00	0.00E+00	2.81E-06	-5.77E+01	
1.20E+02	0.00E+00	0.00E+00	7.21E+02	4.21E+02	0.00E+00	0.00E+00	2.55E-06	-5.43E+01	
3.00E+02	0.00E+00	0.00E+00	3.20E+02	2.65E+02	0.00E+00	0.00E+00	1.12E-06	-3.40E+01	
5.00E+02	0.00E+00	0.00E+00	2.54E+02	2.33E+02	0.00E+00	0.00E+00	5.43E-07	-2.34E+01	
1.00E+03	0.00E+00	0.00E+00	2.21E+02	2.15E+02	0.00E+00	0.00E+00	1.68E-07	-1.31E+01	
3.00E+03	0.00E+00	0.00E+00	2.08E+02	2.07E+02	0.00E+00	0.00E+00	2.20E-08	-4.94E+00	
5.00E+03	0.00E+00	0.00E+00	2.07E+02	2.06E+02	0.00E+00	0.00E+00	8.53E-09	-3.17E+00	
1.00E+04	0.00E+00	0.00E+00	2.05E+02	2.05E+02	0.00E+00	0.00E+00	2.46E-09	-1.82E+00	
3.00E+04	0.00E+00	0.00E+00	2.04E+02	2.04E+02	0.00E+00	0.00E+00	4.07E-10	-8.96E-01	
5.00E+04	0.00E+00	0.00E+00	2.04E+02	2.04E+02	0.00E+00	0.00E+00	1.96E-10	-7.17E-01	
1.00E+05	0.00E+00	0.00E+00	2.04E+02	2.04E+02	0.00E+00	0.00E+00	8.56E-11	-6.26E-01	

CI-826

TestDesc:CI-36 16.688g		Oper:808		Sample:CI sample suite saturated			Comments:saturated		
10g/L		DispB:Q or L/C		Trig:Internal	CktMode:Parallel	Mult:X 1	Dev:OFF		
Date:04/25/2011 Time:13:55:52		L:0	C:0	R:1	Z :1	TimeDelt:0.000	OscLvl:1.000	Mode:No 3488A	FreqMeas:Low Only
Freq	L	C	R	Z	L(B)	C(B)	R(B)	Z (B)	
1.00E+02	0.00E+00	0.00E+00	1.15E+03	5.68E+02	0.00E+00	0.00E+00	2.42E-06	-6.02E+01	
1.20E+02	0.00E+00	0.00E+00	9.01E+02	4.96E+02	0.00E+00	0.00E+00	2.22E-06	-5.64E+01	
3.00E+02	0.00E+00	0.00E+00	3.76E+02	3.08E+02	0.00E+00	0.00E+00	9.87E-07	-3.49E+01	
5.00E+02	0.00E+00	0.00E+00	2.95E+02	2.70E+02	0.00E+00	0.00E+00	4.79E-07	-2.39E+01	
1.00E+03	0.00E+00	0.00E+00	2.56E+02	2.49E+02	0.00E+00	0.00E+00	1.48E-07	-1.34E+01	
3.00E+03	0.00E+00	0.00E+00	2.40E+02	2.39E+02	0.00E+00	0.00E+00	2.00E-08	-5.17E+00	
5.00E+03	0.00E+00	0.00E+00	2.38E+02	2.38E+02	0.00E+00	0.00E+00	7.90E-09	-3.37E+00	
1.00E+04	0.00E+00	0.00E+00	2.37E+02	2.36E+02	0.00E+00	0.00E+00	2.36E-09	-2.00E+00	
3.00E+04	0.00E+00	0.00E+00	2.35E+02	2.35E+02	0.00E+00	0.00E+00	4.23E-10	-1.07E+00	
5.00E+04	0.00E+00	0.00E+00	2.34E+02	2.34E+02	0.00E+00	0.00E+00	2.13E-10	-8.97E-01	
1.00E+05	0.00E+00	0.00E+00	2.34E+02	2.34E+02	0.00E+00	0.00E+00	9.94E-11	-8.33E-01	

CI-835

TestDesc:CI-37 17.870g		Oper:808		Sample:CI sample suite saturated			Comments:saturated		
10g/L		DispB:Q or L/C		Trig:Internal	CktMode:Parallel	Mult:X 1	Dev:OFF		
Date:04/25/2011 Time:14:29:44		L:0	C:0	R:1	Z :1	TimeDelt:0.000	OscLvl:1.000	Mode:No 3488A	FreqMeas:Low Only
Freq	L	C	R	Z	L(B)	C(B)	R(B)	Z (B)	
1.00E+02	0.00E+00	0.00E+00	9.36E+02	4.91E+02	0.00E+00	0.00E+00	2.75E-06	-5.82E+01	
1.20E+02	0.00E+00	0.00E+00	7.44E+02	4.32E+02	0.00E+00	0.00E+00	2.50E-06	-5.44E+01	
3.00E+02	0.00E+00	0.00E+00	3.29E+02	2.76E+02	0.00E+00	0.00E+00	1.05E-06	-3.31E+01	
5.00E+02	0.00E+00	0.00E+00	2.65E+02	2.45E+02	0.00E+00	0.00E+00	4.99E-07	-2.25E+01	
1.00E+03	0.00E+00	0.00E+00	2.33E+02	2.27E+02	0.00E+00	0.00E+00	1.52E-07	-1.25E+01	
3.00E+03	0.00E+00	0.00E+00	2.20E+02	2.19E+02	0.00E+00	0.00E+00	2.06E-08	-4.88E+00	
5.00E+03	0.00E+00	0.00E+00	2.18E+02	2.18E+02	0.00E+00	0.00E+00	8.21E-09	-3.22E+00	
1.00E+04	0.00E+00	0.00E+00	2.17E+02	2.17E+02	0.00E+00	0.00E+00	2.49E-09	-1.94E+00	
3.00E+04	0.00E+00	0.00E+00	2.15E+02	2.15E+02	0.00E+00	0.00E+00	4.48E-10	-1.04E+00	
5.00E+04	0.00E+00	0.00E+00	2.15E+02	2.15E+02	0.00E+00	0.00E+00	2.23E-10	-8.58E-01	
1.00E+05	0.00E+00	0.00E+00	2.14E+02	2.14E+02	0.00E+00	0.00E+00	1.01E-10	-7.75E-01	

CI-902

TestDesc:CI-31h 27.125g		Oper:808		Sample:CI sample suite saturated			Comments:saturated		
10g/L		DispB:Q or L/C		Trig:Internal	CktMode:Parallel	Mult:X 1	Dev:OFF		
Date:04/25/2011 Time:14:50:57		L:0	C:0	R:1	Z :1	TimeDelt:0.000	OscLvl:1.000	Mode:No 3488A	FreqMeas:Low Only
Freq	L	C	R	Z	L(B)	C(B)	R(B)	Z (B)	
1.00E+02	0.00E+00	0.00E+00	7.55E+02	4.91E+02	0.00E+00	0.00E+00	2.45E-06	-4.92E+01	
1.20E+02	0.00E+00	0.00E+00	6.29E+02	4.44E+02	0.00E+00	0.00E+00	2.11E-06	-4.50E+01	
3.00E+02	0.00E+00	0.00E+00	3.55E+02	3.23E+02	0.00E+00	0.00E+00	6.90E-07	-2.48E+01	
5.00E+02	0.00E+00	0.00E+00	3.13E+02	3.00E+02	0.00E+00	0.00E+00	2.98E-07	-1.63E+01	
1.00E+03	0.00E+00	0.00E+00	2.91E+02	2.88E+02	0.00E+00	0.00E+00	8.48E-08	-8.81E+00	
3.00E+03	0.00E+00	0.00E+00	2.83E+02	2.82E+02	0.00E+00	0.00E+00	1.08E-08	-3.29E+00	
5.00E+03	0.00E+00	0.00E+00	2.82E+02	2.81E+02	0.00E+00	0.00E+00	4.19E-09	-2.12E+00	
1.00E+04	0.00E+00	0.00E+00	2.81E+02	2.81E+02	0.00E+00	0.00E+00	1.23E-09	-1.24E+00	
3.00E+04	0.00E+00	0.00E+00	2.80E+02	2.80E+02	0.00E+00	0.00E+00	2.19E-10	-6.59E-01	
5.00E+04	0.00E+00	0.00E+00	2.79E+02	2.79E+02	0.00E+00	0.00E+00	1.11E-10	-5.57E-01	
1.00E+05	0.00E+00	0.00E+00	2.79E+02	2.79E+02	0.00E+00	0.00E+00	5.33E-11	-5.36E-01	

CI-907

TestDesc:CI-32h 100g/l 20.721g		Oper:808		Sample:CI sample suite saturated			Comments:saturated		
10g/L		DispB:Q or L/C		Trig:Internal	CktMode:Parallel	Mult:X 1	Dev:OFF		
Date:04/25/2011 Time:13:27:46		L:0	C:0	R:1	Z :1	TimeDelt:0.000	OscLvl:1.000	Mode:No 3488A	FreqMeas:Low Only
Freq	L	C	R	Z	L(B)	C(B)	R(B)	Z (B)	
1.00E+02	0.00E+00	0.00E+00	1.13E+03	5.72E+02	0.00E+00	0.00E+00	2.40E-06	-5.94E+01	
1.20E+02	0.00E+00	0.00E+00	9.12E+02	5.00E+02	0.00E+00	0.00E+00	2.22E-06	-5.66E+01	
3.00E+02	0.00E+00	0.00E+00	3.78E+02	2.95E+02	0.00E+00	0.00E+00	1.13E-06	-3.88E+01	
5.00E+02	0.00E+00	0.00E+00	2.82E+02	2.49E+02	0.00E+00	0.00E+00	5.98E-07	-2.79E+01	
1.00E+03	0.00E+00	0.00E+00	2.32E+02	2.23E+02	0.00E+00	0.00E+00	1.98E-07	-1.61E+01	
3.00E+03	0.00E+00	0.00E+00	2.13E+02	2.12E+02	0.00E+00	0.00E+00	2.69E-08	-6.18E+00	
5.00E+03	0.00E+00	0.00E+00	2.10E+02	2.10E+02	0.00E+00	0.00E+00	1.05E-08	-3.99E+00	
1.00E+04	0.00E+00	0.00E+00	2.09E+02	2.09E+02	0.00E+00	0.00E+00	2.98E-09	-2.26E+00	
3.00E+04	0.00E+00	0.00E+00	2.08E+02	2.08E+02	0.00E+00	0.00E+00	4.51E-10	-1.02E+00	
5.00E+04	0.00E+00	0.00E+00	2.08E+02	2.08E+02	0.00E+00	0.00E+00	2.02E-10	-7.60E-01	
1.00E+05	0.00E+00	0.00E+00	2.07E+02	2.07E+02	0.00E+00	0.00E+00	7.84E-11	-5.86E-01	

CI-926

TestDesc:CI-43 20.868g		Oper:808		Sample:CI sample suite saturated			Comments:saturated		
10g/L		DispB:Q or L/C		Trig:Internal	CktMode:Parallel	Mult:X 1	Dev:OFF		
Date:04/25/2011 Time:14:20:37		L:0	C:0	R:1	Z :1	TimeDelt:0.000	OscLvl:1.000	Mode:No 3488A	FreqMeas:Low Only
Freq	L	C	R	Z	L(B)	C(B)	R(B)	Z (B)	
1.00E+02	0.00E+00	0.00E+00	7.66E+02	4.60E+02	0.00E+00	0.00E+00	2.77E-06	-5.31E+01	
1.20E+02	0.00E+00	0.00E+00	6.30E+02	4.11E+02	0.00E+00	0.00E+00	2.45E-06	-4.93E+01	
3.00E+02	0.00E+00	0.00E+00	3.21E+02	2.81E+02	0.00E+00	0.00E+00	9.07E-07	-2.88E+01	
5.00E+02	0.00E+00	0.00E+00	2.71E+02	2.56E+02	0.00E+00	0.00E+00	4.13E-07	-1.94E+01	
1.00E+03	0.00E+00	0.00E+00	2.46E+02	2.42E+02	0.00E+00	0.00E+00	1.23E-07	-1.07E+01	
3.00E+03	0.00E+00	0.00E+00	2.35E+02	2.35E+02	0.00E+00	0.00E+00	1.63E-08	-4.14E+00	
5.00E+03	0.00E+00	0.00E+00	2.34E+02	2.34E+02	0.00E+00	0.00E+00	6.46E-09	-2.71E+00	
1.00E+04	0.00E+00	0.00E+00	2.32E+02	2.32E+02	0.00E+00	0.00E+00	1.93E-09	-1.62E+00	
3.00E+04	0.00E+00	0.00E+00	2.31E+02	2.31E+02	0.00E+00	0.00E+00	3.45E-10	-8.61E-01	
5.00E+04	0.00E+00	0.00E+00	2.31E+02	2.31E+02	0.00E+00	0.00E+00	1.71E-10	-7.11E-01	
1.00E+05	0.00E+00	0.00E+00	2.30E+02	2.30E+02	0.00E+00	0.00E+00	7.70E-11	-6.37E-01	

CI-937

TestDesc:CI-33h 24.054g		Oper:808		Sample:CI sample suite saturated					
Comments:saturated 10g/L		DispB:Q or L/C		Trig:Internal		CktMode:Parallel		Mult:X 1	
Dev:OFF		Date:04/25/2011		Time:14:01:31		L:0 C:0 R:1 Z :1		TimeDelt:0.000 OscLvl:1.000 Mode:No 3488A	
FreqMeas:Low Only									
Freq	L	C	R	Z	L(B)	C(B)	R(B)	Z (B)	
1.00E+02	0.00E+00	0.00E+00	8.65E+02	5.11E+02	0.00E+00	0.00E+00	2.52E-06	-5.40E+01	
1.20E+02	0.00E+00	0.00E+00	7.20E+02	4.58E+02	0.00E+00	0.00E+00	2.24E-06	-5.06E+01	
3.00E+02	0.00E+00	0.00E+00	3.56E+02	3.04E+02	0.00E+00	0.00E+00	9.17E-07	-3.17E+01	
5.00E+02	0.00E+00	0.00E+00	2.92E+02	2.71E+02	0.00E+00	0.00E+00	4.46E-07	-2.23E+01	
1.00E+03	0.00E+00	0.00E+00	2.56E+02	2.50E+02	0.00E+00	0.00E+00	1.43E-07	-1.30E+01	
3.00E+03	0.00E+00	0.00E+00	2.40E+02	2.39E+02	0.00E+00	0.00E+00	2.06E-08	-5.36E+00	
5.00E+03	0.00E+00	0.00E+00	2.38E+02	2.38E+02	0.00E+00	0.00E+00	8.43E-09	-3.63E+00	
1.00E+04	0.00E+00	0.00E+00	2.36E+02	2.36E+02	0.00E+00	0.00E+00	2.58E-09	-2.22E+00	
3.00E+04	0.00E+00	0.00E+00	2.34E+02	2.34E+02	0.00E+00	0.00E+00	4.42E-10	-1.13E+00	
5.00E+04	0.00E+00	0.00E+00	2.34E+02	2.34E+02	0.00E+00	0.00E+00	2.12E-10	-9.02E-01	
1.00E+05	0.00E+00	0.00E+00	2.33E+02	2.34E+02	0.00E+00	0.00E+00	8.93E-11	-7.57E-01	

CI-952

TestDesc:CL-44 22.244g		Oper:808		Sample:CI sample suite saturated					
Comments:saturated 10g/L		DispB:Q or L/C		Trig:Internal		CktMode:Parallel		Mult:X 1	
Dev:OFF		Date:04/25/2011		Time:15:43:03		L:0 C:0 R:1 Z :1		TimeDelt:0.000 OscLvl:1.000 Mode:No 3488A	
FreqMeas:Low Only									
Freq	L	C	R	Z	L(B)	C(B)	R(B)	Z (B)	
1.00E+02	0.00E+00	0.00E+00	1.08E+03	5.22E+02	0.00E+00	0.00E+00	2.67E-06	-6.11E+01	
1.20E+02	0.00E+00	0.00E+00	8.57E+02	4.60E+02	0.00E+00	0.00E+00	2.45E-06	-5.78E+01	
3.00E+02	0.00E+00	0.00E+00	3.47E+02	2.78E+02	0.00E+00	0.00E+00	1.15E-06	-3.71E+01	
5.00E+02	0.00E+00	0.00E+00	2.67E+02	2.41E+02	0.00E+00	0.00E+00	5.77E-07	-2.60E+01	
1.00E+03	0.00E+00	0.00E+00	2.27E+02	2.20E+02	0.00E+00	0.00E+00	1.84E-07	-1.48E+01	
3.00E+03	0.00E+00	0.00E+00	2.11E+02	2.10E+02	0.00E+00	0.00E+00	2.52E-08	-5.79E+00	
5.00E+03	0.00E+00	0.00E+00	2.09E+02	2.09E+02	0.00E+00	0.00E+00	1.01E-08	-3.83E+00	
1.00E+04	0.00E+00	0.00E+00	2.08E+02	2.08E+02	0.00E+00	0.00E+00	2.97E-09	-2.25E+00	
3.00E+04	0.00E+00	0.00E+00	2.07E+02	2.07E+02	0.00E+00	0.00E+00	4.76E-10	-1.08E+00	
5.00E+04	0.00E+00	0.00E+00	2.07E+02	2.07E+02	0.00E+00	0.00E+00	2.22E-10	-8.34E-01	
1.00E+05	0.00E+00	0.00E+00	2.06E+02	2.06E+02	0.00E+00	0.00E+00	9.02E-11	-6.75E-01	

CI-965

TestDesc:CI-45 19.982g		Oper:808		Sample:CI sample suite saturated					
Comments:saturated 10g/L		DispB:Q or L/C		Trig:Internal		CktMode:Parallel		Mult:X 1	
Dev:OFF		Date:04/25/2011		Time:15:03:06		L:0 C:0 R:1 Z :1		TimeDelt:0.000 OscLvl:1.000 Mode:No 3488A	
FreqMeas:Low Only									
Freq	L	C	R	Z	L(B)	C(B)	R(B)	Z (B)	
1.00E+02	0.00E+00	0.00E+00	7.82E+02	4.71E+02	0.00E+00	0.00E+00	2.69E-06	-5.29E+01	
1.20E+02	0.00E+00	0.00E+00	6.43E+02	4.19E+02	0.00E+00	0.00E+00	2.40E-06	-4.93E+01	
3.00E+02	0.00E+00	0.00E+00	3.23E+02	2.81E+02	0.00E+00	0.00E+00	9.24E-07	-2.93E+01	
5.00E+02	0.00E+00	0.00E+00	2.70E+02	2.54E+02	0.00E+00	0.00E+00	4.27E-07	-1.99E+01	
1.00E+03	0.00E+00	0.00E+00	2.43E+02	2.38E+02	0.00E+00	0.00E+00	1.29E-07	-1.11E+01	
3.00E+03	0.00E+00	0.00E+00	2.31E+02	2.31E+02	0.00E+00	0.00E+00	1.74E-08	-4.33E+00	
5.00E+03	0.00E+00	0.00E+00	2.30E+02	2.29E+02	0.00E+00	0.00E+00	6.96E-09	-2.87E+00	
1.00E+04	0.00E+00	0.00E+00	2.28E+02	2.28E+02	0.00E+00	0.00E+00	2.13E-09	-1.74E+00	
3.00E+04	0.00E+00	0.00E+00	2.26E+02	2.27E+02	0.00E+00	0.00E+00	3.96E-10	-9.68E-01	
5.00E+04	0.00E+00	0.00E+00	2.26E+02	2.26E+02	0.00E+00	0.00E+00	2.01E-10	-8.18E-01	
1.00E+05	0.00E+00	0.00E+00	2.25E+02	2.25E+02	0.00E+00	0.00E+00	9.26E-11	-7.50E-01	

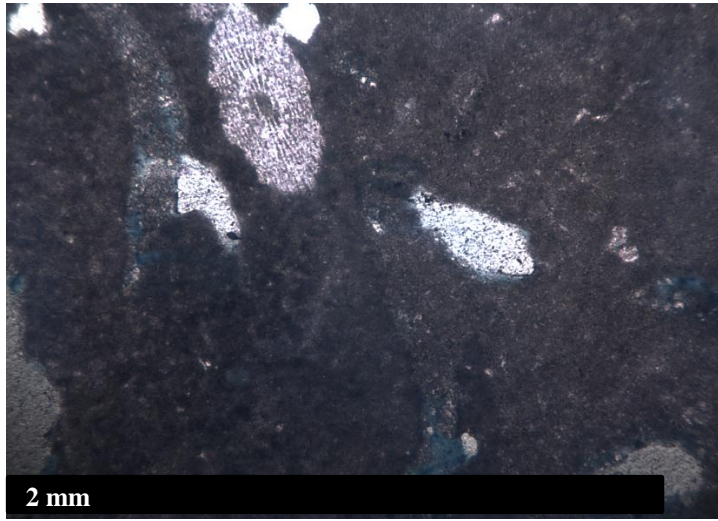
CI-977

TestDesc:CI-46 96.210g		Oper:808		Sample:CI sample suite saturated				
Comments:saturated 10g/L		DispB:Q or L/C		Trig:Internal		CktMode:Parallel		Mult:X 1
Dev:OFF		Date:04/25/2011		Time:16:06:39		L:0 C:0 R:1 Z :1		TimeDelt:0.000 OscLvl:1.000 Mode:No 3488A
FreqMeas:Low Only								
Freq	L	C	R	Z	L(B)	C(B)	R(B)	Z (B)
1.00E+02	0.00E+00	0.00E+00	2.00E+20	9.83E+01	0.00E+00	0.00E+00	1.43E-05	-6.23E+01
1.20E+02	0.00E+00	0.00E+00	1.68E+02	8.56E+01	0.00E+00	0.00E+00	1.33E-05	-5.92E+01
3.00E+02	0.00E+00	0.00E+00	6.54E+01	5.03E+01	0.00E+00	0.00E+00	6.74E-06	-3.97E+01
5.00E+02	0.00E+00	0.00E+00	4.83E+01	4.24E+01	0.00E+00	0.00E+00	3.61E-06	-2.87E+01
1.00E+03	0.00E+00	0.00E+00	3.92E+01	3.75E+01	0.00E+00	0.00E+00	1.25E-06	-1.72E+01
3.00E+03	0.00E+00	0.00E+00	3.51E+01	3.48E+01	0.00E+00	0.00E+00	1.93E-07	-7.27E+00
5.00E+03	0.00E+00	0.00E+00	3.45E+01	3.43E+01	0.00E+00	0.00E+00	8.06E-08	-4.98E+00
1.00E+04	0.00E+00	0.00E+00	3.39E+01	3.38E+01	0.00E+00	0.00E+00	2.59E-08	-3.15E+00
3.00E+04	0.00E+00	0.00E+00	3.33E+01	3.33E+01	0.00E+00	0.00E+00	5.04E-09	-1.81E+00
5.00E+04	0.00E+00	0.00E+00	3.31E+01	3.31E+01	0.00E+00	0.00E+00	2.56E-09	-1.52E+00
1.00E+05	0.00E+00	0.00E+00	3.29E+01	3.29E+01	0.00E+00	0.00E+00	1.12E-09	-1.32E+00

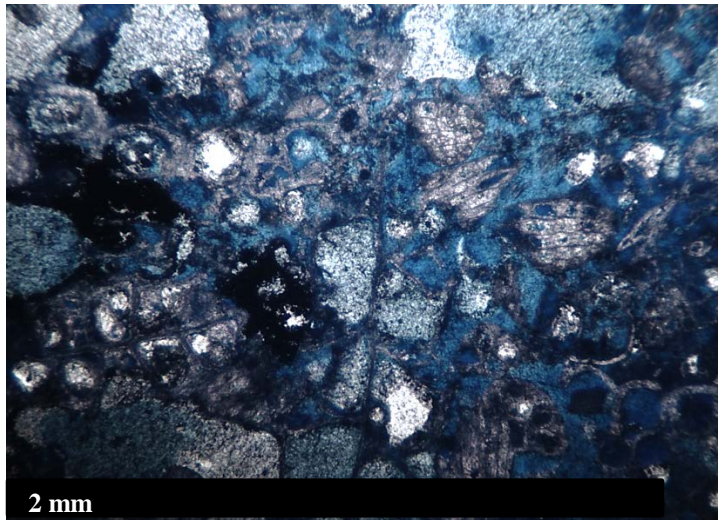
CI-1014

TestDesc:CI-34h 19.526g		Oper:808		Sample:CI sample suite saturated				
Comments:saturated 10g/L		DispB:Q or L/C		Trig:Internal		CktMode:Parallel		Mult:X 1
Dev:OFF		Date:04/25/2011		Time:15:37:17		L:0 C:0 R:1 Z :1		TimeDelt:0.000 OscLvl:1.000 Mode:No 3488A
FreqMeas:Low Only								
Freq	L	C	R	Z	L(B)	C(B)	R(B)	Z (B)
1.00E+02	0.00E+00	0.00E+00	7.81E+02	4.44E+02	0.00E+00	0.00E+00	2.93E-06	-5.50E+01
1.20E+02	0.00E+00	0.00E+00	6.46E+02	3.91E+02	0.00E+00	0.00E+00	2.69E-06	-5.26E+01
3.00E+02	0.00E+00	0.00E+00	2.96E+02	2.39E+02	0.00E+00	0.00E+00	1.30E-06	-3.60E+01
5.00E+02	0.00E+00	0.00E+00	2.27E+02	2.04E+02	0.00E+00	0.00E+00	6.83E-07	-2.60E+01
1.00E+03	0.00E+00	0.00E+00	1.90E+02	1.83E+02	0.00E+00	0.00E+00	2.27E-07	-1.51E+01
3.00E+03	0.00E+00	0.00E+00	1.74E+02	1.73E+02	0.00E+00	0.00E+00	3.19E-08	-5.98E+00
5.00E+03	0.00E+00	0.00E+00	1.72E+02	1.72E+02	0.00E+00	0.00E+00	1.27E-08	-3.94E+00
1.00E+04	0.00E+00	0.00E+00	1.71E+02	1.71E+02	0.00E+00	0.00E+00	3.88E-09	-2.38E+00
3.00E+04	0.00E+00	0.00E+00	1.69E+02	1.69E+02	0.00E+00	0.00E+00	7.37E-10	-1.35E+00
5.00E+04	0.00E+00	0.00E+00	1.68E+02	1.68E+02	0.00E+00	0.00E+00	3.80E-10	-1.15E+00
1.00E+05	0.00E+00	0.00E+00	1.68E+02	1.68E+02	0.00E+00	0.00E+00	1.76E-10	-1.06E+00

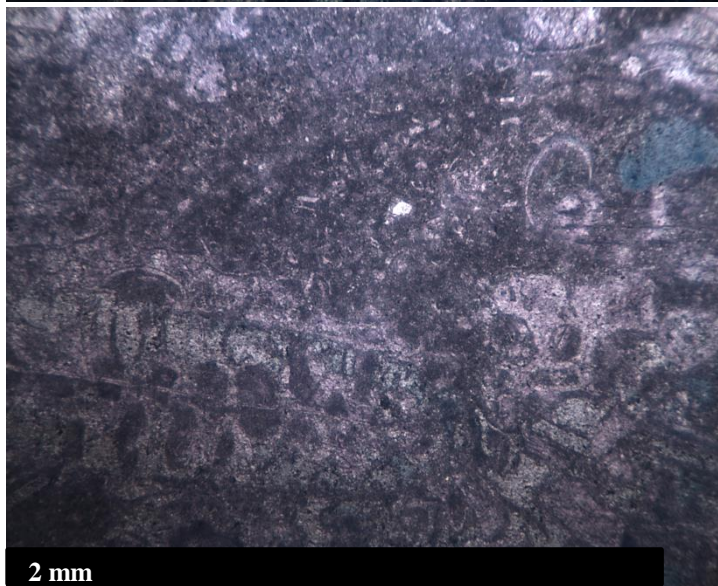
APPENDIX E
PETROGRAPHY



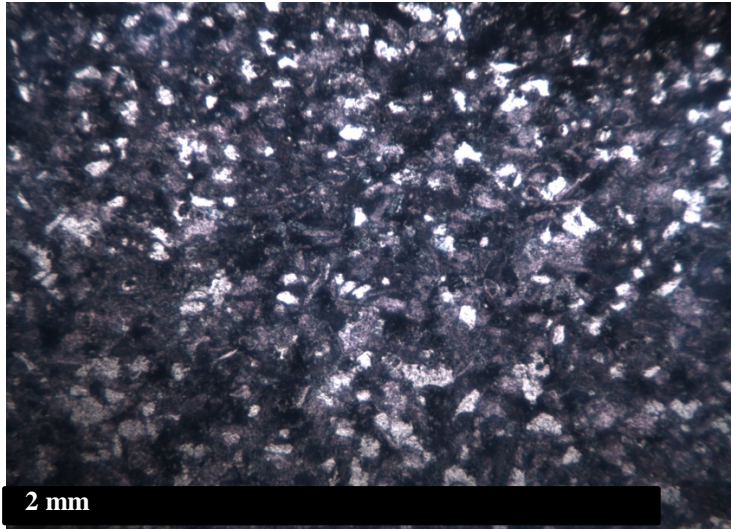
CI-112: Wackestone with vuggy porosity and abundant large angular to subrounded quartz grains. Few echinoderms, and several bryozoans.



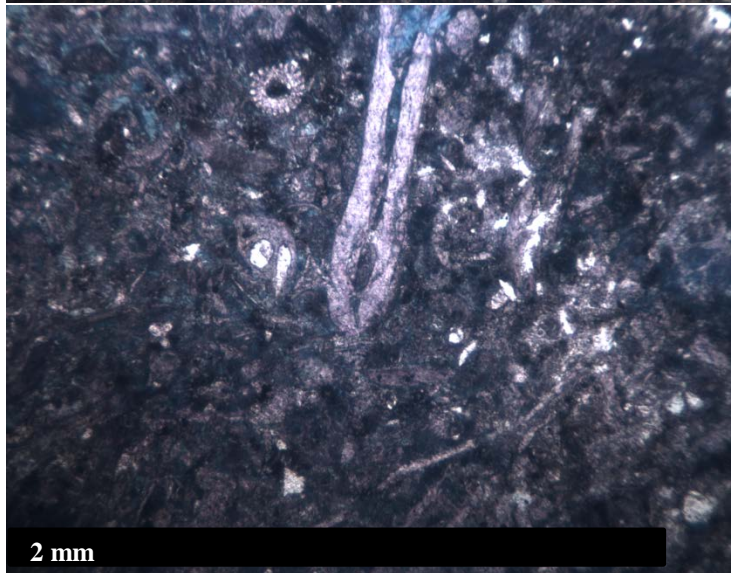
CI-177: Grainstone with abundant intraparticle and minor amounts of interparticle porosity. Abundant bryozoans and few echinoderms.



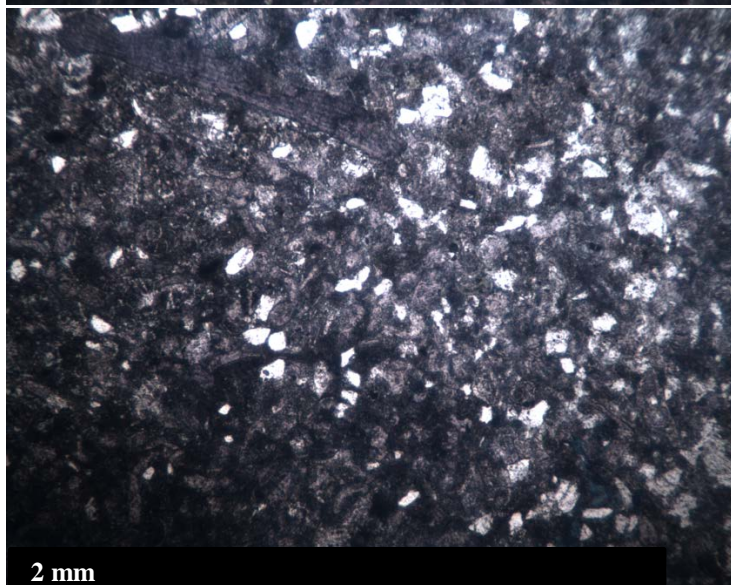
CI-191: Packstone with vugs, and minor amounts of intraparticle porosity. Abundant bryozoans, few echinoderms, few bivalves, and few foraminifera.



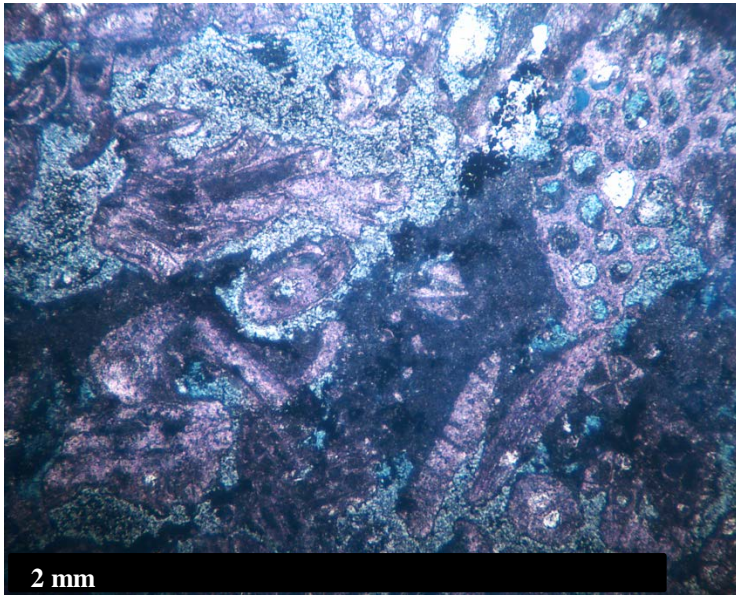
CI-390:Wackestone with abundant small angular to subrounded quartz grains. Poorly consolidate sample with areas of missing sample on thin section.



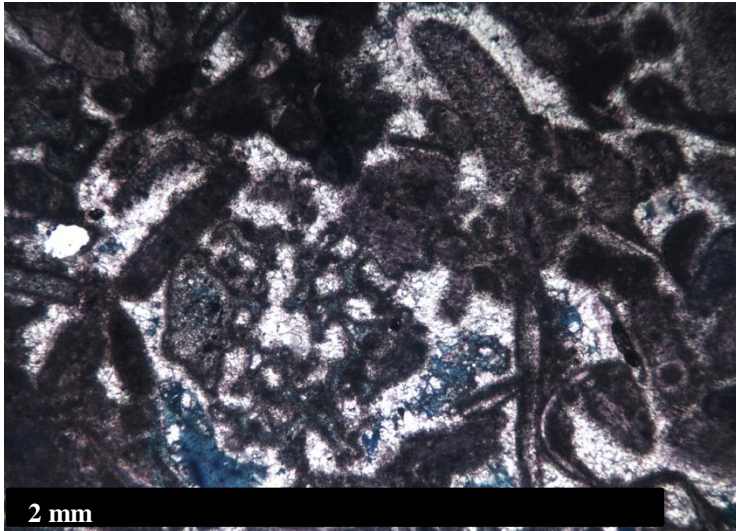
CI-424:Packstone with few small angular to subrounded quartz grains. Foraminifera and bryozoans common. Minor amounts of interparticle and intraparticle porosity. Poorly consolidated sample with areas of missing sample on thin section.



CI-476: Packstone with minor amounts of intraparticle porosity. Abundant small angular to subrounded quartz grains. Few foraminifera and few bryozoans.



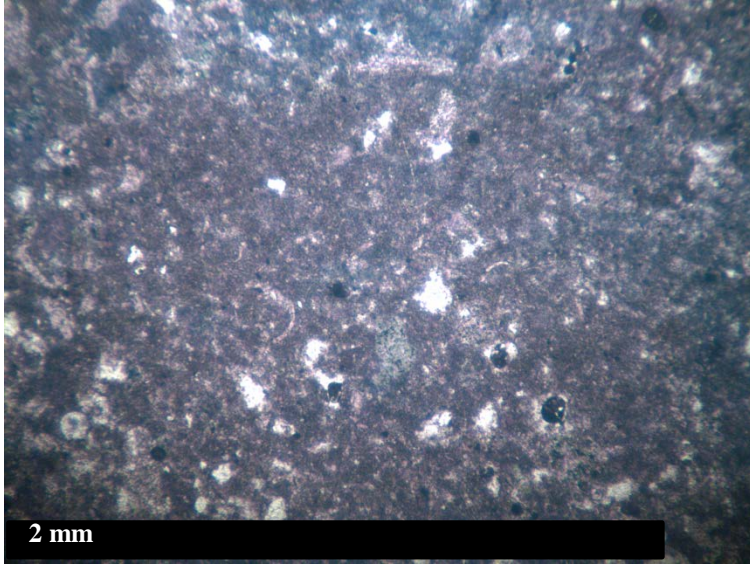
CI-527: Fine-grained grainstone with intraparticle and interparticle porosity. Abundant bryozoans. Glauconite infilling few bryozoans.



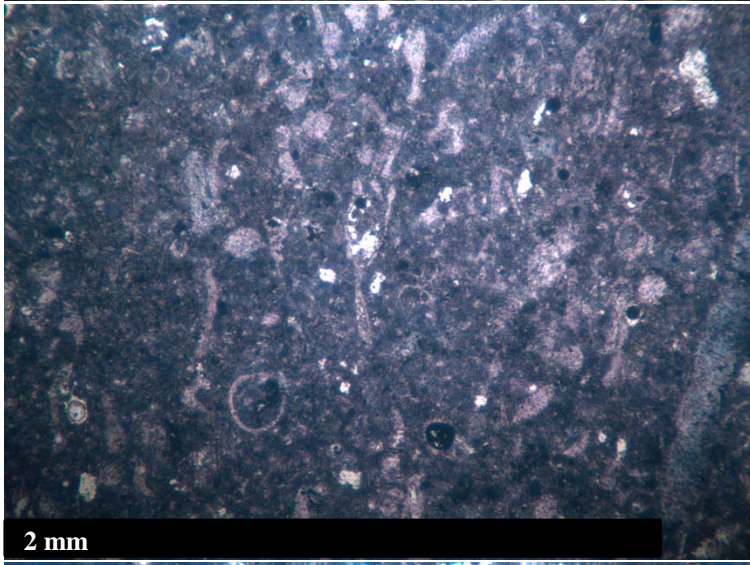
CI-628: Skeletal grainstone with vuggy porosity. Abundant echinoderm spicules and fragments, some bryozoans, and some foraminiferas. Glauconite infilling some bryozoans.



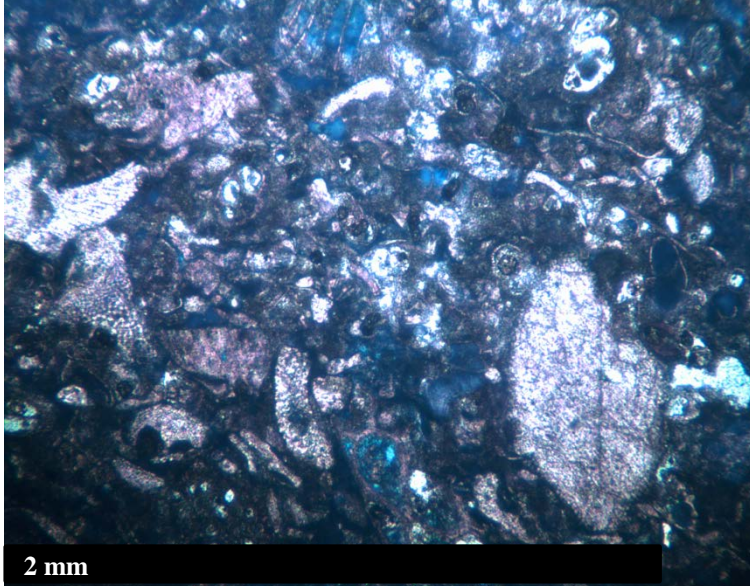
CI-735: Packstone with few bryozoans and some intraparticle and vuggy porosity. Glauconite infilling some bryozoans.



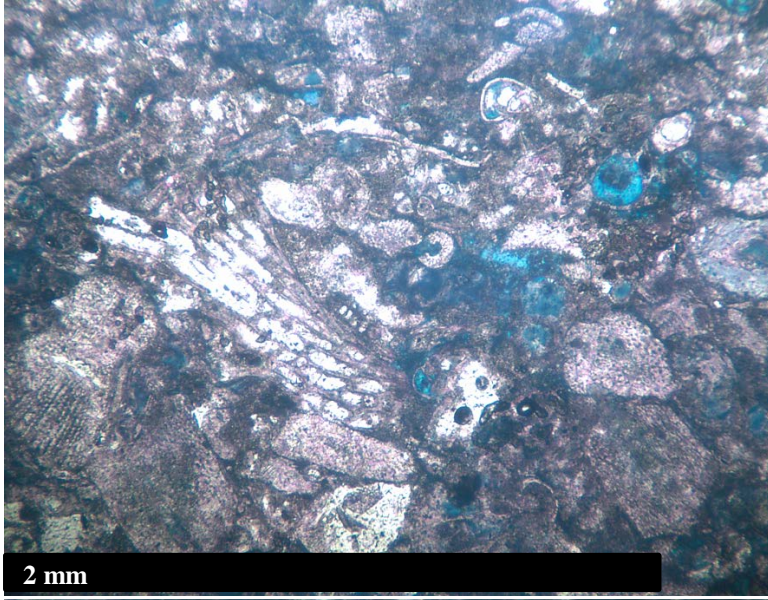
CI-766: Wackestone with some echinoderms, and few gastropods. Sparse glauconite pellets. Poorly consolidated sample with areas of missing sample on thin section.



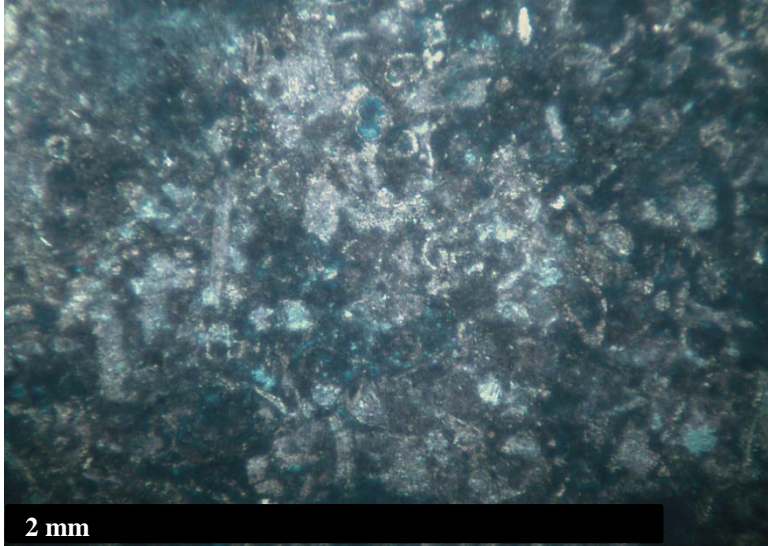
CI-781: Wackestone with some echinoderms, foraminifera, and gastropods.



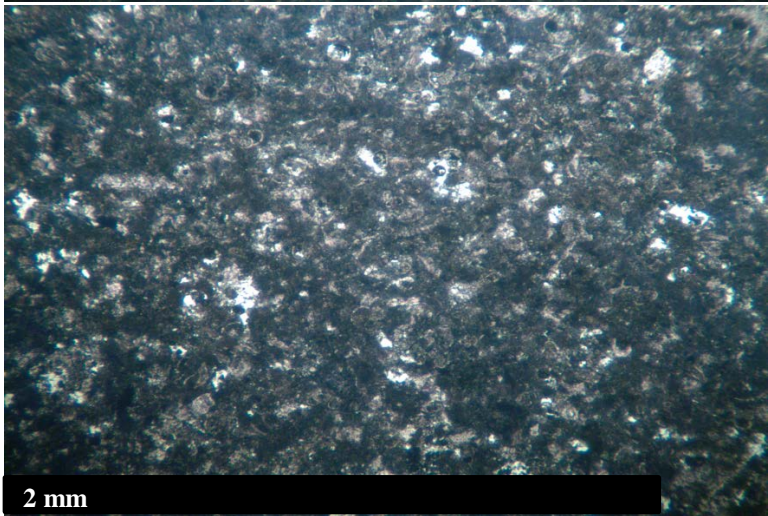
CI-826: Fine-grained packstone with interparticle porosity and abundant intraparticle porosity. Abundant bryozoans, some ostracodes, some echinoderms, and some foraminifera. Glauconite infilling few bryozoans.



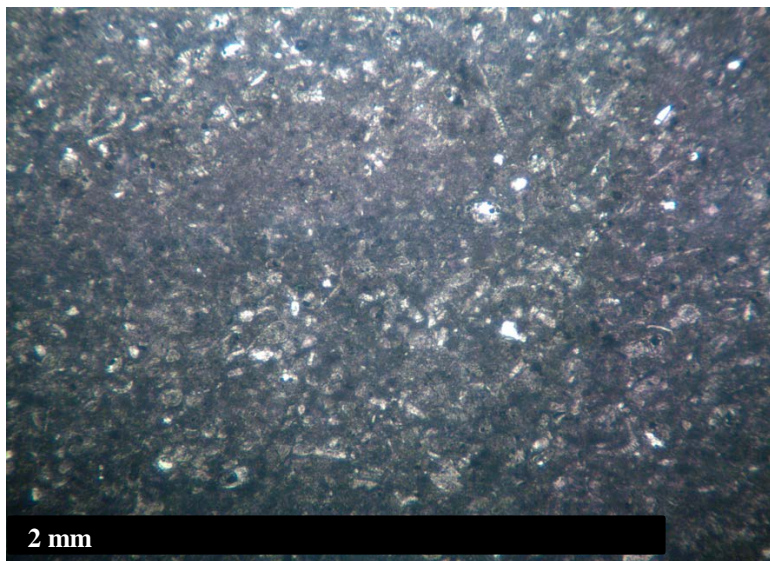
CI-835: Fine-grained packstone with intraparticle porosity. Abundant bryozoans, and some echinoderms. Glaucinite infilling some bryozoans.



CI-902: Fine-grained grainstone with sparse glauconite pellets. Some vugs.



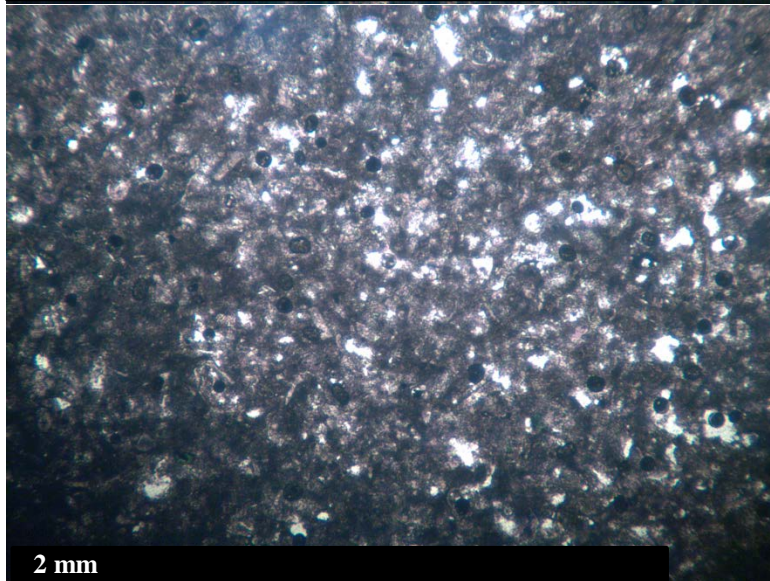
CI-907: Wackestone with sparse glauconite pellets.



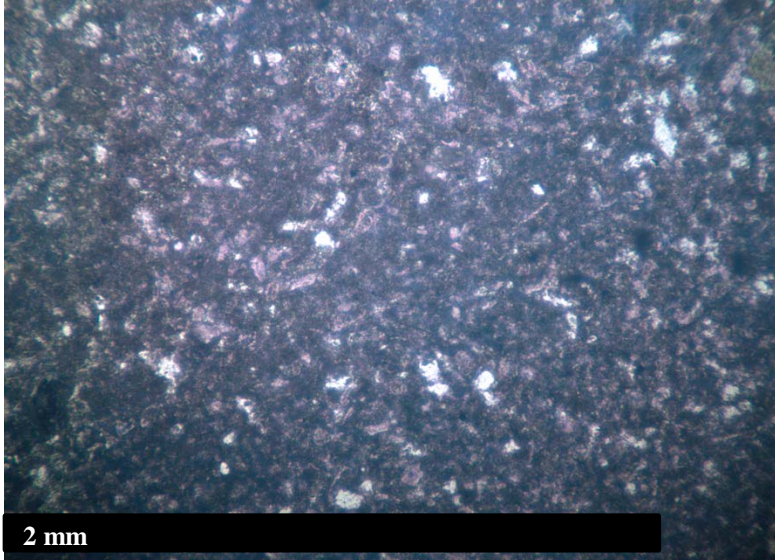
CI-926: Wackestone with few small foraminifera. Sparse glauconite pellets.



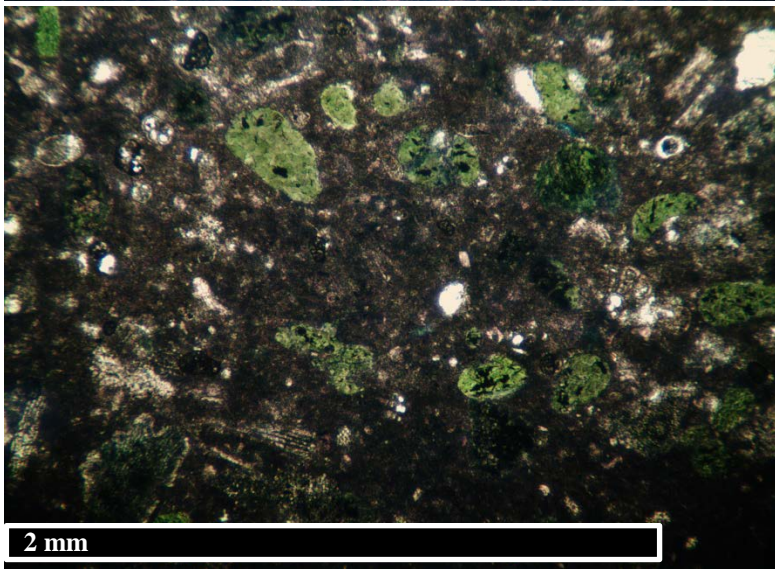
CI-937: Wackestone with sparse glauconite pellets.



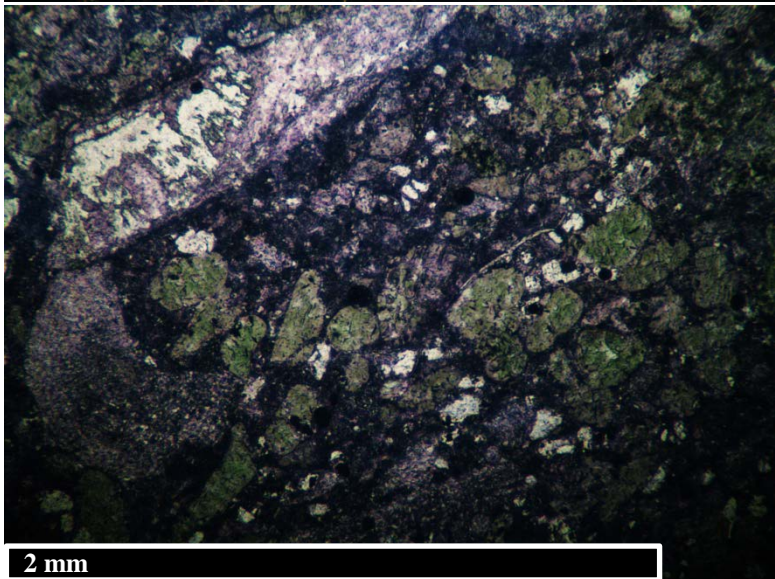
CI-952: Wackestone with few small foraminifera and sparse glauconite pellets. Poorly consolidated sample with areas of missing sample on thin section.



CI-965: Wackestone with large glauconite pellets.



CI-977: Wackestone with abundant glauconite pellets.



CI-1014: Wackestone with abundant glauconite pellets and few echinoderms.